

October 2020

Regulation of the Heat Shock Response and HSF-1 Nuclear Stress Bodies in *C. elegans*

Andrew Deonarine
University of South Florida

Follow this and additional works at: <https://digitalcommons.usf.edu/etd>

 Part of the [Cell Biology Commons](#)

Scholar Commons Citation

Deonarine, Andrew, "Regulation of the Heat Shock Response and HSF-1 Nuclear Stress Bodies in *C. elegans*" (2020). *USF Tampa Graduate Theses and Dissertations*.
<https://digitalcommons.usf.edu/etd/9534>

This Dissertation is brought to you for free and open access by the USF Graduate Theses and Dissertations at Digital Commons @ University of South Florida. It has been accepted for inclusion in USF Tampa Graduate Theses and Dissertations by an authorized administrator of Digital Commons @ University of South Florida. For more information, please contact scholarcommons@usf.edu.

Regulation of the Heat Shock Response and HSF-1 Nuclear Stress Bodies in *C.elegans*

by

Andrew Deonarine

A dissertation submitted in partial fulfillment
of the requirements for the degree of
Doctor of Philosophy
with a concentration in Cellular and Molecular Biology
Department of Cell Biology, Microbiology, and Molecular Biology
College of Arts and Sciences
University of South Florida

Major Professor: Sandy D. Westerheide, Ph.D.
Meera Nanjundan, Ph.D.
Younghoon Kee, Ph.D.
Margaret Park, Ph.D.

Date of Approval:
October 21, 2020

Keywords: heat shock response, HSF1, heat shock proteins, *C. elegans*, longevity

Copyright © 2020, Andrew Deonarine

Dedication

I dedicate this work to my family who have provided endless warmth, support, and encouragement. To my mom and dad Lynette and Joclyn and my brother and sister Michael and Andrea. To my friends Kayleigh Walters, Angel Cheong, Douglas Silva, Ian Aranca who have shown me how a few good friends can keep you feeling renewed and motivated to bring science and understanding to all. To my high school teacher, Mrs. Randa Flinn, who was instrumental in laying down the foundation of my interest in biology and cultivating a passion for teaching. To my mentor Dr. Sandy Westerheide for allowing me the freedom to grow and develop as scientist. And finally, to my previous mentor Dr. Keith Choe, whose invaluable training in *C. elegans* and experimental design served as the foundation into my scientific creativity and professional scientific development.

Acknowledgements

I would like to thank my committee members Dr. Meera Nanjundan, Dr. Younghoon Kee, and Dr. Margaret Park as well as my colleagues Doreen Lugano and Lindsey Barrett for insightful guidance and discussion throughout the years. I would also like to thank previous Choe lab members who were instrumental in patiently teaching and training me in all things worm: Dr. Yiva Wang, Dr. David Leung, and Dr. Lanlan Tang. I would also like to thank undergraduate students Mark Noble, Lori-Ann Bowie, and Erik Black for their contributions to this work.

Table of Contents

List of Figures.....	iv
List of Acronyms.....	vii
Abstract.....	viii
Chapter 1 Introduction.....	1
History of the Heat Shock Response.....	1
Heat Shock Proteins and Molecular Chaperones.....	2
HSF-1 Structure.....	3
HSF1 Post-translational Modifications.....	4
The HSF1 Activity Cycle Feedback Hypothesis.....	5
HSF1 Localization Changes.....	6
Utilizing <i>C. elegans</i> as a Model Organism.....	6
Studies of the Heat Shock Response in <i>C. elegans</i>	7
Aging and the Heat Shock Response.....	8
Insulin Signaling in <i>C. elegans</i>	9
Sirtuin SIRT1 and the Heat Shock Response.....	10
Decline of the Heat Shock Response in <i>C.elegans</i>	11
Previous Fluorescently Tagged HSF-1 Models.....	11
CRISPR/Cas9 as a Tool for Genetic Modification.....	13
Chromatin remodeling and the Heat Shock Response.....	14
Inorganic Pyrophosphatases and PYP-1.....	16
The <i>C.elegans</i> Cuticle and Collagens.....	17
Studies Proposed.....	19
Chapter 2. HSF-1 displays nuclear stress body formation in multiple tissues in <i>Caenorhabditis elegans</i> upon stress and following the transition to adulthood.....	21
Abstract.....	21
Introduction.....	22
Results.....	23
A <i>C. elegans</i> HSF-1::GFP CRISPR model shows that HSF-1::GFP in young worms is localized to nuclei of hypodermal cells and forms nuclear stress bodies in response to heat shock.....	23
HSF-1::GFP shows diffuse nuclear expression in multiple tissues in young worms, and forms nuclear stress bodies in the absence of exogenous stress in some germline cells.....	24
HSF-1::GFP provides thermotolerance, allows the induction of <i>hsp</i> mRNA upon heat shock, and does not alter thermotolerance,	

brood size, or lifespan	25
Multiple cytotoxic stressors induce HSF-1 nuclear stress body formation	27
HSF-1::GFP forms nuclear stress bodies upon the transition to adulthood in hypodermal cells and germline cells, an effect that is suppressed by genetic loss of the germline	28
HSF-1::GFP in various types of neurons escapes the formation of nuclear stress bodies during the transition to adulthood.....	29
Discussion	31
Materials and Methods	36
Chapter 3. Regulation of the Heat Shock Response by NuRF subunit <i>pyp-1</i>	47
Abstract	47
Introduction.....	48
Materials and Methods	49
Results	52
<i>pyp-1</i> acts as a specific negative transcriptional regulator on the HSR.....	52
<i>pyp-1</i> regulates <i>C. elegans</i> growth and reproduction, but does not affect lifespan	53
<i>pyp-1</i> knockdown improves proteostasis in a metastable protein folding assay and suppresses Amyloid-beta induced paralysis	53
Late <i>pyp-1</i> RNAi initiation is not sufficient to induce negative regulation of the HSR and knockdown of isoform <i>pyp-1C</i> is required	54
<i>pyp-1</i> RNAi negatively regulates lipid staining.....	55
Discussion	55
Chapter 4. Modulation of the Heat Shock Response by O-GlcNAc in <i>C. elegans</i>	64
Introduction.....	64
Materials and Methods	65
Results	68
Modulation of O-GlcNAc cycling transcriptionally regulates the HSR in <i>C. elegans</i>	68
Modulation of O-GlcNAc regulates a model of metastable protein folding.....	68
Modulating O-GlcNAc cycling affects the localization of intestinal HSF-1::GFP.....	69
<i>oga-1</i> knockdown suppresses Polyglutamine Aggregates in a Huntington's Disease model.....	69
Modulating O-GlcNAc levels regulates thermotolerance.....	69
Discussion	71
Chapter 5. RNAi of Cuticle and Collagen Genes May Regulate the HSR	79
Introduction.....	79
Materials and Methods	80

Results	80
Cuticle and Collagen genes may regulate the HSR transcriptionally	80
Discussion	81
Chapter 6. Analysis of Genetic Regulation of HSF-1 Nuclear Stress Bodies	90
Introduction.....	90
Materials and Methods	93
Results	96
p38 MAPK Signaling May Support the HSR in Germline lacking <i>C.elegans</i>	96
SIR-2.1 Overexpression May Support Diffuse Nuclear HSF-1::GFP During the Transition to Adulthood Which Requires <i>jmjd-3.1</i>	96
Insulin Signaling May Regulate HSF-1::GFP localization During the Transition to Adulthood.....	97
HSB-1 Negatively Regulates HSF-1::GFP nSBs	97
<i>hsb-1</i> delays full recovery of HSF-1::GFP nSBs Following Heat shock.....	97
<i>hsb-1</i> Regulates Germline Apoptosis and Brood Size	97
<i>hsb-1</i> May Regulate Embryogenesis in <i>C.elegans</i>	97
<i>hsb-1</i> Negatively Regulates <i>hsf-1</i> Target <i>hsp</i> Expression Dependent on <i>jmjd-3.1</i>	98
Discussion	99
Chapter 7. Implications and Future Directions	112
HSF-1 Localization in <i>C.elegans</i>	112
PYP-1 as a Regulator of the HSR	114
O-GlcNAc Cycling as a Regulator of the HSR.....	116
Collagen and the Cuticle as a Regulator of the HSR.....	117
HSB-1 as a Regulator of the HSR	116
References.....	120
Appendix A: Supporting Figures for Chapter 2.....	149
Appendix B: Supporting Figures for Chapter 3.....	155
Appendix C: Extended Protocols.....	158

List of Figures

Figure 2.1 - The <i>C. elegans</i> HSF-1::GFP CRISPR model shows that HSF-1::GFP forms nuclear stress bodies (nSBs) in hypodermal cells in response to heat shock	40
Figure 2.2 - The <i>C. elegans</i> HSF-1::GFP CRISPR model shows that HSF-1::GFP forms nuclear stress bodies (nSBs) in hypodermal cells in response to heat shock	41
Figure 2.3 - The <i>C. elegans</i> HSF-1::GFP CRISPR model shows that HSF-1::GFP provides thermotolerance, allows the induction of <i>hsp</i> mRNA upon heat shock, and does not alter thermotolerance or brood size	42
Figure 2.4 - The <i>C. elegans</i> HSF-1::GFP CRISPR model shows that HSF-1::GFP does not alter thermotolerance or brood size	43
Figure 2.5 - Confocal fluorescence images show the formation of HSF-1::GFP nSBs in response to multiple cytotoxic stressors.....	44
Figure 2.6 - HSF-1::GFP forms nSBs upon transition to adulthood in hypodermal cells and germline cells, an effect that is suppressed by genetic loss of the germline.....	45
Figure 2.7 - The transition to adulthood does not induce the localization of HSF-1::GFP into nuclear stress bodies in Touch Receptor Neurons (TRNs) PLM and ALM neurons, an effect that is independent of neuronal ensheathment.....	46
Figure 3.1 - Knockdown of <i>pyp-1</i> negatively regulates two HSR transcriptional reporters	58
Figure 3.2 - Analysis of knockdown of <i>pyp-1</i> negatively regulates two HSR transcriptional reporters.....	59
Figure 3.3 - <i>pyp-1</i> knockdown regulates growth and reproduction, but does not affect lifespan	60
Figure 3.4 - <i>pyp-1</i> knockdown improved metastable protein folding and suppresses Amyloid-beta toxicity.....	61

Figure 3.5 - Late <i>pyp-1</i> RNAi initiation is not sufficient to induce negative regulation of the HSR and knockdown of isoform <i>pyp-1C</i> is required.....	62
Figure 3.6 - <i>pyp-1</i> RNAi negatively regulates lipid staining	63
Figure 4.1 - Modulation of O-GlcNAc cycling transcriptionally regulates the HSR in <i>C. elegans</i>	73
Figure 4.2 - Modulation of O-GlcNAc regulates a model of metastable protein folding.....	74
Figure 4.3 - Modulating O-GlcNAc cycling affects the localization of intestinal HSF-1::GFP.....	75
Figure 4.4 - <i>oga-1</i> knockdown suppresses Polyglutamine Aggregates in a Huntington's Disease model.....	76
Figure 4.5 - Modulating O-GlcNAc levels regulates thermotolerance.....	77
Figure 4.6 - <i>ogt-1</i> mutants induce <i>hsf-1</i> target genes <i>hsp-70/hsp-16.2</i> more robustly <i>oga-1</i> mutants.....	78
Figure 5.1 - RNAi of Cuticle and Collagen Related Genes Identified with Increased or Decreased GFP Intensity.....	86
Figure 5.2 - RNAi of Cuticle and Collagen Related Genes Identified with Increased or Decreased GFP Intensity.....	87
Figure 5.3 - RNAi of Cuticle and Collagen Related Genes Identified with Increased or Decreased GFP Intensity.....	88
Figure 5.4 - RNAi of Cuticle and Collagen Related Genes Identified with Increased or Decreased GFP Intensity.....	89
Figure 6.1 - p38 MAPK Signaling May Support the HSR in Germline Lacking <i>C. elegans</i>	103
Figure 6.2 - SIR-2.1 Overexpression May Support Diffuse Nuclear HSF-1::GFP During the Transition to Adulthood Which Requires <i>jmjd-3.1</i>	104
Figure 6.3 - Insulin Signaling May Regulate HSF-1::GFP Localization During the Transition to Adulthood.....	105
Figure 6.4 - HSB-1 Negatively Regulates HSF-1::GFP nSBs	106

Figure 6.5 - <i>hsb-1</i> delays full recovery of HSF-1::GFP nSBs Following Heat Shock	107
Figure 6.7 - <i>hsb-1</i> Regulates Germline Apoptosis and Brood Size	108
Figure 6.8 - <i>hsb-1</i> May Regulate Embryogenesis in <i>C.elegans</i>	109
Figure 6.9 - <i>hsb-1</i> Negatively Regulates <i>hsf-1</i> Target <i>hsp</i> Expression Dependent on <i>jmjd-3.1</i>	110

List of Acronyms

HSF1/HSF-1: Heat Shock Factor 1
HSR: Heat Shock Response
HS: Heat Shock
HSE: Heat Shock Element
HSP: Heat Shock Protein
HSBP1/HSB-1: Heat Shock Binding Protein 1
OGT1: O-GlcNAc Transferase 1
OGA1: O-GlcNAcase 1
nSB: Nuclear Stress Body
SIRT1/SIR-2.1: Sirtuin 1
GFP: Green Fluorescent Protein
YFP: Yellow Fluorescent Protein
CRISPR: Clustered Regularly Interspaced Palindromic Repeats
NURF: Nucleosome remodeling factor complex
L1: Larval Stage 1
L2: Larval Stage 2
L3: Larval Stage 3
L4: Larval stage 4
YA: Young adult
GA: Gravid adult
ALM: Anterior lateral microtubule cells
PLM: Posterior lateral microtubule cells
qPCR: quantitative Polymerase Chain Reaction
RNAi: RNA interference
Acs: Fatty acid CoA synthetase genes
Bli: Blistered genes
Col: Collagen genes
Dpy: Dumpy genes
Sqt: Squatty genes

Abstract

The Heat Shock Response (HSR) is a highly conserved stress responsive molecular pathway that functions to promote appropriate protein folding in the cell. The HSR accomplishes this primarily through the use of molecular chaperones that serve to bind to misfolded or unfolded proteins to assist in stabilizing and folding proteins back to their native functional state. The master regulator of this pathway is a transcription factor known as Heat Shock Factor 1 (HSF1). HSF1 regulates molecular chaperone expression in the cell's basal state, but can also be stress induced by diverse biotic and abiotic signals including thermal shock, oxidative stress, osmotic imbalance, pathogenic invasion, cell transformation, and other pathological disease states. Thus, it is essential to understand how HSF1 function is regulated to better appreciate how the compromise of protein homeostasis (proteostasis) underlies many clinical disease pathologies. Evidence from invertebrates suggests that the HSR undergoes a rapid decline very early in adulthood and may explain the physiological effect of aging across many cell and tissue types.

To better understand this process, we sought to develop an endogenously tagged fluorescent model of HSF1 in *C. elegans*. We utilized CRISPR/Cas9 mediated transgenesis and found that our tagged model behaves very similar to wildtype animals and displays similar phenotypes to previously published low-copy fluorescent models of

HSF-1 which is the *C. elegans* homolog of mammalian HSF1. Using this novel model, we find that HSF-1 is capable of responding to novel cell stressors including Juglone, Peroxide, Paraquat, Osmotic stress, and UV exposure. This model also displays tissue-specific localization changes during the transition to adulthood. This time period of around 24 hours has been shown to be the critical window where the HSR collapses. The formation of these age-related HSF-1::GFP nuclear stress bodies (nSBs) is typically correlated with an increase in HSR activity, yet multiple measurements of proteostasis in the worm suggest that HSF-1 cannot mount an adequate response to meet acute stress demands. Genetic loss of the germline that has been shown previously to enhance longevity and stress resistance was able to suppress the formation of nSBs suggesting that the HSR remains robust and retains the youthful phenotype. Our data suggests that most cells in the worm form HSF-1:GFP nSBs during this early timepoint except the neurons. We hypothesized that this may be due to physical contact and examined the effect of ensheathment defective mutants, but found no difference in the appearance of nSBs after the transition to adulthood.

Recent data in the literature suggested that chromatin remodel may underlie the abrupt decline in the HSR has previously stated. To identify other candidate chromatin remodeling genes we performed a targeted RNAi screen to search for other regulators of the HSR across the transition to adulthood. Our work identified *pyp-1*, an inorganic pyrophosphatase, that when suppressed is capable of enhancing the activity of HSR transcriptional reporters and can also support metastable protein folding reporter animals. Interestingly, we did not find a subsequent benefit in longevity due to this increased HSF-1 dependent activity. Additionally, the effect of *pyp-1* knockdown on

our reporter animals appeared to require initiation of RNAi prior to the transition of adulthood. Taken together, this data may suggest that *pyp-1* performs a specific function during the transition to adulthood and that when this process is suppressed it results in increased HSF-1 activity in adulthood, but it is not sufficient to more broadly enhance proteostasis. This suggests further investigation into *pyp-1* expression and activity to better understand its role in regulating the HSR.

The literature suggests that mammalian HSF1 can be post-translationally modified by O-GlcNAcylation. This modification, which is similar to phosphorylation, is thought to be very dynamic and highly dysregulated in many metabolic disorders including diabetes, cancer, and neurodegeneration. The overall effect of O-GlcNAcylation on the HSR at the organismal level is still unknown. To investigate the role of O-GlcNAcylation in *C. elegans*, we utilized knockdown of the two O-GlcNAcylation modifying enzymes, *oga-1* and *ogt-1*, to examine the effect of hyper-O-GlcNAcylation and hypo-O-GlcNAcylation on the HSR in the worm. We found that in larval animals disruption O-GlcNAc cycling typically results in the enhancement of proteostasis. However, in adults, we found that knockdown of *oga-1* typically resulted in increased HSF-1 activity and *ogt-1* knockdown compromised proteostasis. Interestingly, we found that modulating O-GlcNAc cycling appeared to alter HSF-1::GFP localization specifically in the intestine suggesting further research. Intriguingly, when performing experiments to confirm the modulation of O-GlcNAc cycling on the HSR was HSF-1 dependent we found a dramatic reversal of the phenotypes of *oga-1* and *ogt-1* genetic dosage. This conflict may suggest that the bacterial food source, RNAi pathway activation, or other factors may synergize with O-GlcNAcylation to specifically regulate the HSR and suggests future experimentation.

Previous research from our lab suggests that HSF-1 may regulate a number of collagen and cuticle genes in *C. elegans* both in basal conditions and during acute stress. It was suggested that these collagen and cuticle genes may themselves regulate the HSR. To address this, we performed a RNAi subscreen of all available cuticle and collagen genes using a *hsf-16.2* fluorescent transcriptional reporter. We found a number of candidate genes that both enhanced and suppressed stress induction relative to control knockdown. Further research is required to determine if these candidates also regulate endogenous HSF-1 target gene expression and by what mechanism this is performed with.

Lastly, we utilized our validated HSF-1::GFP CRISPR/Cas9 model to examine the genetic regulation of HSF-1::GFP nSBs. It has been shown that the formation of HSF1 nSBs are typically correlated with an increase in HSR activity, but prolonged HSF1 nSBs is associated with a compromise in proteostasis. Similar to our previous research we find that longevity enhancing genetic backgrounds typically suppress HSF-1::GFP nSB formation during the transition to adulthood. Previously, we found that genetic loss of the germline conferred by a *glp-1* mutation blocked the formation of these nSBs. Here we found that this effect requires p38 MAPK signaling as a *pmk-1* mutant in the *glp-1* mutant background reversed the effect of *glp-1*. Next, we found that SIR-2.1 overexpression also suppressed nSBs that form during the transition to adulthood and that this required the lysine demethylase *jmjd-3.1*. We also examined the role of disrupting insulin signaling which is well known to dramatically enhance longevity and stress resistance. Interestingly, we did find less nSBs relative to wildtype but the effect was not completely suppressed as seen in *glp-1* and SIR-2.1 OE genetic backgrounds.

Finally, we examined the role of *hsb-1* in regulating HSF-1::GFP nSBs and found that *hsb-1* mutants typically had increased nSBs and a delay in restoring the basal level of nSBs after acute stress. Also, in the *hsb-1* mutant background, we found that *jmjd-3.1* expression is enhanced which has been previously shown to regulate HSF-1's chromatin accessibility to its target *hsps*. Taken together, this entire work establishes an endogenously tagged whole-organism model of HSF-1 and expands upon the knowledge of stress conditions that regulate HSF-1. We also identify novel genetic pathways at the whole organism level to regulate the HSR including age-specific modulation of inorganic pyrophosphatase, post-translation modification pathways, and manipulation to the worm cuticle. These identified signaling cascades require further research work to fully understand how each contributes to HSF-1 regulation and in what tissue types this regulation is present in.

Chapter 1

Introduction

History of the Heat Shock Response

The initial discovery of heat shock response (HSR) was the result of an unintentional incubator accident in the lab of Ferruccio Ritossa [1]. In Ritossa's lab work involving *Drosophila melanogaster* was being performed to study DNA. After the incubator was left at an elevated temperature it was found that puffing patterns emerged in the chromosomes of the flies suggesting those regions were experiencing increased access and transcriptional activity [2]. Although Ritossa was unable to understand why the pattern emerged in the DNA, we now understand that the significance of those puffs to be a highlight of an ancient and highly conserved proteostatic stress response now known as the HSR. Since those initial observations, multiple studies across model organisms and mammalian cell models have shown that in response to diverse endogenous and exogenous proteotoxic insults such as thermal stress, oxidative stress, pH changes, UV damage, and others result in the rapid transcriptional and translational production of cytoprotective proteins known as heat shock proteins (HSPs) [3]. Upon heat stress, one of the most highly upregulated proteins was a protein product, now called HSP70, that was observed to be approximately 70 kDa in molecular weight [4]. This led to the convention of naming these proteins which are highly enriched in

response to thermal stress by their molecular weights. Further studies identified the master transcriptional regulator of the HSR known as heat shock factor 1 (HSF1) [5, 6]. Given that thermal stress is a highly detrimental and a universal abiotic stress for all cells, it is unsurprising that HSF1 or a functionally identical gene is highly conserved across both eukaryotes and prokaryotes. Studies have revealed that upstream of HSF1 target genes, such as *hsps*, there is a HSF1 target sequence referred to as a heat shock element (HSE). These target sequences consist of a pattern of inverted triplicate repeats of nGAAn [5-7]. Identification of these HSEs within the promotor elements of genes provided a method to study the genes induced during the HSR. That is, the presence of HSEs within the promotor element would suggest the gene is likely regulated by HSF-1.

Heat Shock Proteins and Molecular Chaperones

Under both normal cellular activity and during proteotoxic stress, HSF1 regulates the expression of numerous *hsps* which function as molecular chaperones to assist in protein folding. Chaperones typically recognize an unfolded or misfolded polypeptide via hydrophobic amino acids [8, 9]. These residues which are usually found on the interior of the functional protein would normally be shielded from the aqueous environment of the cytoplasm. Many chaperones can have overlapping or sometimes distinct client proteins to fold. Given their broad function to support overall cellular function it then follows that these chaperones are essential in maintaining protein homeostasis (proteostasis) at the cellular and organismal level. Chaperones also have been found to be stress inducible or constitutive. Both inducible or constitutive chaperones are also divided by subcellular locations such as within the mitochondria [10].

The different classes of chaperones are divided up typically by their molecular weight as stated previously. One of the most well studied chaperone families is the 90 kDa weight chaperone known as HSP90. This chaperone is known to function as a dimer with ATP acting as an essential component of the protein folding pathway. The working model for HSP90 folding cycle involves HSP90 forming an open conformation when bound to ADP and the target protein to be folded. After a nucleotide exchange factor replaces ADP with ATP hydrolysis follows which enables a conformational shift in the HSP90 which attempts to fold the client protein [11]. This cycle is thought to repeat until the client protein is successfully folded. Similar hsp folding cycles have been shown for other families of hsps including the HSP70 subfamily. Further regulation of protein folding by co-chaperones such as HSP40s or J-domain containing proteins (DNAJs) can assist in guiding unfolded proteins or specificity of client proteins [4, 12].

HSF-1 Structure

HSF1 structure is defined by multiple domains which regulate its transcriptional activity. HSF1 has been shown to experimentally contain four distinct domains including a DNA binding domain, trimerization domain, regulatory domain, and transactivation domain. The DNA binding domain has been shown to have a helix-turn-helix motif which “embraces” DNA segments containing the HSE [13-16]. A key characteristic of HSF1 is the ability to form trimers which can be homotrimers, but also heterotrimers which another closely related heat shock factor called heat shock factor 2 (HSF2). Contained within the trimerization domain are hydrophobic heptad repeats A, B, and C. (HR-A/B/C). As a monomer HSF1 can be self inhibited by having HR-C fold back onto the HR-A/B region preventing trimerization [17-19]. In mammalian cells there are also other

heat shock factor genes, HSF1-4, which have some, but mostly few overlapping target genes and cellular expression locations [20, 21]. It is canonically thought that mammalian HSF1 forms homotrimers in its active state, but evidence has also shown that HSF1 and HSF2 can form heterotrimers as well [22]. Interestingly, within the mouse testes cells, in response to heat shock co-occupation of target sites of HSF1/2 were dramatically reduced and now reflected the presence of only HSF1 [23].

HSF1 Post-translational modifications

The activity of HSF1 has been shown to be related to extensive post-translational modification including phosphorylation, acetylation, and O-GlcNAcylation. Some function of these modifications have been described. Phosphorylation is arguably the most well studied with its functionality described. Hyperphosphorylation of HSF1 is usually associated with increased transcriptional activity and is performed by kinases including MAPK, PLK1, and PKA [24-28]. However, specific phosphorylation events may also reduce DNA binding and transcriptional activity such as the action of GSK-3 β or MK2 [29, 30].

Deacetylases and acetyltransferases have also been shown to target HSF1. Most acetylation sites do not have a function on HSF1 described except for acetylation to lysine 80 within the DNA binding domain [31]. This lysine can be acetylated by the acetyltransferase p300 and deacetylated by SIRT1 which serves to decrease and increase HSF1's DNA binding, respectively.

O-GlcNAcylation is the addition of a modified glucose group derived from the hexosamine biosynthesis pathway to a molecule [32]. Its addition to proteins is

controlled only by two proteins, OGT1 and OGA1, which add and remove O-GlcNAc, respectively [32]. HSF1 has been shown to be O-GlcNAcylated in response to increased glutamine presence in the cell, which is itself a part of the rate limiting step in the production of O-GlcNAc groups [33-36]. This effect is associated with increased expression of HSP70 which is dependent on HSF1 activity. However, no specific residues on HSF1 where the O-GlcNAcylation is placed have been described nor has the HSF1 O-GlcNAcylation been described in the context of heat shock similarly to phosphorylation and acetylation. To address this gap in understanding, I present the results of modulating global O-GlcNAcylation on the HSR in *C. elegans* in chapter 4 of this dissertation.

The HSF-1 Activity Cycle Feedback Hypothesis

It is suggested that HSF1 and the HSPs it regulates form a self-correcting mechanism to maintain appropriate proteostasis. As a monomer, HSF1 may associate with HSPs including HSP70 and HSP90 keeping it inactive (refs). However, with an increase in the population of misfolded/unfolded proteins, it is thought that those HSPs titrate away from HSF1 to assist folding of proteins at risk. Subsequent trimerization, DNA binding, and transactivation of HSF1 occur which leads to the upregulation of the concentration of HSPs [37-39]. Once enough chaperones are produced and have reduced the number of misfolded/unfolded species, they then reduce HSF1 activity by associating with it once again.

HSF1 Localization Changes

Changes to HSF1 localization have been reported to occur during cell stress or within pathological conditions. Upon heat shock, as HSF1 trimerizes it has been shown to translocate to the nucleus where it is observed to form distinct foci termed nuclear stress bodies (nSBs) [40]. HSF1 nSBs have been shown to colocalize with sites of transcription using RNA Pol II in immunohistochemistry [41]. However, a large majority of HSF1 nSBs do not overlap with such specific functional markers, suggesting other molecular functions of nSBs. These structures are not specific to induction by thermal stress, as many diverse cytotoxic stressors can elicit HSF1 nSBs including oxidative stress, mitochondrial stress, heavy metals such as cadmium, proteasome inhibition, and other small molecule modulators [42, 43]. A common finding in the states that induces HSF1 nSBs is the upregulation of HSPs, which has led to the thought that HSF1 nSBs are a hallmark of increased HSF1 activity [41, 44]. However, recent evidence suggests that chronic stress which leads to an extended time of HSF1 nSB formation is detrimental to cell survival [45]. Outside of exogenously applied cell stress, pathological conditions such as cancer may also exhibit the formation of HSF1 nSBs [45, 46]. The presence or absence of these HSF1 nSBs may be used as predictive markers to assess the prognosis and behavior of tumors [46, 47].

Utilizing *C. elegans* as a Model Organism

The roundworm *C. elegans* is an ideal model organism for studying the molecular basis of many biological processes in humans such as aging and pathological conditions. It is genetically tractable, has a short lifespan, has transparent anatomy for visualizing fluorescent proteins *in vivo* in live cells, and is economic to culture in laboratory settings.

Starting from a newly hatched worm they undergo three larval molts before finally molting into an adult hermaphrodite and initiating reproduction shortly thereafter [48]. Feeding on *E. coli* on agar plates researchers can easily manipulate genetic expression via RNA interference (RNAi) [49]. By generating RNAi feeding vectors it is possible to use *E. coli* to produce the double stranded RNAi which is ingested and then processed into the single stranded RNA species within the worm's cells themselves [50]. This effect is also systemic and can spread from tissue to tissue but has been shown to be less effective in some tissue types than others notably neuronal cells. *C. elegans* also has well defined genetics. It was the first multicellular organism to have its genome sequenced and has been fully annotated [51].

Studies of the Heat Shock Response in *C. elegans*

For this research's studies on the HSR the worm is especially well suited.

Transcriptional reporters for HSF1 target genes have already been generated and characterized. Similarly, to mammalian cells, the *C. elegans* homolog of human HSF1 is also known as Heat Shock Factor 1 (HSF-1). Within the worm HSF-1 has been shown to drive the expression of HSPs as well as regulating diverse cellular processes. Similar to mammalian cell-based experiments, worm HSF-1 can also exhibit localization changes either in response to cell stress or optogenetic based stimulation [52, 53].

However, a complete understanding of the function of these structures remains unclear as worms lack the DNA satellite sequences described from mammalian investigations.

Experimental evidence also suggests that the HSR can be regulated cell non-autonomously by sending signals from one tissue type to distal tissues [54-56].

Overexpression of HSF-1 in the worm can replicate longevity enhancement similar to

mouse experiments as well [57]. Modulation to the actin cytoskeleton has also been shown to regulate HSF-1 activity in the worm [58]. Notably, there is evidence suggested that the germline regulates multiple cell stress pathways in the worm including the HSR [59, 60]. Very early in the worm lifespan there is also a radical change in the robustness of stress activated HSR that is related to chromatin access and mitochondrial function [61, 62]. It has been shown that mild mitochondrial stress can modulate the decline in the HSR associated with the transition to adulthood to improve worm health and this acts through the HSR. However, a complete understanding of the expression of HSF-1 in all tissues and throughout aging in the worm is not well described.

Aging and the Heat Shock Response

The HSR has been shown to regulate aging in many metazoan model systems and has become a very attractive system to pharmaceutically target in order to promote healthier lifespans in humans. Experiments in which HSF-1 is overexpressed or activated with small molecules results in the higher expression of its target genes, including molecular chaperones, which act to stabilize the proteome and protect it from damage [47, 57, 63, 64]. As such, understanding how to utilize the HSR is thought to be essential to develop therapies to promote human health. It has been shown that modest stressors such as mild heat shocks may activate HSF-1 enough to provide a lasting benefit, which is partially mediated through histone acetylation and the activation of autophagy [63, 65]. Genetically, the HSR can also be modulated to promote longevity by the suppression of negative regulators of the HSR. First described in mammalian cells, a binding partner of HSF1, heat shock binding protein 1 (*hsbp-1*), can bind to HSF1 and block HSR activity by interacting with the oligomerization domain of HSF1 [66-68]. The homologous gene

in the worm is heat shock binding protein 1 (*hsb-1*) and its effect on the activity of the HSR and longevity is also conserved [69, 70].

Insulin Signaling in *C. elegans*

Interestingly, it has been shown that insulin signaling, a well-studied regulator of stress resistance and aging in *C. elegans*, has been shown to regulate *hsb-1*'s ability to bind to and suppress HSF-1 activity [69]. Insulin signaling, and more importantly the disruption of insulin-signaling, is one of the most well studied genetic pathways that regulate *C. elegans* lifespan, stress resistance, metabolism, immunity, and development is the Insulin/IGF-1 signaling pathway [71-73]. The *C. elegans* genome encodes many insulin or insulin-like peptides to mediate essential developmental signals and respond to changes in food availability, temperature, pH, and other biological challenges [71, 74, 75]. One of the key insulin receptors is a gene called *daf-2* which was first described in 1993 as a mutant that lives twice as long as wildtype animals [76]. This receptor is classified as a tyrosine kinase. Active insulin signaling leads to a downstream cascade of phosphoinositide-3-kinase (PI3K), Ras/mitogen activated protein kinase (MAPK), and target of rapamycin (mTOR) pathway activation [77]. This gene was identified for its role in promoting dauer formation which is an alternative life cycle stage for *C. elegans* that results in morphological, behavioral, and feeding changes. The disruption in insulin signaling conferred by *daf-2* mutants has been shown to dramatically increase general stress resistance including thermotolerance and requires stress responsive transcription factors such as *daf-16*, *hsf-1*, and *skn-1* [57, 78, 79]. Most notably, the regulation of the FoxO transcription factor DAF-16 within the insulin signaling pathway is the most well studied. Once insulin or insulin like peptides bind to DAF-2 they lead to the activation of

the downstream phosphorylation cascade starting with the phosphoinositide-3-kinase AGE-1 [80]. This then results in a series of serine/threonine kinase activations including PDK-1, AKT-1, and AKT-2 which result in the phosphorylation of DAF-16 which plays a major role in DAF-16 subcellular localization [77, 81, 82]. Phosphorylated DAF-16 is predominantly cytoplasmic where dephosphorylated DAF-16 can accumulate in the nucleus and drive expression of its target genes [83]. In the wildtype *daf-2* background, DAF-16 has been shown to be mostly diffuse in the cytoplasm, but can quickly redistribute in response to heat shock or other stressors for activation. However, In the *daf-2* mutant background, DAF-16 is constitutively nuclear in expression which suggests increased transcriptional activity supporting its role in enhancing lifespan and overall stress resistance [83]. As stated previously, a connection between insulin-signaling and the heat shock response was made 2012 showing that the DDL-1-containing HSF-1 inhibitory complex (DHIC) are disrupted by reduced insulin-signaling [69]. These findings suggested that DDL-1/2 acted together with HSB-1 to negatively regulate HSF-1 activity. However, it remains unclear if the characterized phosphorylation signaling cascade may directly target HSF-1 or how changes to insulin-signaling may regulate HSF-1 localization.

Sirtuin SIRT1 and the Heat Shock Response

Direct negative regulation with HSF-1 is not necessary as research from our group has also shown that it is possible to suppress negative regulators of other HSF-1 modifying genes to affect longevity. SIRT1 in human mammalian cells functions as an acetylation transferase and has been shown to modify many conserved client proteins and when overexpressed leads to increased stress resistance and longevity [84-86]. This effect is

also recapitulated in the worm and has been another attractive target for pharmaceutical targeting [87]. SIRT1 can deacetylate HSF1 within its DNA binding domain and this effect causes enhanced binding and an increased HSR [88]. It was then hypothesized that by suppressing a negative regulator of the worm homolog of SIRT1 termed CCAR-1, it should enhance the HSR in the worm and promote stress resistance and longevity [89]. In the worm the homolog of SIRT1 is *sir-2.1* and it still remains unclear how *sir-2.1* may regulate HSF-1 activity or localization is still unknown.

Decline of the Heat Shock Response in *C.elegans*

The effect of aging on the HSR is also a large interest in *C. elegans*. A striking feature of the HSR is that it undergoes a dramatic decline very early in adulthood [61, 90]. This effect is related to chromatin remodeling that leads to decreased access for HSF-1 to its target gene promoter elements such as *hsp-70* and *hsp-90*. Interestingly, this event can be suppressed by restoring histone modifying enzymes, modulation of mitochondrial stress, or genetic removal of the germline [61, 62, 91]. However, there is still not a complete understanding of how these signals may transmit from the germline to the soma nor between two somatic tissue types. Further, how these signals affect HSF-1 localization is very unclear. In this dissertation research, I have conducted studies to examine how tagged HSF-1 behaves under some of these conditions, revealing critical insights into understanding HSF-1 at the whole organism level within chapter 2

Previous Fluorescently Tagged HSF-1 Models

To address the aims of chapter 2 of this dissertation I will need to examine the localization of HSF-1 under various stressors, in different genetic backgrounds, and

during aging using a fluorescently labeled *hsf-1* transgene. There are multiple methods to insert transgenic DNA into the genomes of model organisms. Previous techniques such as TALENs and Zinc-finger nucleases have been used for years to modifying an assortment of different organisms [92-95]. These techniques both rely on DNA cleaving enzymes to break and/or then repair a particular genetic locus depending on the researcher's applications. I utilized CRISPR/Cas9 based genome editing to produce an endogenously tagged HSF-1::GFP worm model. There are other *C. elegans* HSF-1::GFP models that are currently available. The first model produced was based on standard extrachromosomal array integration of a HSF-1::GFP transgene driven under the control of the *hsf-1* promoter [69]. In this strain the exogenous DNA element is randomly integrated into the worm's genome during the recovery period after the application of mutagenic agents [96]. These models will overexpress your transgene, but may represent the behavior of the protein at endogenous expression levels. To improve on this, the creation of low-dose transgene models utilizing a predetermined genomic locus to insert the transgene was developed. This method uses the Mos1 mediated single copy insertion (Mos-SCI) [97]. In this approach, Mos1 transposable elements from *Drosophila* were introduced into the worm genome which then are able to react with a plasmid carrying your DNA of interest flanked by the corresponding homology arms [97]. This method was used to create a HSF-1::GFP model that showed *C. elegans* HSF-1::GFP is predominately nuclear and is able to respond to diverse stressors [52]. However, one issue with both of these approaches is silencing of the transgene which has been shown to be regulated by the choice of 3' untranslated region

in the transgene and they will not reflect the regulation of the endogenous *hsf-1* locus [98].

CRISPR/Cas9 as a Tool for Genetic Modification

Recently, a new approach using the enzyme Cas9 derived from *Streptococcus pyrogenes* has dramatically altered the accessibility of genetic modifications to scientists. Cas9 revolutionized genetic recombination because it is an endonuclease that is readily reprogrammable to cleave a particular target sequence. Once bound to a guiding RNA molecule, it scans the DNA until the site is located and creates a double strand break [99]. This endonuclease activity is dependent on a particular motif called the protospacer adjacent motif located at the end of the target sequence corresponding to the general sequence nGG. In prokaryotes, research suggests that Cas9 acts as an adaptive immunity molecule by searching for sequences from bacteriophage integrated into the genome from previous infections [100]. First identified in 1987, these clustered regularly interspaced palindromic repeats (CRISPR) serve as the sequence obtained from phage or plasmid DNA previously infecting the cell [101]. These sequences are then used as templates to produce guiding RNAs that load onto Cas9 to search out and inactivate invading viral genomes. Researchers have adapted this programmable endonuclease to achieve a variety of genetic modifications. It is possible to adapt the CRISPR/Cas9 system to perform genetic activations, inactivations, knock-in, or knock-out animals or cell lines at specific sites within the genome with relative ease. Because CRISPR/Cas9 insertion is thought to bypass the concerns regarding transgene silencing and should faithfully reflect endogenous expression and regulation of the *hsf-1*

locus I chose this approach to generate my HSF-1::GFP model for research in chapter 2.

Chromatin remodeling and the Heat Shock Response

hsp promoters and other regions of the chromatin undergo changes both during and after heat shock. Multiple conserved chromatin remodeling factors and complexes have been implicated in regulating *hsp* promoters across a variety of cell types and organisms. Starting in *C. elegans*, it has been shown that mild heat shock enables a more robust response to an otherwise lethal heat shock given afterward [63, 102]. One mechanism that regulates this is histone acetylation [65]. The effect of this modification is thought to relax the chromatin state and enable more efficient access of transcription factors like HSF-1 to bind and activate HSPs in response to stress [103]. It has also been shown that modulation of the histone balance by perturbing chromatin remodeling factors such as ISW-1, a member of the Nucleosome remodeling factor complex (NURF) also upregulates the HSR in the worm [104]. Relatedly in yeast, another chromatin remodeling complex SWI/SNF and ISWI has also been shown to play a major role in both the normal activation of the HSR and repression of other genes during heat shock [105, 106]. One of the hallmarks of the response of cells to heat shock is a global reorganization of chromatin which typically results in the prioritization of the robust induction of *hsp* genes and few other genes [107-111]. To explain this, within the mammalian literature it is suggested that HSF-1 itself acts as a chromatin remodeling factor due to its ability to recruit histone deacetylases HDAC1 and HDAC2 to initiate heat shock-dependent histone deacetylation [112].

In *C. elegans*, it has also been shown that a specific lysine demethylase, *jmjd-3.1*, is capable of specifically regulating *hsf-1* target genes across the transition to adulthood [61]. Lysine demethylases function to remove a methyl group from histone lysines and this functions to regulate chromatin structure and gene expression [113]. These genes have been shown to become dysregulated in many disease states including cancer and are a growing area of interest for therapeutic manipulation. In the worm, the transition to adulthood is a particularly early timepoint in aging and it also marks the striking decline in the inducibility of many *hsf-1* dependent *hsps* [90]. The literature suggests that *jmjd-3.1*'s gene expression declines very rapidly during this point in early adulthood which results in the repression of chromatin accessibility of HSF-1 to its *hsp* target gene promoters. Transgenic overexpression of JMJD-3.1 is sufficient to suppress the decline in *hsp* expression and results in lifespan extension and increased stress resistance in the worms [61]. However, given *jmjd-3.1*'s important role in regulating *C. elegans* lifespan, a complete understanding of the genetic control of the expression of *jmjd-3.1* is still unclear.

Another common finding in response to heat shock is the expression of Satellite III repeat sequence RNAs dependent on HSF1 in human cells. The DNA regions that contain these repeats is typically found in the heterochromatin state prior to heat shock. It has been shown that heat shock can cause HSF1 nuclear stress bodies to form near Satellite III repeats and regulates histones at these locations and temporarily alters the chromatin state to euchromatin facilitating the transcription [114, 115]. It has also been shown that the SWI/SNF complex is also required for the expression of these Satellite

III repeats and the formation of HSF1 nuclear stress bodies which is thought to represent active HSF1 [116, 117].

One interesting aspect is that these repetitive sequences have not been described in the *C. elegans* genome, yet fluorescently tagged worm HSF-1 displays similar nuclear stress bodies in response to heat shock [52]. Taken together, these results suggest that multiple chromatin remodeling complexes regulate HSR target genes and thermal stress itself may play an important role in regulating chromatin dynamics and HSF-1 activity across metazoans. Specifically in *C. elegans*, it prompts unanswered questions regarding how chromatin remodeling factors regulate HSF-1 target gene expression as well as how thermal stress may also directly mediate HSF-1 target gene accessibility. To identify candidate chromatin remodeling factors that affect the worm HSR I will perform an unbiased RNAi screen and characterize hits in chapter 3 of this dissertation.

Inorganic Pyrophosphatases and PYP-1

A hit identified in our collagen/cuticle screen was the gene *pyp-1*. It is not very well studied beyond basic characterization in *C. elegans* [118]. PYP-1 is expressed in the intestine and nervous system where it functions as an inorganic pyrophosphatase (PPase) [118]. Inorganic pyrophosphatases function enzymatically to hydrolyze inorganic pyrophosphate (PPi) to two molecules of orthophosphate (Pi). This reaction is highly exergonic which may be coupled to catalyze otherwise energetically unfavorable reactions [119]. The types of reactions inorganic pyrophosphatase include biosynthetic reactions of DNA, RNA, protein, and polysaccharides [120]. There are two classes of PPases, soluble PPase and membrane bound H⁺ translocating PPases and are not

very related in sequence similarity [121]. Within the soluble PPases the active site structure is evolutionarily conserved [122]. Changes in their activity lead to alterations of metabolism and growth in some plants [123]. The most widely studied soluble PPase is NURF38 in *Drosophila* is a member of the NURF complex and functions in nucleosome remodeling [124]. In *Drosophila*, NURF38 is required for appropriate development and regeneration after radiation damage and during metamorphosis [125, 126]. It also plays a role in maintaining germline stem cells in the *Drosophila* testis [127]. Interestingly, in the parasitic roundworm *Ascaris*, PPase has been shown to play a role in the development and molting of the cuticle [121]. Our data regarding the identification and phenotypes of *pyp-1* regulating the HSR in *C. elegans* are detailed in chapter 3 of this dissertation work.

The *C.elegans* Cuticle and Collagens

Given our findings related to *pyp-1* in chapter 3 in conjunction with previous results of our groups data we also sought to screen cuticle and collagen genes as regulators of the HSR [111]. Similar to the mammalian cuticle, the worm cuticle serves as a physical barrier to pathogens and small molecules, and assists in maintaining internal cellular physiology [128, 129]. The worm undergoes five total molts throughout its lifespan. The cuticle serves as an essential attachment point for body wall muscles for locomotion [130, 131]. The collagens that comprise the cuticle are highly conserved ubiquitous proteins that have a regular tripeptide repeat which consists of Glycine-A-B, where A is proline and B hydroxyproline [132]. In order to form a collagen fiber, three procollagen peptides trimerize in the endoplasmic reticulum before being exported from the cell. After secretion from the ER, procollagens are further processed and crosslinked

together for cuticle synthesis [133]. Appropriate cuticle synthesis and patterning results in specific structures called alae along the dorsal and ventral and circumferential furrows along the entire length of the worm body [134]. Mutations in collagen genes may lead to changes in the morphology of the cuticle affecting the alae, furrows, and overall motility of the worm. Cuticle phenotypes are typically named for the resulting observable phenotype including dumpy (dpy), squat (sqt), long (lon), roller (rol), and blister (bli) [132]. The cuticle genes undergo cyclic expression that correspond to molting timing [135].

Beyond the worm cuticle, collagens serve as essential components of the extracellular matrix in other cellular compartments and organs. Dysregulation of collagen processing also underlies a variety of human disease such as Ehlers-Danlos syndrome, chondrodysplasia, osteogenesis imperfecta, and wound healing defects [132]. The worm cuticle has distinct characteristics and features within its underlying mechanisms regarding its synthesis and processing which are highly conserved in many metazoans. One growing technology that will benefit from a better understanding of ECM synthesis is organoid technology. In this technique, cells are cultured to form more accurate representative structures of organs to facilitate a variety of research applications [136, 137].

It has been reported that the cuticle plays a role in regulation of osmotic and oxidative stress [138-140]. Changes to intracellular osmolarity can lead to increases or decreases in cell volume which may result in mechanical stress on cellular components. Interestingly, changes to the morphology of the cuticle has been shown to activate both oxidative stress and antimicrobial defenses. This data suggests that the cuticle itself

may act as a sensor to adverse environmental conditions and the presence of pathogens. One relatively new approach to enhance longevity is the modulation of collagens to mediate aging effects. It has been suggested that in long-lived genetic mutants collagen remodeling may be a mechanism by which worms exhibit anti-aging behavior [141]. Some collagen genes have been shown to be regulated by HSF-1 during stress conditions and independent of stress [111]. These results suggest that the HSR can be co-opted in order to promote increased longevity and stress resistance to enhance the human condition. It is unknown if the modulation of cuticle morphology affecting oxidative and osmotic stress responses described above may also regulate HSF-1 activity as well. To begin answering these questions, the worm presents an amenable screening tool to identify novel candidate regulators of the HSR. We performed a RNAi subscreen of all available cuticle/collagen genes and the results can be found in chapter 5 of this dissertation.

Studies Proposed

Analysis from the literature reveals many aspects of the HSR that need to be addressed. Specifically in *C. elegans*, to better understand the regulation of the HSR, I propose the following aims. The construction of an endogenously tagged HSF-1 fluorescent model will allow for high fidelity analysis of the expression and localization of HSF-1 *in vivo* during acute cell stress and aging. This will be examined in chapter 2 of this work. Following construction and validation of this model I propose to test the genetic regulation of longevity promoting mutant backgrounds on the localization of HSF-1::GFP to better understand how HSF-1 may be regulated to promote enhanced survival. This will be examined in chapter 6 of this work. Chromatin remodeling has

been shown to regulate the HSR, but a wide analysis of multiple chromatin remodeling factors has not been performed. I propose a targeted RNAi subscreen of available chromatin remodeling factors to potentially identify novel regulators of the HSR. This will be addressed in chapter 3 of this work. The post-translation modification O-GlcNAc has been shown to modify mammalian HSF1, but its effect at the organismal level is still not well understood. To address this, I propose to examine the effect of both hyper-O-GlcNAcylation and hypo-O-GlcNAcylation on the HSR in *C. elegans*. This will be presented in chapter 4 of this work. Lastly, previous research in our lab has revealed HSF-1 dependent regulation of collagen genes both dependent on cell stress and independent of stress. To examine a potential role of collagens themselves regulating the HSR I propose a RNAi subscreen of collagen or collagen modifying genes to identify potential novel regulators of the HSR via collagen/cuticle remodeling. This work will be presented in chapter 5 of this work.

Chapter 2

HSF-1 displays nuclear stress body formation in multiple tissues in *Caenorhabditis elegans* upon stress and following the transition to adulthood

Text adapted from manuscript submitted to Cell Stress and Chaperones in revisions.

Abstract

The transcription factor Heat Shock Factor-1 (HSF-1) regulates the heat shock response (HSR), a cytoprotective response induced by proteotoxic stresses. Data from model organisms has shown that HSF-1 also has non-stress biological roles, including roles in the regulation of development and longevity. To better study HSF-1 function, we created a *C. elegans* strain containing HSF-1 tagged with GFP at its endogenous locus utilizing CRISPR/Cas9-guided transgenesis. We show that the HSF-1::GFP CRISPR worm strain behaves similarly to wild-type worms in response to heat and other stresses, and in other physiological processes. HSF-1 was expressed in all tissues assayed. Immediately following the initiation of reproduction, HSF-1 formed nuclear stress bodies, a hallmark of activation, throughout the germline. Upon the transition to adulthood, HSF-1 nuclear stress bodies appeared in most somatic cells. Genetic loss of the germ line suppressed nuclear stress body formation with age, suggesting that the germ line influences HSF-1 activity. Interestingly, we found that various neurons did not form nuclear stress bodies

after transitioning to adulthood. Therefore, the formation of HSF-1 nuclear stress bodies upon the transition to adulthood does not occur in a synchronous manner in all cell types. In sum, these studies enhance our knowledge of the expression and activity of the aging and proteostasis factor HSF-1 in a tissue-specific manner with age.

Introduction

The heat shock response (HSR) is a conserved stress response that maintains proteostasis within cells and organisms. Heat shock transcription factor 1 (HSF1), the master regulator of the HSR, drives expression of heat shock protein (*hsp*) genes following exposure to high temperature [142]. HSPs then act as molecular chaperones to restore proteostasis [143]. In addition to functions in stress-induced gene expression, HSF1 is now known to orchestrate diverse normal physiological processes including development, reproduction and aging [142]. HSF1 is also central to a number of diseases of aging including neurodegenerative diseases, cancer, and metabolic disorders [144]. Understanding how HSF1 function can be co-opted or compromised with age is thus critical for understanding the normal aging process and for elucidating novel therapeutic strategies for diseases of aging.

Caenorhabditis elegans is a useful model organism in which to study the function of the conserved HSF-1 transcription factor during stress, development, and aging. A number of HSF-1::GFP worm strains have been created to visualize HSF-1 localization and activity during these conditions. Overexpression models of HSF-1::GFP have shown gain-of-function phenotypes, including increased stress resistance and longevity [69, 78, 145, 146]. More recently, HSF-1::GFP models created using the direct genome insertion MosSCI technique have allowed the study of HSF-1::GFP when expressed at levels that

are closer to physiological levels [52, 147]. HSF-1::GFP is expressed primarily in the nucleus of *C. elegans* cells, where it localizes into distinct granules upon heat shock [52]. These granules are similar to the nuclear stress bodies formed by mammalian HSF1, markers of activation [40, 44].

Many questions remain regarding HSF-1 activation in a whole organism. For instance, more could be learned about the effects of diverse stressors besides heat shock on HSF-1 activity. Also, a whole organism model is useful to uncover the effects of naturally occurring developmental programs on HSF-1 activity. Additionally, the effect of aging on HSF-1 activity in a tissue-specific manner deserves more research. To address these questions, we utilized CRISPR/Cas9 technology to add a GFP tag onto the endogenous *hsf-1* gene in *C. elegans*. This model has the advantage that HSF-1::GFP expression comes from the endogenous chromatin location, so expression should be highly similar to wild-type expression. Using this model, we characterized the localization and nuclear stress body formation of HSF-1 in response to diverse cytotoxic stressors and across age in a tissue-specific manner.

Results

A *C. elegans* HSF-1::GFP CRISPR model shows that HSF-1::GFP in young worms is localized to nuclei of hypodermal cells and forms nuclear stress bodies in response to heat shock.

Previously published studies of *C. elegans* HSF-1 have utilized fluorescently tagged HSF-1 that was either overexpressed or integrated at a non-endogenous location in the

genome [52, 69, 147]. To improve upon our understanding of HSF-1 physiology and its expression and function during the transition to adulthood in *C. elegans*, we sought to knock in GFP in the endogenous locus to avoid overexpression and locus-specific effects. We utilized CRISPR/Cas9 transgenesis to knock in a homologous repair template carrying a direct GFP *hsf-1* C-terminal fusion, retain its endogenous 3' UTR, and select transgenic animals via *unc-119(+)* rescue (Figure S1) allowing expression of endogenous HSF-1 tagged with GFP (Figure 1A-B). Hypodermal cells of the resulting worm strain, SDW015, were then examined at the L4 larval/young adult stage (L4/YA) for HSF-1::GFP expression patterns with and without heat shock (Figure 1 A-B). We found that HSF-1::GFP is diffusely expressed in nuclei under non-stress conditions (Figure 2.1A). HSF-1::GFP redistributed into nuclear stress bodies, a well-established hallmark of HSF-1 activation [115, 148], following heat shock (Figure 1B). We obtained similar results using a MosSCI single-copy HSF-1::GFP strain [52] for comparison (Figure 2.1C-D). Upon examining hypodermal cells from multiple worms ($n \geq 8$) from both the CRISPR knock-in and the MosSCI HSF-1::GFP strains, we found nearly 100% of the cells showed diffuse nuclear HSF-1 prior to stress (negative for the appearance of nSBs (-nSBs)), which redistributed into nuclear stress bodies following heat shock (Figure 2.1E).

HSF-1::GFP shows diffuse nuclear expression in multiple tissues in young worms, and forms nuclear stress bodies in the absence of exogenous stress in some germline cells.

To determine the full organismal expression pattern of HSF-1::GFP using our endogenous HSF-1::GFP CRISPR model, we analyzed multiple tissues via fluorescence microscopy in L4/YA worms. (Figure 2.2- A-H complete images, Figure 2- I-N magnified inserts). HSF-1::GFP expression was observed in all cell types examined. In unstressed

worms, HSF-1::GFP was predominantly localized diffusely in the nucleus and was visible in all cells examined including hypodermal cells, intestinal cells, pharyngeal muscle cells, amphid neurons, phasmid neurons, adult nerve ring neurons and germ cells. Interestingly, HSF-1::GFP was observed to form nuclear stress bodies in different regions of the germline including both the distal and proximal ends as well as the loop (Figure 2.S2), even though the worms were not exposed to any external stressors, suggesting that HSF-1 activity may be affected by the germ cell maturation process.

HSF-1::GFP provides thermotolerance, allows the induction of *hsp* mRNA upon heat shock, and does not alter thermotolerance, brood size, or lifespan.

To validate that the addition of the GFP tag to HSF-1 did not cause any gross organismal alterations to HSF-1 function, we first examined whether the worm strain induced *hsp* mRNA upon heat shock, and whether the worms displayed alterations to thermotolerance (Figure 2.3). In L4/YA worms, we assessed the heat shock inducibility of *hsp-16.2* mRNA (Figure 2.3A) and *hsp-70* (C12C8.1) mRNA (Figure 2.3B). We found that both genes were highly inducible in the HSF-1::GFP CRISPR strain, although the maximum induction levels were lower than in the wild-type N2 strain. We found no significant changes in thermotolerance levels between the HSF-1::GFP CRISPR strain and the wildtype N2 strain 24 hours post subjection of L4/YA worms to a 37°C heat shock for 2 hours (Figure 2.3C). Thus, while the HSF-1::GFP CRISPR strain was not able to reach the same maximal *hsp* mRNA induction as wild-type worms, the modified *hsf-1* gene still allowed for significant activation of molecular chaperone genes in response to thermal stress and the same degree of protection of the organism from thermal stress.

Continuing to validate our HSF-1::GFP model, we next performed experiments using *hsf-1* or GFP RNAi to test whether targeting HSF-1::GFP in our CRISPR strain had physiological consequences on brood size, thermotolerance, and lifespan, all processes which are known to be modulated by HSF-1 [145]. *hsf-1* RNAi decreased brood size by over 50% in both the N2 strain and in the HSF-1::GFP CRISPR strain (Figure 2.3D). As predicted, RNAi targeting GFP specifically eliminated offspring in the HSF-1::GFP CRISPR worms as compared to the N2 strain. Therefore, HSF-1 with the GFP tag retains its ability to modulate the number of offspring. To test for resistance to heat stress, we found that *hsf-1* RNAi decreased thermotolerance in both the N2 and in the HSF-1::GFP CRISPR strain (Figure 2.4E). GFP RNAi, on the other hand, only decreased thermotolerance in the HSF-1::GFP CRISPR strain, as expected. We note that the effect of the *hsf-1* RNAi on both the number of offspring and on thermotolerance was greater in the SDW015 strain than it was in the N2 strain for unknown reasons. For longevity studies, we observed that both N2 and HSF-1::GFP CRISPR animals displayed similar lifespans with control RNAi (Figure 2.4F) and both have reduced longevity after *hsf-1* RNAi treatment, but only the HSF-1::GFP CRISPR animals were affected by GFP RNAi (Figure 2.4G). A similar pattern for the median lifespan was also observed (Figure 2.4H). Both strains had significant reductions in median lifespan when fed *hsf-1* RNAi, but only the HSF-1::GFP CRISPR strain was affected by GFP RNAi. Thus, our HSF-1::GFP CRISPR strain can be targeted by RNAi against either *hsf-1* or GFP to affect known HSF-1-dependent physiological processes.

Multiple cytotoxic stressors induce HSF-1 nuclear stress body formation.

Heat shock is one of many proteotoxic stressors that can activate HSF-1. We thus tested the effectiveness of several other stressors on the formation of nuclear stress bodies in the hypodermal cells of HSF-1::GFP CRISPR animals at the L4/YA stage (Figure 2.5). We found that severe hypertonicity (600 mM NaCl/ 30 min) induced HSF-1::GFP nuclear stress body formation (Figure 2.5B), likely due to a disruption in proteostasis caused by osmotic stress. We then tested a panel of oxidative stressors, including the naturally occurring oxidants juglone and peroxide, and the synthetic compounds paraquat and acrylamide, for their abilities to induce HSF-1 nuclear stress bodies. Juglone (38 μ M/30 mins), paraquat (5 mM/2 hrs), and peroxide (7.5 mM/2 hrs), were all able to induce nuclear stress bodies, but acrylamide (7 mM) was not (Figure 2.5B-F). Since acrylamide is reported to act as a neurotoxin, we wondered if cells still responded to thermal stress following acrylamide exposure, and indeed we observed strong HSF-1::GFP nuclear stress body formation after heat shock (Appendix A3, A-E). To confirm our acrylamide was functional, we exposed strain CL2166 (*pgst-4::GFP*), an oxidative stress transgenic transcriptional reporter strain, to 7 mM acrylamide and observed strong activation of the reporter (Appendix A3, F).

Next, we tested whether HSF-1::GFP could respond to UV-induced DNA damage. We found that UV damage also activated HSF-1, as we observed the formation of stress bodies in nuclei of stressed animals immediately following UV exposure (Figure 2.5G). Lastly, we tested whether sodium azide induced HSF-1::GFP nuclear stress bodies. Sodium azide inhibits cytochrome oxidase and ATP production, and can be often used as an anesthetic to immobilize *C. elegans* [149]. Similar to a previous report [52], we

found strong nuclear stress body formation in hypodermal cells upon exposure to 5 mM sodium azide for 5 mins (Figure 2.5H). Therefore, HSF-1::GFP can form nuclear stress bodies in hypodermal cells in response to diverse cytotoxic stressors in addition to heat shock.

HSF-1::GFP forms nuclear stress bodies upon the transition to adulthood in hypodermal cells and germline cells, an effect that is suppressed by genetic loss of the germline.

C. elegans is an ideal model to study organismal aging and it has been reported that the HSR declines precipitously upon the transition to adulthood [61, 90]. To investigate how HSF-1 localization is affected during this period, we aged our HSF-1::GFP CRISPR animals without applying outside stressors and recorded the localization of HSF-1::GFP in the hypodermal cells and in the germline. During the last larval stage, L4, we observed HSF-1::GFP diffusely expressed in the nuclei of both hypodermal cells and germ cells (Figure 2.6 A,G). Approximately 6-8 hrs after the L3/L4 molt, *C. elegans* animals complete their final molt into the adult cuticle, becoming young adults (YA). Five to seven hrs after becoming young adults, the worms begin reproduction and become fully gravid adults (GA). We observed that upon the transition to adulthood just after the L4/adult molt, HSF-1::GFP formed nuclear stress bodies in some hypodermal cells and germ cells (Figure 2.6 B-C and H-I). In addition, a higher proportion of the hypodermal cells of gravid adults displayed nuclear stress bodies as compared to young adults, suggesting that the transition to adulthood enhances HSF-1 foci formation. Beyond the transition to adulthood, we also assessed the behavior of HSF-1::GFP in normally aging animals. Starting at the L4 stage we assessed the individually number of HSF-1::GFP nSBs

present per hypodermal cell (Appendix A4 A-B). We find that throughout aging stress bodies are always observable in every hypodermal cell, but the individual number of nSBs per cell can vary dramatically. The *C. elegans* germline has been linked to the regulation of somatic proteostasis and overall longevity, with loss of the germline having a pro-survival effect [150, 151]. We tested whether the formation of nuclear stress bodies that appear in the adult could be suppressed by the genetic loss of the germline by crossing the HSF-1::GFP CRISPR strain with a strain carrying the temperature sensitive *glp-1(e2144)* mutation (Figure 2.6 D-F). After shifting to the non-permissive temperature of 25°C, we observed that the *glp-1* mutant animals lost the formation of nuclear stress bodies upon the transition to adulthood. We next tested whether or not this suppression of nSBs conferred by the genetic loss of the germline is capable of retaining cells largely absent of nSBs throughout aging in 25°C. Intriguingly, we did not observe any dramatic increases in hypodermal cells displaying HSF-1::GFP nuclear stress bodies up to day 9 of adulthood (Figure 2.6K). Thus, the transition to adulthood can cause the formation of nuclear stress bodies, a marker of active HSF-1, and the genetic loss of the germline can suppress this effect.

HSF-1::GFP in various types of neurons escapes the formation of nuclear stress bodies during the transition to adulthood.

We wondered whether cell-cell communication may be important in HSF-1::GFP nuclear stress body formation that occurs during the transition to adulthood. To test this hypothesis, we asked whether nuclear stress body formation would occur in cells that are physically shielded from other cells. In *C. elegans*, the touch receptor neurons (TRNs) become ensheathed by the hypodermis during development. As a result, they are not

exposed to the worm's pseudocoelom and are thus largely protected from other cells. We crossed a strain expressing a fluorescent marker for TRNs, *pmec-17::RFP*, into our HSF-1::GFP CRISPR strain to create strain SDW077. We then observed a subset of TRNs, the posterior lateral microtubule (PLM) and anterior lateral microtubule (ALM) touch receptor neurons, for the presence or absence of HSF-1::GFP nuclear stress bodies during the transition to adulthood (Figure 2.7). Interestingly, unlike the other cell types we studied, we did not observe an increase in the number of PLM neurons with nuclear stress bodies upon the transition to adulthood or in gravid adults (Figure 2.7A). Indeed, upon analysis of both the PLM and ALM neurons at gravid adulthood, neither type of TRN neuron showed an increase in nuclear stress bodies (Figure 2.6B-F). We then crossed an ensheathment mutation, *mec-1* (e1292) [152], with our HSF-1::GFP; *pmec-17::RFP* CRISPR strain, and found that the PLM and ALM neurons in these animals still escape age-induced formation of nuclear stress bodies (Figure 2.7B, G-J). Thus, an alternative mechanism must exist to prevent the formation of HSF-1 nuclear stress bodies with age in these cells. To confirm that PLM neurons are capable of producing HSF-1::GFP nuclear stress bodies, we exposed them to heat stress and observed strong focus formation immediately following exposure (Appendix A5). We then wondered whether neurons in general have decreased formation of nuclear stress bodies with age. We analyzed the neurons in the adult nerve ring, and we observed that these neurons also did not show enhanced nuclear stress body formation with age (Appendix A6). We thus conclude that PLM, ALM and adult nerve ring neurons contrast from other cells in that they do not form nuclear stress bodies upon the transition to adulthood.

Discussion

Given the critical role of HSF-1 in regulating cellular proteostasis, organismal viability, and aging, we sought to generate a biologically relevant expression model to study this transcription factor in *C. elegans*. We utilized CRISPR/Cas9 genome editing to insert GFP as a direct fusion to the endogenous *hsf-1* locus, while retaining the natural 3' untranslated region. This approach has an advantage over other *C. elegans* HSF-1 expression models as it restricts the cell to express only GFP-tagged HSF-1 instead of both tagged and untagged variants. We characterized this strain to understand the localization and activation of HSF-1 during cell stress and during the transition to adulthood in a tissue-specific fashion. We observed that HSF-1 is nuclear in all cell types examined, and that it formed nuclear stress bodies, a marker of activated HSF-1, in response to diverse proteotoxic stressors. Immediately following the initiation of reproduction, we observed the formation of HSF-1::GFP nuclear stress bodies in multiple cell types including germ cells. Overall, these studies enhance our knowledge of the expression and activation of the proteostasis factor HSF-1 in a tissue-specific manner over age.

While the addition of the GFP tag decreased maximal hsp induction by heat shock, other biological readouts of the HSR remained unaltered. There was no statistical difference in survival after thermal stress, brood size, or lifespan in wild-type N2 versus our HSF-1::GFP CRISPR strain. We note that there appears to be a blunted maximal induction of *hsp-16.2* and *hsp-70* mRNA expression after heat stress as compared to wildtype animals, indicating that the GFP tag may moderately hinder the activity of HSF-1, but this

reduction was not sufficient to cause obvious phenotypic differences in the assays tested. Thus, our strain provides a valid model in which to study HSF-1 expression and activity.

We observed that the HSF-1::GFP fusion protein is a predominately nuclear protein which can quickly redistribute its localization to form nuclear stress bodies after heat shock and other cytotoxic stresses. We note that it could be possible for GFP tagging to alter fusion protein localization. Many models of mammalian HSF1 suggest that it is cytoplasmic in the resting state, and only moves to the nucleus upon proteotoxic stress that allows the titration away of inhibitory cytoplasmic chaperones [153]. Conversely, other studies have found HSF1 to be predominantly nuclear under control conditions [154, 155]. Initial results with overexpressed *C. elegans* HSF-1::GFP indicated diffuse nucleo-cytoplasmic localization for HSF-1 under control conditions, which switched to weak nuclear localization after heat shock [69]. Our results that HSF-1::GFP is nuclear prior to stress agree with recent *C. elegans* studies in which HSF-1::GFP was expressed at more physiological levels via the MosSCI insertion technique [52, 147]. As our strain expresses HSF-1::GFP from the endogenous locus and is thus unlikely to have enhanced HSF-1 levels, our results support the previous findings that HSF-1 is a constitutively nuclear protein in *C. elegans*.

The formation of nuclear stress bodies has been associated with HSF1 activation in mammalian cells [115, 148]. As reported in previous studies with *C. elegans* HSF-1::GFP generated by MosSCI [52, 147], we find that heat shock induces the localization of HSF-1 into nuclear stress bodies. Thus, *C. elegans* HSF-1 is a nuclear protein in all cells examined, and it forms classical nuclear stress bodies upon heat shock.

Interestingly, we find robust HSF-1::GFP expression in germ cells. While this was not reported in a HSF-1::GFP MosSCI strain utilizing the *unc-54* 3'UTR [52], this was observed in a HSF-1::GFP MosSCI strain utilizing the endogenous *hsf-1* 3'UTR [156]. This difference in HSF-1 models is likely attributed to strong germline silencing of transgenes that can be alleviated with the usage of particular 3' UTRs that allow for germline expression [98]. In our studies, we have found a striking formation of HSF-1::GFP nuclear stress bodies throughout the germline immediately following the initiation of the *C. elegans* reproductive cycle. This finding has not been previously described, and it is unknown what the function of the HSF-1 nuclear stress bodies is in these cells. Prior to fertilization, protein aggregates are cleared to avoid the transmission of protein damage across generations [157]. It is possible that HSF-1 nuclear stress body formation in the germline is a marker of HSF-1 activation that may be required for this process.

As a central regulator of cellular proteostasis, worm HSF-1 should be capable of responding to diverse forms of cytotoxic agents. To test this hypothesis, we exposed worms to several stress conditions in addition to heat shock, including hypertonic stress, different forms of oxidative stress, and DNA damage. While mild hypertonic stress did not activate HSF-1 (data not shown), we found that severe hypertonic stress (600 mM NaCl) could, perhaps due to the macromolecular crowding that occurs under this condition [158]. With a panel of oxidative stressors, we found that juglone, paraquat, and peroxide were all able to induce nuclear stress bodies. This data fits with previous results showing that redox reactions can regulate the HSR [159, 160]. It is unclear why acrylamide, which also induces oxidative stress, does not induce nuclear stress body formation. It may be that the specific type of oxidative stress is important in determining whether HSF-1 can

become activated. Because the HSR is subject to non-cell autonomous signaling via the worm nervous system [54] and acrylamide has been reported to act as a neurotoxin [161], we wondered whether HSF-1::GFP would be capable of responding to a thermal stress after acrylamide exposure, and found that prior treatment with acrylamide did not block heat-induced HSF-1 activation. We showed that sodium azide, a common anesthetic used to paralyze worms for imaging [149], also caused the formation of HSF-1 nuclear stress bodies. Additionally, UV treatment induced nuclear stress body formation. Therefore, we conclude that diverse cytotoxic stressors can activate the formation of HSF-1 nuclear stress bodies. Future work with our HSF-1::GFP CRISPR model will allow a more detailed analysis of which stressors, or stress combinations, can cause nuclear stress body formation and the mechanisms by which this happens.

Why do we observe an increase in HSF-1 nuclear stress bodies upon the transition to adulthood? Previous studies have shown that HSR promoters are subjected to dramatic transcriptional silencing upon the transition to adulthood in *C. elegans* via chromatin repression [61]. As HSF-1 nuclear stress body formation has been associated with activated HSF-1, how can we reconcile these two disparate observations? HSF-1 nuclear stress bodies may reflect an attempt to respond to a decline in proteostasis capacity that occurs upon the transition to adulthood. HSF-1 could become activated and form nuclear stress bodies at distinct genomic loci, but would be unable to activate the transcription of most *hsp* target genes due to chromatin inaccessibility. A recent study of HSF-1 nuclear stress body formation in human cancer cells also has an interesting link with our data. In this study, it was found that while HSF1 nuclear stress body formation correlates with HSF1 activity at the cell population level, at the single cell level it is actually the dissolution

of the foci, not the formation of the foci, that correlates with HSF1 activity [45]. It is possible that once stress induces the HSF1 foci, the foci then have two options: to dissolve, allowing HSF1 activity, or to solidify, permanently trapping and inactivating HSF1. It is possible that the appearance of HSF-1 nuclear stress bodies that we are seeing with age is thus indicative of inactive, trapped HSF-1, correlating with the dramatic decrease in the activity of the HSR.

Well-established methods to support overall proteostasis and longevity in *C. elegans* are by physical destruction of germline precursor cells or by genetic loss of the germline [59, 91]. Raising HSF-1::GFP CRISPR animals carrying the *glp-1* (e2144) mutation at the non-permissive temperature to eliminate the germline, we found that the formation of nuclear stress bodies upon the transition to adulthood is lost. Thus, there is a transcellular signaling mechanism that signals between the germline and the somatic cells to regulate nSBs formation. It will be interesting in future work to determine the mechanism by which the transition to adulthood induces HSF-1 nuclear stress bodies, how the elimination of the germline prevents this, and what the biological significance of formation of nuclear stress bodies is at the cellular and organismal level across age.

Interestingly, we observed that the PLM, ALM and nerve ring neurons did not recapitulate the rapid shift in HSF-1::GFP nuclear stress body formation across the transition to adulthood that occurs in the cells of other tissues. PLM neurons did form HSF-1 nuclear stress bodies in response to heat shock, so they do express HSF-1 that can respond to stress. It will be informative in future work to test whether other neuronal types also behave similarly, and to investigate what is protecting these neuronal cells from nuclear stress body formation with age.

Collectively, our studies suggest that HSF-1 is expressed in the nuclei of multiple cell types within *C. elegans* and can respond to diverse stresses, biological processes, and age to become activated. Our HSF-1::GFP CRISPR model provides a new tool to further understand how this critical protein integrates stress, development, and aging in a whole organism model.

Materials and Methods

C. elegans strains and maintenance. *C. elegans* strains were grown and maintained at 20°C on NGM plates with *Escherichia coli* OP50-1, unless otherwise noted. Bristol N2 was used as the wild-type strain for these studies. Additional strains used were OG497 [drSi13 II; unc-119(ed3) III] [52], SDW015 *hsf-1*(*asd002*(*hsf-1*::*GFP* + *unc-119*(+)) (this work), SDW050 *hsf-1*(*asd002*(*hsf-1*::*GFP* + *unc-119*(+))); *glp-1*(*e2144*) (this work), SDW077 *hsf-1*(*asd002*(*hsf-1*::*GFP* + *unc-119*(+))); *uls115*[*pmec-17*::*RFP*] (this work), and TU6773 *hsf-1*(*asd002*(*hsf-1*::*GFP* + *unc-119*(+))); *uls115*[*pmec-17*::*RFP*]; *mec-1*(*e1292*). Age synchronization was accomplished by standard hypochlorite treatment.

Creation of CRISPR HSF-1::GFP strain (SDW015). CRISPR/Cas9 transgenesis was performed as described with modifications [162]. Briefly, upstream and downstream homology arms consisting of 2 kb of genomic sequence flanking either side of the desired double strand break was amplified via PCR and followed by subsequent Gibson Assembly to insert GFP directly following exon 8 directly before the stop codon of *hsf-1*. Unc-119(+) rescue was used to detect homologous repair template insertion. The homologous repair template was injected at a final concentration of 10 ng/μl. A Cas9/sgRNA-producing plasmid (pDD162) was edited using NEB Q5 Site Directed Mutagenesis per the manufacturer's instructions to insert the sgRNA targeting exon 8 of

hsf-1 and was injected by Knudra Transgenics (Murray, UT) at a final concentration of 50 ng/ μ l. The negative selection vector pMA122 and the fluorescent co-injection vector pCFJ90 were injected at 10 ng/ μ l and 5 ng/ μ l, respectively.

RNA interference (RNAi). To perform RNAi, animals were fed HT115(DE3) *E. coli* transformed with the indicated RNAi vectors (J. Ahringer, University of Cambridge, Cambridge, U.K.) as previously described [163]. Individual RNAi clones were sequence-verified prior to use. To induce dsRNA production, NGM plates were supplemented with 1 mM IPTG and inoculated plates were left to mature overnight at room temperature. RNAi feeding was initiated at the L1 developmental stage unless otherwise noted.

Stress exposures. Worms were subjected to heat shock for the specific duration and temperatures described, 600 mM NaCl for 30 mins, 7 mM acrylamide for 5 hrs, 38 μ M juglone for 30 mins, 5 mM paraquat for 2 hrs, 7.5 mM hydrogen peroxide for 2 hrs, 300 J/cm² UV using a Stratalinker UV crosslinker (Stratagene, La Jolla, CA), or 5 mM sodium azide for 5 min.

Fluorescence microscopy and nuclear stress body assessment. Confocal images were obtained using a Zeiss Axiovert 200M inverted confocal microscope (Jena, Germany) and a Zeiss LSM 700 laser scanning microscope (Jena, Germany). Animals were picked free of bacteria and anesthetized with 10 mM levamisole. Nuclear stress body formation was quantified by assessing for the presence of nuclear foci containing HSF-1::GFP. The heat shock conditions for nuclear stress body assessment was 5 mins in a 33°C water bath on plates wrapped in parafilm. After anesthetizing and placing the cover slip on top of the worms, they were imaged within 10-15 mins to avoid the formation of nuclear stress bodies which may be due to hypoxia or other cytotoxic stress. Quantification was

performed in GraphPad Prism (GraphPad Software, www.graphpad.com). A minimum of eight individual animals ($n > 8$) were imaged per stress condition.

Brood Size Analysis. Animals were grown on gene-selected RNAi plates until L4 and then individual worms were transferred to 6-well plates. Parental worms were transferred to fresh plates daily for 6 days and total live offspring were counted per worm. Brood assay data reflects three biologically independent trials with 4-6 replicate animals per condition. Significance was determined by conducting a One-Way ANOVA using GraphPad Prism (GraphPad Software, www.graphpad.com) followed by a Tukey post-hoc test comparisons of all columns.

Lifespan Analysis. Worms were grown on gene-selected RNAi plates and transferred to fresh RNAi plates every other day starting on day 3 of adulthood to avoid progeny contamination. Worms were considered alive if they physically responded to a gentle touch with a metal worm pick. Animals that were observed to display hatched offspring within the parental worm (bag of worms) or that underwent intestinal expulsion were censured. Longevity assay data reflects three biologically independent trials with approximately 30-80 individual replicate lifespans recorded per trial per condition. Deaths over time were recorded, plotted, and statistically analyzed as a survival curve using GraphPad Prism (GraphPad Software, www.graphpad.com).

Thermotolerance analysis. Thermotolerance was tested by exposing L4 animals to 37°C for 2 hrs and then determining survival 24 hrs later by assessing response to a gentle touch. Data was plotted as the fraction alive using GraphPad Prism (GraphPad Software, www.graphpad.com), and was analyzed with a two tailed t-test. Thermotolerance assay data reflects three biologically independent trials with an approximate total of 100-175

individual animal's survival assessed per trial per condition. Significance was determined by conducting a One-Way ANOVA using GraphPad Prism (GraphPad Software, www.graphpad.com) followed by a Tukey post-hoc test comparisons of all columns.

qPCR analysis. Approximately 250-300 animals were grown on OP50-1 plates until L4 and then subjected to either a 1 hr HS at 33°C or left at 20°C. Following HS, all plates were washed twice with NGM buffer and worms were washed clean of bacteria before immediately being snap frozen at -80°C. Trizol was added to the frozen worm pellet prior to sonication for 10 cycles of 30 seconds on/off in a Bioruptor sonicator (Diagenode, Inc., Denville, NJ). RNA was extracted via Direct-Zol RNA Miniprep kit (Zymo Research, Irvine, CA) and reverse transcribed into cDNA via the High Capacity cDNA Reverse Transcription Kit (Thermo Fisher Scientific, Waltham, MA) according to manufacturer's instructions. Expression levels for *hsp-70* (C12C8.1) and *hsp-16.2* (Y46H3A.3) were analyzed via qPCR using the Step-One Plus Real-time PCR machine (Applied Biosystems, Waltham, MA) using the the $\Delta\Delta C_t$ method. The housekeeping gene *cdc-42* (R07G3.1) was used for normalization. qPCR analysis reflect three biologically replicate trials. Significance was determined by conducting a One-Way ANOVA using GraphPad Prism (GraphPad Software, www.graphpad.com) followed by a Tukey post-hoc test comparisons of all columns.

Primers used - *hsp-16.2* (Y46H3A.3) Fwd-ACGCCAATTTGCTCCAGTCT Rvs-TGATGGCAAACCTTTTGATCATTGT, *hsp-70* (C12C8.1) Fwd-TTCAATGGGAAGGACCTCAACT Rvs-GGCTGCACCAAAGGCTACTG, *cdc-42* (R07G3.1) Fwd-CTTCTGAGTATGTGCCGACAGTCT Rvs-GGCTCGCCACCGATCAT

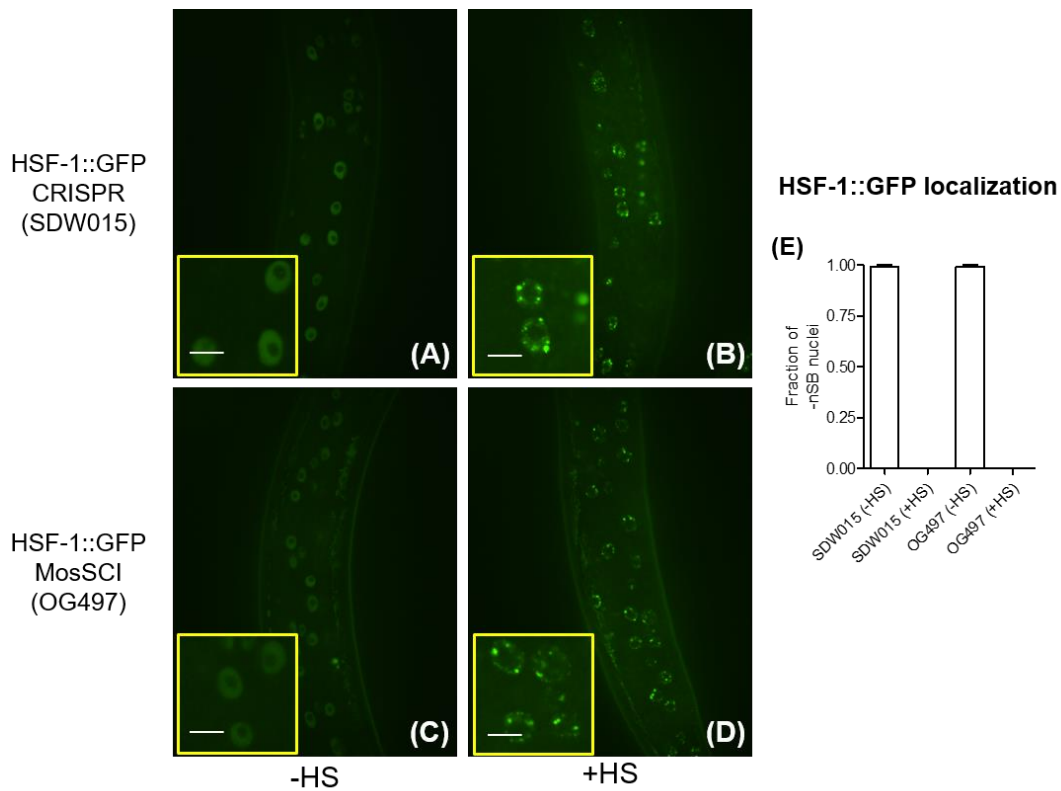
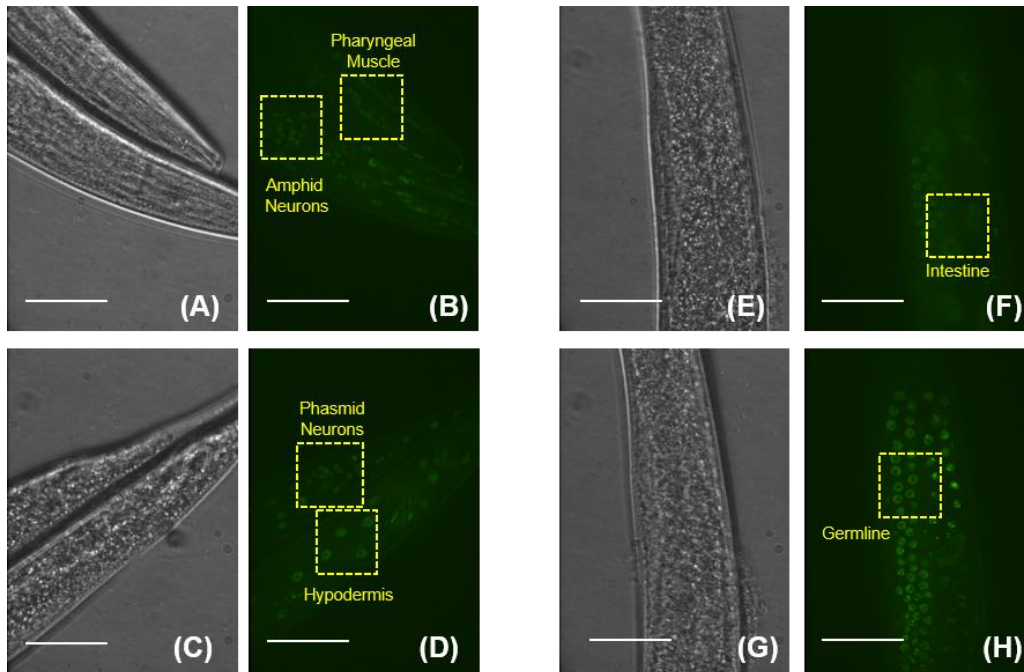


Figure 2.1 – The *C. elegans* HSF-1::GFP CRISPR model shows that HSF-1::GFP forms nuclear stress bodies (nSBs) in hypodermal cells in response to heat shock. (A-B) Expression of HSF-1::GFP from the HSF-1::GFP CRISPR strain (SDW015) was analyzed by fluorescence microscopy with and without heat shock (HS) for 5 min at 33°C. Without heat shock, HSF-1::GFP exhibits a diffuse nuclear pattern in the hypodermal cells examined. Upon heat shock, there is a redistribution of signal into nuclear stress bodies (nSBs). (C-D) Expression of HSF-1::GFP from an HSF-1::GFP MosSCI strain (OG497), with and without HS for 5 min at 33°C. This strain is shown as a comparison to the HSF-1::GFP CRISPR strain and displays similar results. (E) Hypodermal nuclei from SDW015 and OG497 were scored for the appearance of nSBs in A-D and the fraction of those containing no nSBs was calculated and plotted for $n \geq 8$ replicate worms. Scale bar within zoomed image insert represents 5 microns.



Magnified inserts

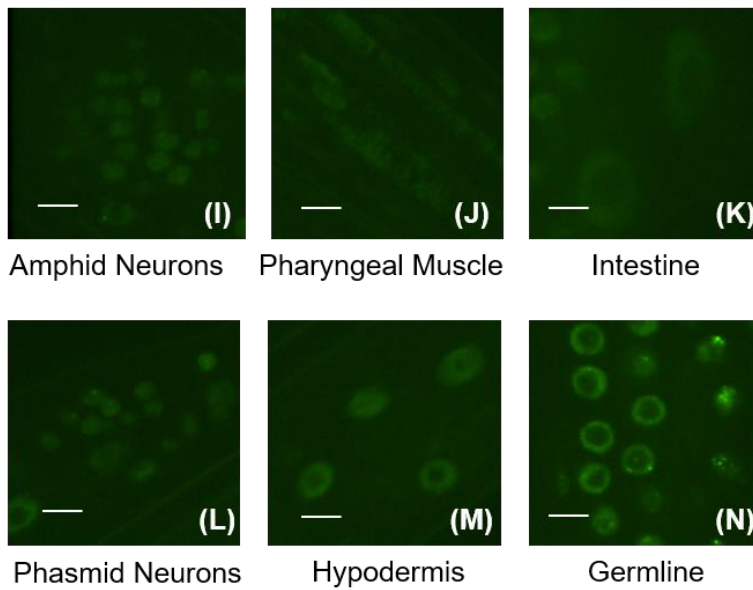


Figure 2.2 – HSF-1::GFP CRISPR is expressed in multiple cell types and forms spontaneous nuclear stress bodies in some oocytes. HSF-1::GFP from strain SDW015 shows nuclear expression in the amphid neurons (A/I), pharyngeal muscle (A/J), intestine (F/K), phasmid neurons (D/L), hypodermis (D/M) and germline (H/N), as indicated. Scale bar in (A-H) represents 45 microns. Scale bar in (I-N) represents 5 microns.

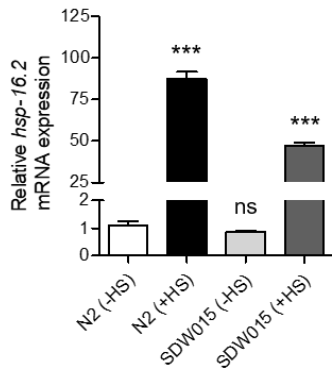
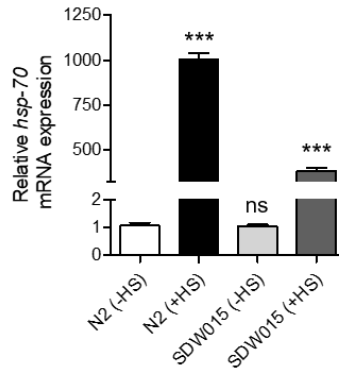
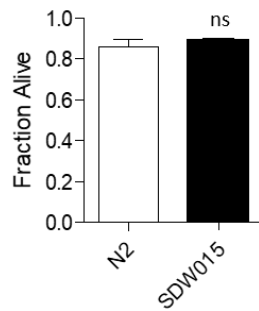
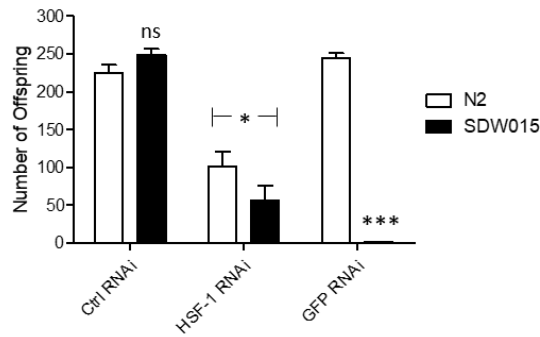
(A) *hsp-16.2* mRNA expression**(B) *hsp-70* mRNA expression****(C) Thermotolerance****(D) Brood size**

Figure 2.3 – The *C. elegans* HSF-1::GFP CRISPR model shows that HSF-1::GFP provides thermotolerance, allows the induction of *hsp* mRNA upon heat shock, and does not alter thermotolerance or brood size. (A-B) N2 (wildtype) and SDW015 (HSF-1::GFP CRISPR) animals at the L4/YA stage were subjected to a 1 hour HS at 33°C followed by immediate RNA extraction for qRT-PCR analysis of *hsp-16.2* and *hsp-70* (c12C8.1) expression. Three independent biological replicates were assessed in technical triplicate using the $\Delta\Delta C_t$ analysis method. *** p-value < 0.0001. For significance, all samples are compared to N2 (-HS). (C) Survival of N2 (wildtype) and SDW015 (HSF-1::GFP CRISPR) worm strains after being subjected to 37°C for 2 hours. Survival was assessed 24 hours post heat shock via response to gentle touch with a platinum wire. 150 worms were used for each experiment in three independent biological replicates. Results were analyzed using a two-tailed t-test. The difference between the two results was not statistically significant, with a p-value of 0.39. (D) RNAi targeting HSF-1::GFP alters brood size. N2 (wildtype) and SDW015 (HSF-1::GFP CRISPR) animals were grown on empty L4440 RNAi feeding vector (Control), HSF-1, or GFP RNAi starting from L1. Total brood size of N2 (wildtype) and SDW015 (HSF-1::GFP CRISPR) animals was determined by assessing live hatched offspring measured during the first five days of adulthood. Eighteen worms were used for each experiment in three independent biological replicates. For significance, all samples are compared to N2 (Ctrl RNAi) unless otherwise indicated with brackets.

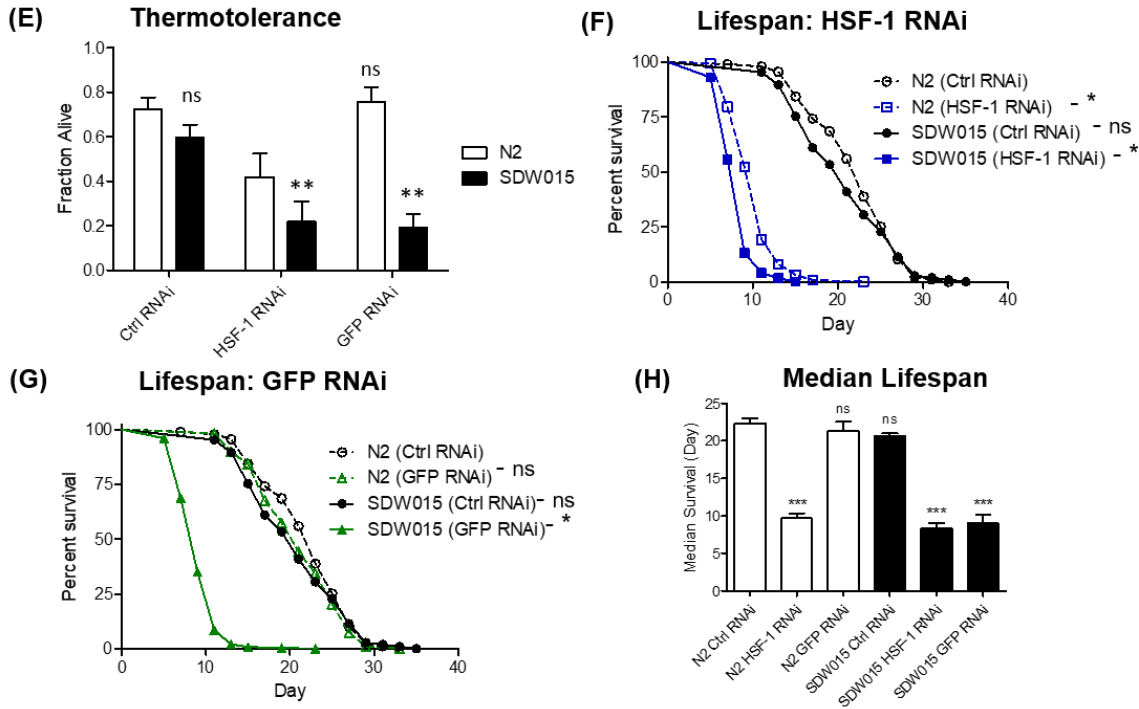


Figure 2.4 - The *C. elegans* HSF-1::GFP CRISPR model shows that HSF-1::GFP does not alter thermotolerance or lifespan. (E) RNAi targeting HSF-1::GFP inhibits thermotolerance. N2 (wildtype) and SDW015 (HSF-1::GFP CRISPR) animals were grown on empty L4440 RNAi feeding vector (EV), HSF-1, or GFP RNAi starting from L1. Thermotolerance was conducted by exposure to 37°C for 2 hours at the L4/YA stage and assessing for survival 24 hours later. Animals were considered alive if they responded to a gentle touch via a platinum wire. 150 worms were used for each experiment in three independent biological replicates. For significance, all samples are compared to N2 (Ctrl RNAi). (F) *hsf-1* RNAi inhibits lifespan in N2 and in HSF-1::GFP CRISPR animals. N2 (wildtype) and SDW015 (HSF-1::GFP CRISPR) animals were grown on empty L4440 RNAi feeding vector (EV) or *hsf-1* RNAi starting from L1 and measured for live/dead every other day starting at day 5 of adulthood. Worms were considered alive if they responded to a gentle touch via worm pick. Greater than 120 worms were used for each experiment, in three biological replicates. For significance, all samples are compared to N2 (Ctrl RNAi). (G) GFP RNAi inhibits lifespan in HSF-1::GFP CRISPR animals. N2 (wildtype) and SDW015 (HSF-1::GFP CRISPR) animals were grown on empty L4440 RNAi feeding vector (EV) or GFP RNAi starting from L1 and measured for live/dead every other day starting at day 5 of adulthood. Worms were considered alive if they responded to a gentle touch via worm pick. Greater than 120 worms were used for each experiment, in three biological replicates. For significance, all samples are compared to N2 (Ctrl RNAi). (H) Median survival for figures F/G plotted as bar graph. For significance, all conditions were compared to N2 (Ctrl RNAi). Significance was determined by conducting a One-Way ANOVA followed by a Tukey post-hoc test comparisons of all columns (D-E,H) or survival curve analysis (F-G) in GraphPad Prism. Significance is indicated by * p-value<0.05. "ns": not significant.

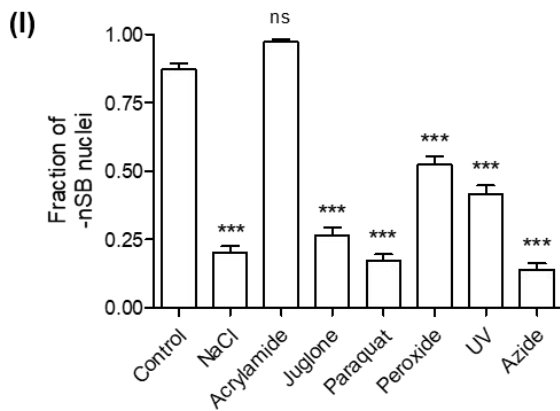
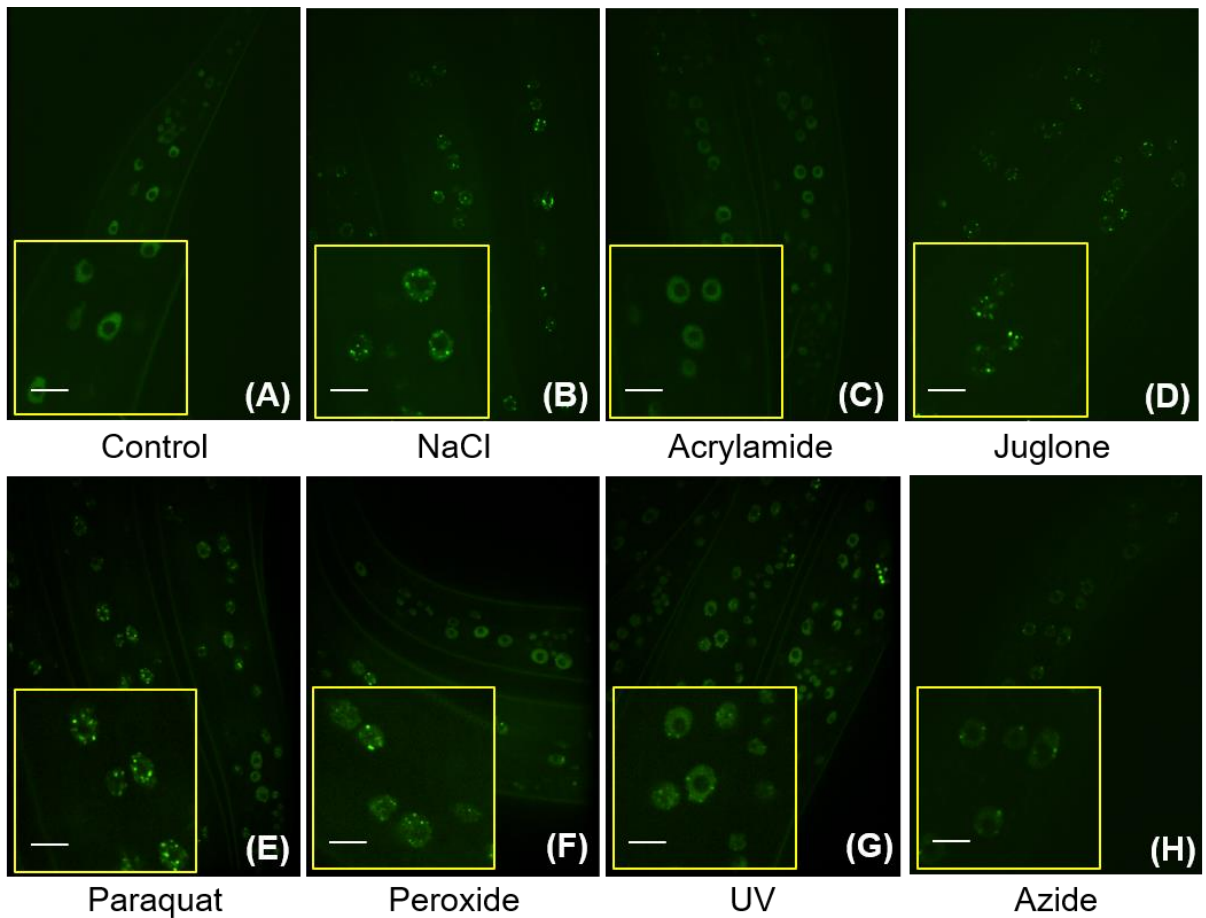


Figure 2.5 – Confocal fluorescence images show the formation of HSF-1::GFP nSBs in response to multiple cytotoxic stressors. (A-H) SDW015 animals at the L4/YA stage were exposed to control conditions (A), sodium chloride at 600 mM for 30 mins (B), acrylamide at 7 mM (C), juglone at 38 μ M for 30 mins (D), paraquat at 5 mM for 2 hrs (E), peroxide at 7.5 mM for 2 hrs (F), UV radiation at 300 J/cm² (G), or azide at 5 mM for 5 mins (H), and then assessed for the presence of nSBs in hypodermal nuclei as previously described. Confocal images are zoomed-in images of those in Figure S4. (I) Hypodermal nuclei were scored for the appearance of HSF-1::GFP nSBs and the fraction of cells displaying no nSBs (-nSBs) in conditions A-H was calculated and plotted for n \geq 8 replicate worms. For significance, A One-Way ANOVA was performed with Tukey Post-Hoc test of all comparisons. For indicated significance, all conditions were compared to control. *** p-value < 0.0001. Scale bar within zoomed image represents 5 microns.

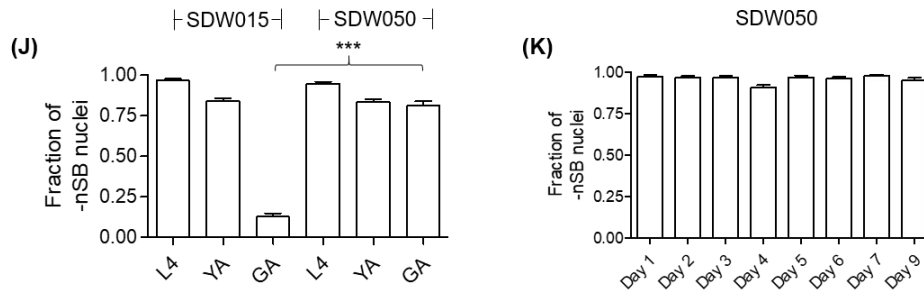
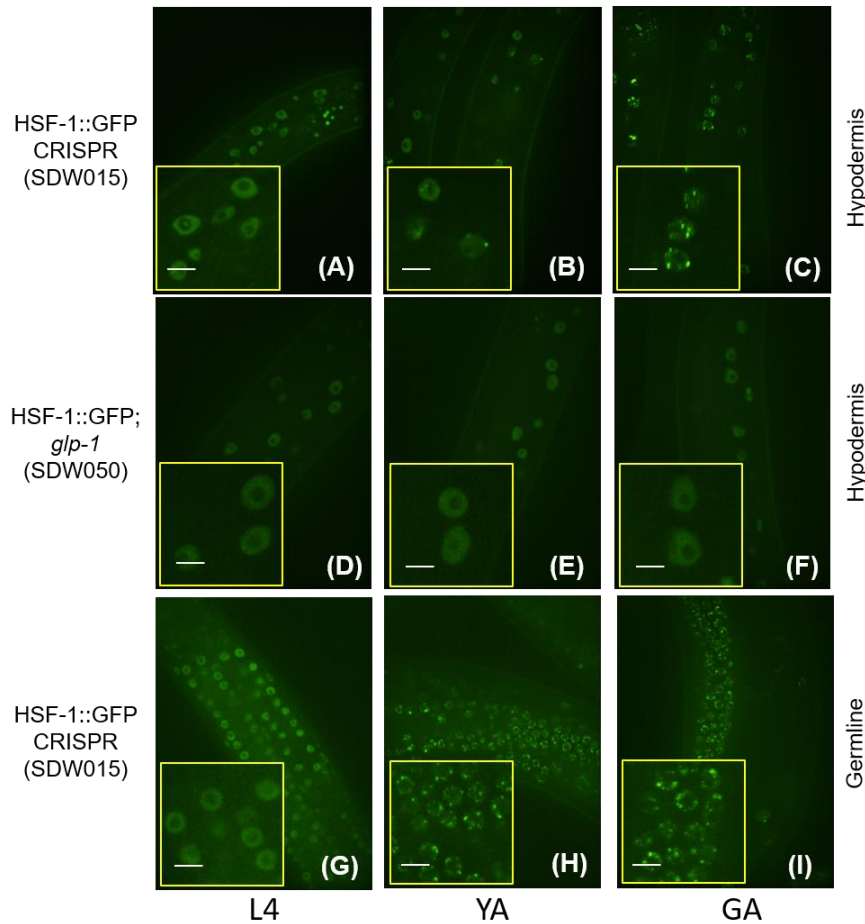


Figure 2.6 – HSF-1::GFP forms nSBs upon transition to adulthood in hypodermal cells and germline cells, an effect that is suppressed by genetic loss of the germline. (A-C) Confocal fluorescence images of HSF-1::GFP CRISPR worms (SDW015) show expression of HSF-1::GFP in hypodermal cell nuclei during the transition to adulthood in *C. elegans*. The formation of nSBs occurs in hypodermal cell nuclei within a 24 hr window between the L4 stage (0 hr) to young adulthood (YA) (~4-6 hrs post L4), and gravid adulthood (GA) (24 hrs post L4). (D-F) Confocal fluorescence images show that the formation of nSBs upon transition to adulthood is suppressed in HSF-1::GFP CRISPR animals carrying the *glp-1* (e2144) mutation strain name (SDW050). (G-I) Confocal fluorescence images show the robust formation of nSBs upon the transition to adulthood throughout the germline. (J) Hypodermal nuclei from HSF-1::GFP (SDW015) or HSF-1::GFP; *glp-1*(e2144) (SDW050) animals at the last larval stage (L4), young adult (YA), or gravid adult (GA) were scored for the appearance of HSF-1::GFP nSBs and the fraction of cells displaying no nSBs (-nSBs) was calculated and plotted in GraphPad Prism for $n \geq 8$ replicate worms from images (A-F). Significance indicated compares the gravid adult condition of HSF-1::GFP (SDW015) to the gravid adult condition of HSF-1::GFP; *glp-1*(e2144) (SDW050), *** indicates $p < 0.0001$. (K) HSF-1::GFP; *glp-1* (e2144) (SDW050) animals were grown to the 9th day of adulthood on OP50-1 plates and hypodermal nuclei were scored for the appearance of HSF-1::GFP nSBs and the fraction of cells displaying no nSBs (-nSBs) was calculated and plotted in GraphPad Prism for $n \geq 8$ replicate worms per timepoint. Scale bar in zoomed in images represents 5 microns.

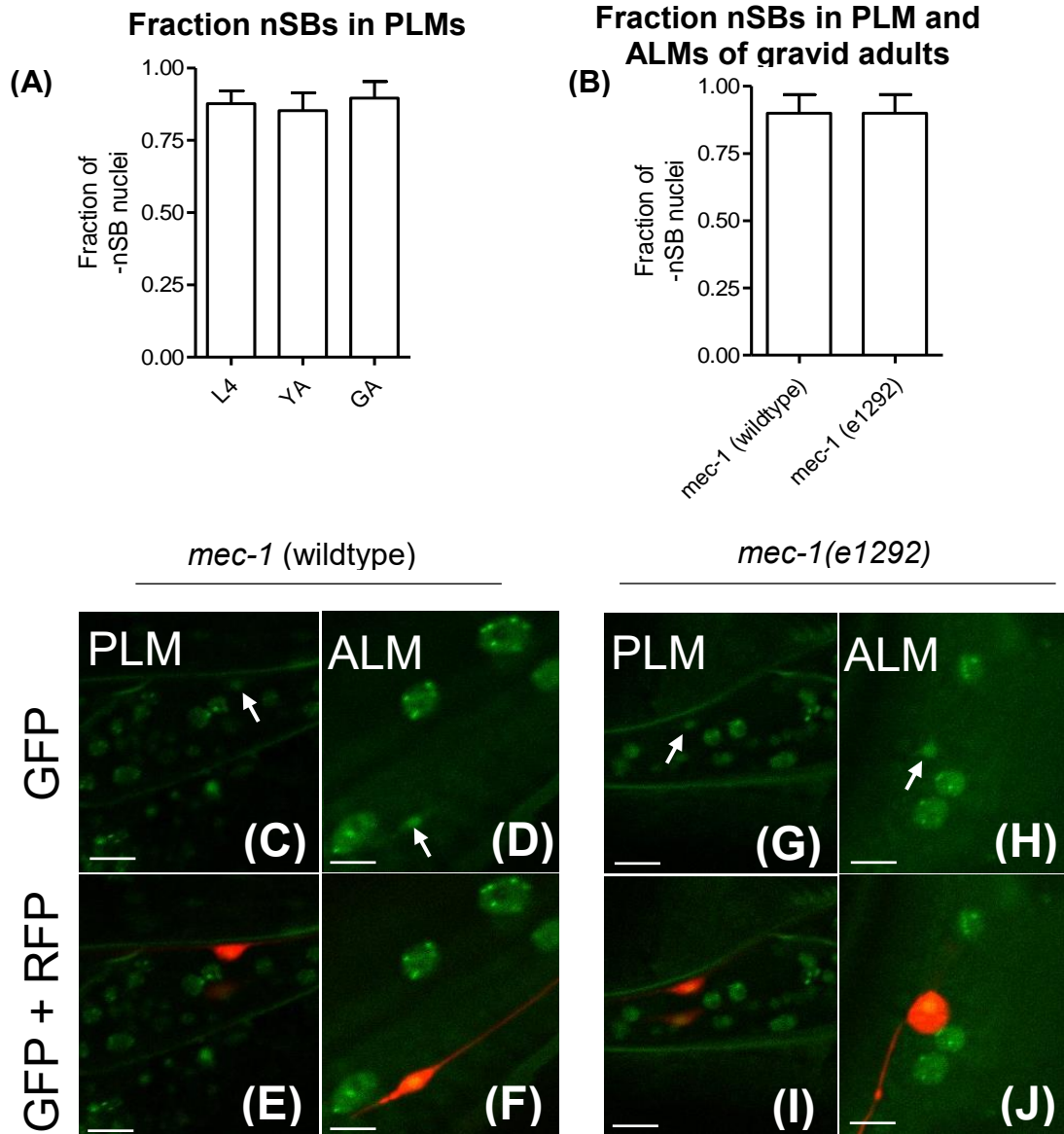


Figure 2.7 – The transition to adulthood does not induce the localization of HSF-1::GFP into nuclear stress bodies in Touch Receptor Neurons (TRNs) PLM and ALM neurons, an effect that is independent of neuronal ensheathment. The Touch Receptor Neuron (TRN) co-marker *p_{mec-17}::RFP* was genetically crossed into HSF-1::GFP CRISPR (SDW015) to generate HSF-1::GFP CRISPR; *p_{mec-17}::RFP* (SDW077). (A) For each age, $n \geq 28$ replicate animals of HSF-1::GFP CRISPR; *p_{mec-17}::RFP* (SDW077) were examined and scored for the appearance of HSF-1::GFP nSBs within the PLM neuron at the L4 stage, young adult (YA), and gravid adult (GA) and the fraction of cells displaying no nSBs (-nSBs) was calculated and plotted in GraphPad Prism. (B) SDW077 animals carrying the wildtype sequence variant of *mec-1* or genetically crossed to the ensheathment defective *mec-1* (e1292) were grown to gravid adulthood (24 hours post L4) and scored for the appearance of HSF-1::GFP nSBs within the PLM and ALM neurons and the fraction of cells displaying no nSBs (-nSBs) was calculated and plotted in GraphPad Prism for $n=20$ replicate individuals. (C-J) Confocal images of PLM and ALM neurons as graphed in (B) scale bar represents 5 microns.

Chapter 3

Regulation of the Heat Shock Response by NuRF subunit *pyp-1*

Abstract

The transcription factor Heat Shock Factor 1 (HSF-1) regulates the heat shock response (HSR), a highly conserved cytoprotective pathway induced by proteotoxic stress. The HSR has been shown to be epigenetically regulated in early adulthood leading to a collapse in proteostasis and loss of robust induction of chaperones. We performed a targeted RNAi screen of chromatin remodeling factors and identify *pyp-1*, a Nucleosome Remodeling Complex Factor (NuRF), as a negative regulator of the HSR. Reduction of *pyp-1* activity was shown to lead to increased proteostasis as measured through a metastable protein assay and suppression of Amyloid Beta toxicity. *pyp-1* also required for appropriate brood size, growth, lipid accumulation, but not longevity. Interestingly, we find that in order for *pyp-1* to act as a negative regulator gene suppression is required to be initiated during larval development. Negative regulation was also specific to *pyp-1* as knockdown of other NuRF complex members did not alter HSR reporter activity. Our results show that a specific member of the NuRF complex negatively regulates the HSR which can improve proteostasis in *C. elegans*.

Introduction

The Heat Shock Response (HSR) is a highly conserved stress pathway that responds to the increased presence of unfolded or misfolded proteins. In response to this disruption in protein homeostasis (proteostasis) the major transcriptional regulator of the HSR Heat Shock Factor 1 (HSF-1) increases the expression of molecular chaperones known as heat shock proteins (HSPs) [164]. These HSPs serve to assist in the folding of proteins to maintain their functional state [3, 165-169]. Experimental evidence across metazoans suggests that increases in HSR activity is associated with increased stress resistance, longevity, and healthspan [57, 63, 170]. Recent evidence suggests that the HSR undergoes an abrupt decline in activity early in adulthood in *C. elegans* which is regulated by decreased chromatin access of HSF-1 to target gene loci [61]. As worms molt from their last larval stage (L4) to adulthood they lose the ability to mount a robust induction of HSPs within six to eight hours post the L4 molt. However, a complete understanding of how chromatin remodeling pathways regulates this sharp temporal window is lacking.

To address this, we performed an unbiased RNAi screen of annotated and predicted chromatin remodeling factors to identify targets that may regulate the HSR across the transition to adulthood. Of the genes assessed we found a component of the Nucleosome Remodeling Factor (NuRF) complex able to induce HSR transcriptional GFP reporters in the absence of applied thermal stress. The NuRF complex is most well studied in *Drosophila* which has identified it as a critical pathway that serves to regulate transcription [171]. NuRF consists of four members including an ISWI ATPase that facilitates chromatin remodeling by nucleosome sliding after binding to histones [172-

176]. Outside of *Drosophila*, NuRF has also been identified to regulate cellular differentiation and maturation [177].

From our subscreen, we find that *pyp-1*, an inorganic pyrophosphatase, is a negative regulator of the HSR which when knocked down can alter brood size, growth rate and lipids content. Furthermore, *pyp-1* knockdown can enhance proteostasis as measured via a metastable protein folding assay and in Alzheimer's Disease model animals by suppression of Amyloid Beta toxicity and both effects are dependent on HSF-1. Interestingly, we find that the negative regulation effects of *pyp-1* knockdown appear to be linked to initiation of RNAi before adulthood.

Materials and Methods

C. elegans strains. *C. elegans* strains were grown and maintained at 20°C unless otherwise noted [48]. Strains used in this study: wildtype Bristol N2, TJ375 [*gpls1* (*phsp-16.2::GFP*)], AM446 [(*pC12C8.1::GFP*; *pRF4* (*rol-6*)], HE250 [*unc-52*(*e669su250*) II], AM140 [*rmls132* [*punc-54::Q35::YFP*], CL2006 [*dvl2* (*pCL12*(*unc-54*/human Abeta peptide 1-42 minigene)) + *pRF4*]. Age synchronization was accomplished by standard hypochlorite treatment.

RNA interference. To perform RNAi animals were fed HT115(DE3) *E. coli* that are engineered to transcribe double-stranded RNA (dsRNA) [50, 163, 178]. Clones were obtained from the Ahringer RNAi feeding library (Geneservice, Cambridge, United Kingdom) and individual RNAi clones were obtained and sequenced verified prior to use. To induce dsRNA production NGM plates were supplemented with 0.2% β -lactose [179]. RNAi was initiated at the L1 stage unless otherwise indicated.

Fluorescence analysis. TJ375 and AM446 Animals were grown to the indicated timepoints and anesthetized by picking individual worms to a drop of 10 mM levamisole on 1% agarose pads and then covered with a cover slip. Slides were imaged on an EVOS Fluorescence microscope. Fluorescent images analyzed using ImageJ (NIH) to quantify fluorescent intensity [180].

Thrashing analysis. HE250 animals were fed HT113(DE3) E. coli containing plasmids targeting *pyp-1*, *hsf-1*, or non-targeting empty vector control. Dual *pyp-1/hsf-1* conditions were prepared by mixing overnight cultures of *pyp-1* and *hsf-1* RNAi in equal parts at equal density. Animals were grown at 20°C until day 2 of adulthood and then shifted to 25°C for 24 hours and then thrashing was assayed. Animals were scored as number of body bends per 30 seconds floating in a drop of NGM buffer.

Amyloid Beta paralysis CL2006 animals were fed HT113(DE3) E. coli containing plasmids targeting *pyp-1*, *hsf-1*, or non-targeting empty vector control. Dual *pyp-1/hsf-1* conditions were prepared as described above. Animals were grown until Day 6-10 of adulthood and then assayed for paralysis. Animals that can twitch the pharynx but are non-motile upon gentle stimulation with a platinum wire were scored as paralyzed while motile animals were scored as non-paralyzed. Animals were picked to fresh plates as needed to avoid progeny contamination.

Lifespan/Worm length/Brood analysis. N2 wildtype animals were fed HT113(DE3) E. coli containing plasmids targeting *pyp-1*, *hsf-1*, or non-targeting empty vector control. Dual *pyp-1/hsf-1* conditions were prepared as described above. Lifespan analysis: Animals were picked to fresh plates as needed to avoid progeny contamination. Animals were scored as alive if they responded to gentle stimulation with a platinum wire or dead

if there was no response. Animals that formed a “bag of worms” phenotype or protruded intestines were scored as censured. Worm length: Brightfield images of animals were taken with an EVOS FL microscope and worm length was calculated utilizing ImageJ to trace the length of the worm as measured from the tip of the pharynx to tail following the midline of the animal. Brood size measurements: At the L4 stage individual animals were isolated to one well of a 6-well RNAi plate and picked every day for 5 days to fresh plates. Hatched offspring were counted two days after the parental worms were moved to fresh plates.

Oil Red O staining- Staining was performed as previously described [181]. Briefly, on the day of staining working stocks were prepared by a 3:2 dilution of 5 mg/ml Oil Red O (ORO) from 100% isopropanol to 60% isopropanol and filtered. Worms were washed free of bacteria and worms were fixed using 40% isopropanol for 3 minutes with rotation. Working stock of ORO was added to each sample and left rotating at RT for 2 hours. Worms were then washed free of ORO and placed onto a 1% agarose pad on a glass slide and covered with a cover slip for imaging.

pyp-1 isoform RNAi – To generate isoform specific RNAi clones of *pyp-1* genetic sequences unique to *pyp-1* isoform A, C, or D were amplified according to the appendix figure B1 utilizing the primers listed in appendix table B1. Those PCR products were cloned into L4440 gtwy following standard Gateway Cloning technology BP reactions. All clones generated for *pyp-1A* RNAi, *pyp-1C* RNAi, and *pyp-1D* RNAi were fully sequenced verified. TJ375 animals were then fed the isoform specific RNAi including the original Ahringer library clone of *pyp-1* used previously.

Liquid RNAi. Inoculate RNAi cultures in 96 deep well plates overnight at 37°C and then induced to produce dsRNA by adding 4 mM of IPTG and shaking for 1 hour at 37°C. Cultures were then pelleted and resuspended with 100 microliters of NGM/Carbenicillin (25 µg/ml)/IPTG (5 mM) buffer. In a 96 well plate 20 microliters of TJ375 L1 worms in liquid were added to each well and 30 microliters of the resuspended RNAi cultures were added to each well. Plates were sealed with breathable tape, placed in a humidified sealed box, and set on a rotating platform at 20°C. Worms were grown to day 1 and day 3 of adulthood and then manually screened for brightness of the GFP reporter.

Results

***pyp-1* acts as a specific negative transcriptional regulator on the HSR**

After performing our targeted RNAi subscreen we identified *pyp-1* as a candidate negative regulator of the HSR (Supplemental figure 3.1). We confirmed this hit by measuring the effect of *pyp-1* knockdown in two transcriptional reporters of the HSR. These animals have integrated HSF-1 regulated gene promoters driving the expression of GFP which have already been characterized. We observe that *pyp-1* knockdown in both reporters induce a GFP signal (Figure - 3.1 A/B). Interestingly, we observe that the reporter signal is only apparent in the adult stages (Day 3) which is indicated as two days post the last larval stage L4. Importantly, this signal is also dependent on *hsf-1* as the dual knockdown of *pyp-1* and *hsf-1* abolishes the day 3 GFP expression. We confirmed this result using ImageJ analysis of the fluorescent images (Figure 3.2 A/B). The NuRF complex consists of four members in *Drosophila*. We were curious if the negative regulation we observed was due to a disruption of the entire NuRF complex or

pyp-1 acting independently. To test this, we performed RNAi of the *C. elegans* homologs of the other complex members utilizing the HSR transcriptional reporter used in previous experiments. We find that no other members are able recapitulate an increase in GFP signals as *pyp-1* did (Supplemental figure 3.2 A-E). Thus, *pyp-1* specifically appears to negatively regulate the HSR transcriptionally in adulthood rather than in larval development.

***pyp-1* regulates *C. elegans* growth and reproduction, but does not affect lifespan**

Next, we were interested in whether or not *pyp-1*'s regulation of the HSR affected worm healthspan. We first examined growth and found that *pyp-1* is required for normal growth into adulthood (Figure 3.3 A). We observed that during larval development *pyp-1* knockdown does not appear to cause any growth defects, but around after 48 hrs, when animals are transitioning into adulthood, they appear shorter in length than control RNAi animals. We next assessed reproduction by measuring the number of hatched live offspring during the first five days of adulthood. We found that *pyp-1* knockdown resulted in the failure of any live offspring (Figure 3.3 B/C). Lastly, we assessed lifespan by moving animals to fresh plates as needed recording deaths as failure to respond to touch. Interestingly, we observed no significant difference in longevity of worms after *pyp-1* RNAi (Figure 3.3 D). Taken together, these results suggest *pyp-1* is required for reproduction and appropriate maturation into adulthood, but does not regulate overall longevity.

***pyp-1* knockdown improves proteostasis in a metastable protein folding assay and suppresses Amyloid-beta induced paralysis.**

Because we observed an increase in the transcriptional activity of the HSR we hypothesized that this effect may be able to improve proteostasis in the worm. To address this, we utilized a mutation in *unc-52* that confers a metastable protein that induces paralysis in at the non-permissible temperature of 25C. We observed that *pyp-1* knockdown can increase motility as measured by increased body bends of swimming worms which was dependent on *hsf-1* (Figure 3.4 A). Next, we utilized Alzheimer's Disease model worms that express amyloid beta in body wall muscle that leads to age-related paralysis. We observed that *pyp-1* RNAi is able to suppress this paralysis relative to control animals and that this effect was dependent on *hsf-1* (Figure 3.4 B). Thus, *pyp-1* knockdown is able to increase proteostasis as measured in a metastable protein folding assay and amyloid-beta toxicity.

Late *pyp-1* RNAi initiation is not sufficient to induce negative regulation of the HSR and knockdown of isoform *pyp-1C* is required.

Because there was no change in longevity we were curious if initiating RNAi later would be able to induce the negative regulation we observed previously. We devised a different RNAi paradigm that will expose animals to the same length of time on RNAi from hatching in previous experiments, but now initiate it after two days of growing on control RNAi (Figure 3.5 A). This is within the period when animals would transition into adulthood and where we observed the beginning of previous *pyp-1* effects manifesting such as growth dysregulation. Interestingly, we did not observe an increase in the GFP signal from our transcriptional reporters (Figure 3.5 B). From this result, we suggest that

pyp-1's negative regulation on the HSR may require knockdown within larval development. PYP-1 has three protein isoforms reported via Wormbase. We were interested to determine which, if any, may be responsible for the negative regulation of the HSR we have observed thus far. We devised an approach to knockdown each isoform by utilizing unique exonic sequence for each isoform where possible and place it into the standard RNAi feeding vector L4440. As a control, we also utilized the original *pyp-1* RNAi clone obtained from the Ahringer RNAi library used in previous experiments. After performing knockdown from hatching again, we found that knockdown of *pyp-1a* and *pyp-1c* were insufficient to induce any GFP signal, but we were able to recapitulate the effects of *pyp-1* RNAi with our *pyp-1d* clone (Figure 3.5 C). From these results we suggest that PYP-1D may be the isoform required to suppress to induce negative regulation of the HSR.

***pyp-1* RNAi negatively regulates lipid staining**

During our experiments we observed that *pyp-1* RNAi appeared to result in adults that varied in their overall pigmentation compared to control which we hypothesized may be a change in lipid content. To assess lipid content we employed Oil Red O staining which is known to stain all lipid droplets contained in the cell. We performed RNAi from hatching and then analyzed total lipid content on day 3 of adulthood and found that *pyp-1* RNAi resulted in less lipid content compared to control RNAi (Figure 3.6 A/B). This may indicate that *pyp-1* regulates lipid metabolism in *C. elegans*.

Discussion

Our data suggests that *pyp-1* acts as a negative regulator of the HSR, but can only do so if suppressed early in life. From our RNAi screen we show that *pyp-1* regulates the HSR, but of all the candidates tested it was the only one that showed an effect in non-stress conditions. Further, there appeared to be no effect of *pyp-1* knockdown at day one (L4/YA) of the screen which is just prior to adulthood. Our data confirm this negative regulation as another previous study also identified it as a negative regulator. Importantly, in that study RNAi knockdown was initiated after one day of feeding on control RNAi before being assessed in adulthood 2.5 days later. Taken together, we suggest that these two studies indicate in order to obtain *pyp-1*'s effect on the HSR it must be suppressed prior to the transition to adulthood.

We show that *pyp-1* knockdown completely eliminates reproduction in *C. elegans*, but interestingly this does not lead to an increase in longevity. In *C. elegans* cells within the germline are unique stem cells that have distinct regions which remain mitotic before completing meiosis prior to fertilization [182]. Previous research on the NuRF complex indicates that it regulates stem cell maintenance in *Drosophila* [127]. Our data may indicate that by disrupting this complex via *pyp-1* RNAi we may be compromising germ cell division possibly resulting in poor cell viability. Additionally, previous literature suggests that there is a trade off between reproductive effort and healthspan in *C. elegans*. Manipulations such as laser ablation of the precursor germ cells or other mutations that reduce reproduction typically result in increased longevity of the animal [91]. Our data suggests that *pyp-1* may be an exception to this general aging phenomena described in *C. elegans*. Nevertheless, the negative regulation observed is

not merely an artifact of a reporter system. We observe benefits to proteostasis in metastable protein folding and a neurodegenerative disease model animal both of which require *hsf-1*. Activation of *hsf-1* is a stepwise ordered process which is tightly regulated at the transcriptional, post-translational level, and via protein-protein interactions from target gene HSPs most notably HSP90/HSP70 [183]. Understanding how *pyp-1* knockdown leads to higher *hsf-1* activity will be important to reveal how the NuRF complex affects proteostasis in *C. elegans*. We performed one preliminary experiment to suggest a mechanism in this regard by measuring the abundance of lipids with and without *pyp-1* knockdown. Since we observed a modest, but statistically significant decrease in lipid droplets we propose a dysregulation in fatty acid metabolism caused by *pyp-1* RNAi. Metabolic regulation of the HSR is generally not well understood as compared to its function in acute cytotoxic stress. Additionally, because we did not note any effect if *pyp-1* is suppressed post 48 hours of growth we suggest that this metabolic regulation is critical to the successful metabolic transition into adulthood. Thus, further study is warranted to understand how changes to lipid biology via the NuRF complex regulates proteostasis in *C. elegans*.

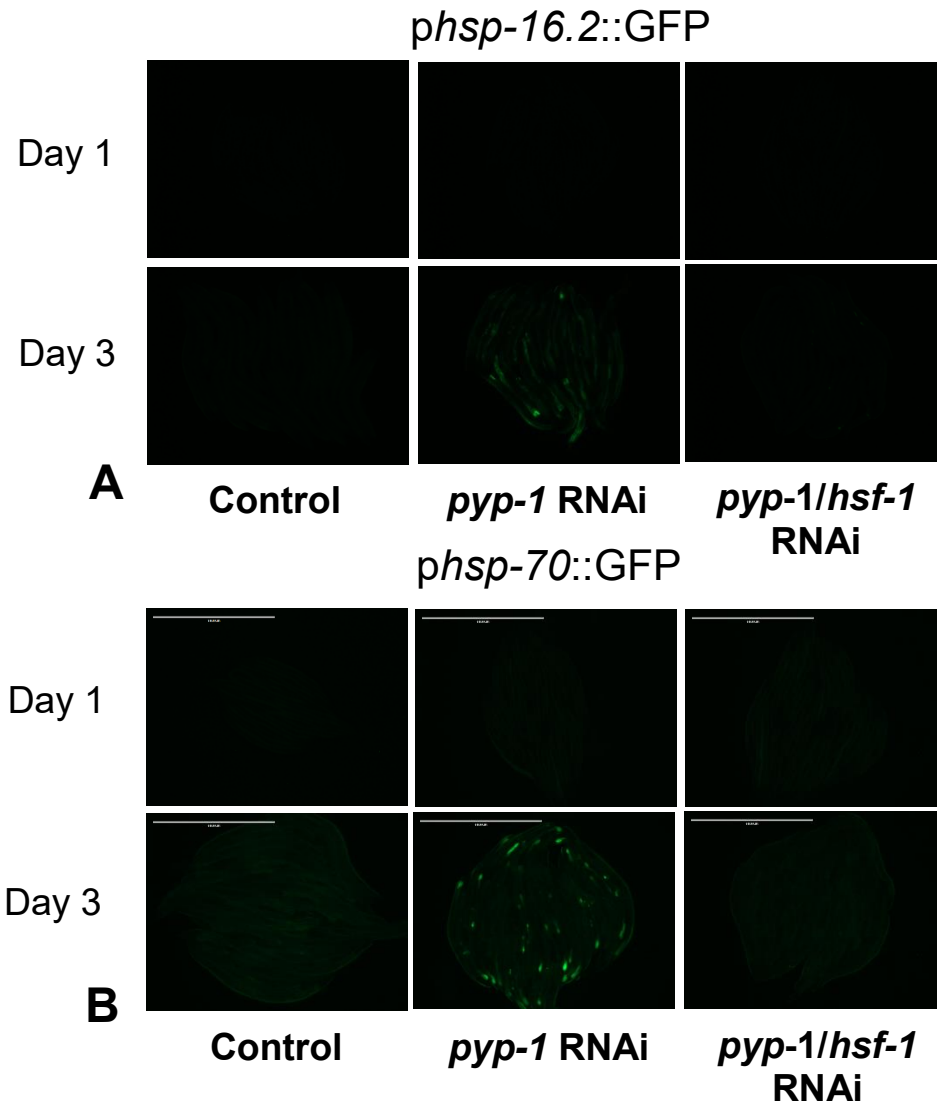


Figure 3.1 – Knockdown of *pyp-1* negatively regulates two HSR transcriptional reporters. (A) TJ375 (*phsp-16.2::GFP*) or (B) AM446 (*phsp-70::GFP*) animals were fed control, *pyp-1*, or *pyp-1/hsf-1* RNAis from hatching. At L4/YA (Day 1) or two days later (Day 3) worms were anesthetized using 10 mM Levamisole and mounted on agarose pads and imaged.

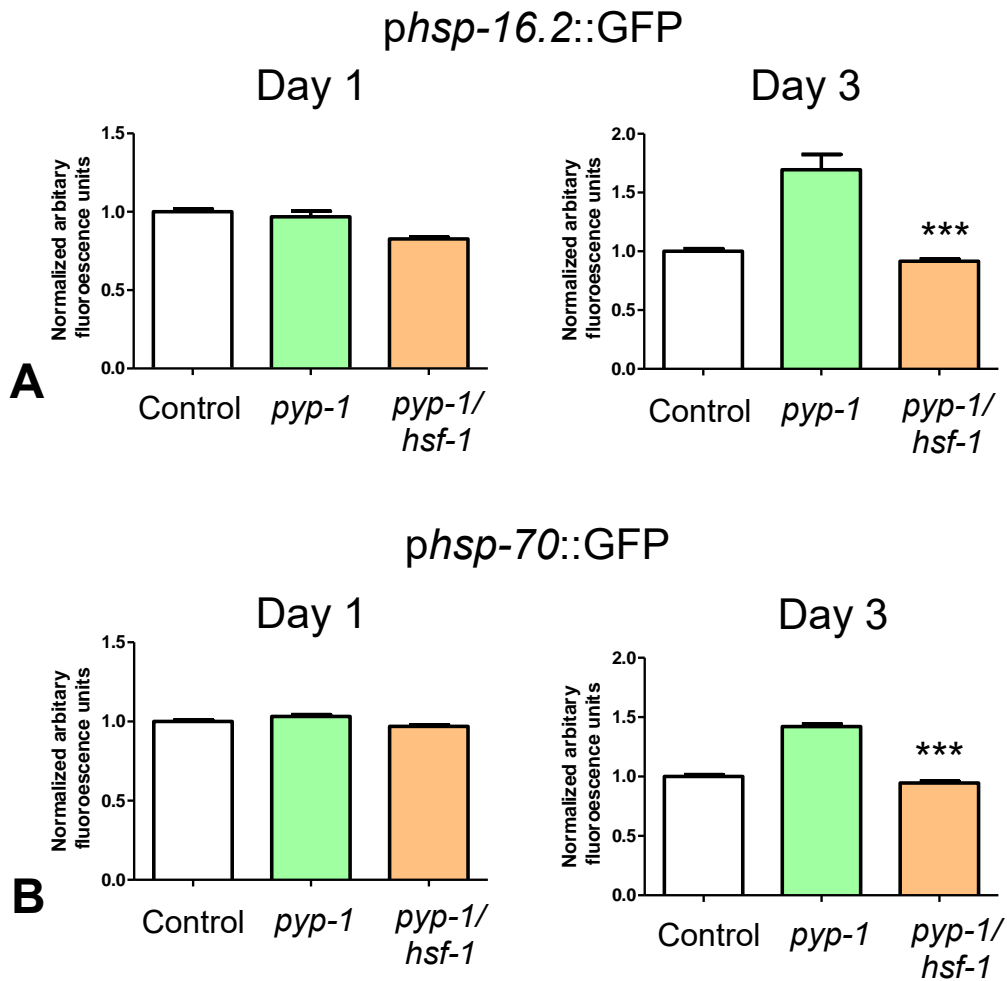


Figure 3.2 – Analysis of knockdown of *pyp-1* negatively regulates two HSR transcriptional reporters. (A) TJ375 (*phsp-16.2::GFP*) or (B) AM446 (*phsp-70::GFP*) animals were fed control, *pyp-1*, or *pyp-1/hsf-1* RNAis from hatching. At L4/YA (Day 1) or two days later (Day 3) worms were anesthetized using 10 mM Levamisole and mounted on agarose pads and imaged. Fluorescent images were analyzed using ImageJ and normalized to each days control RNAi sample and plotted using GraphPad Prism. Data was analyzed using a OneWay ANOVA. (***) indicates $p < 0.0001$

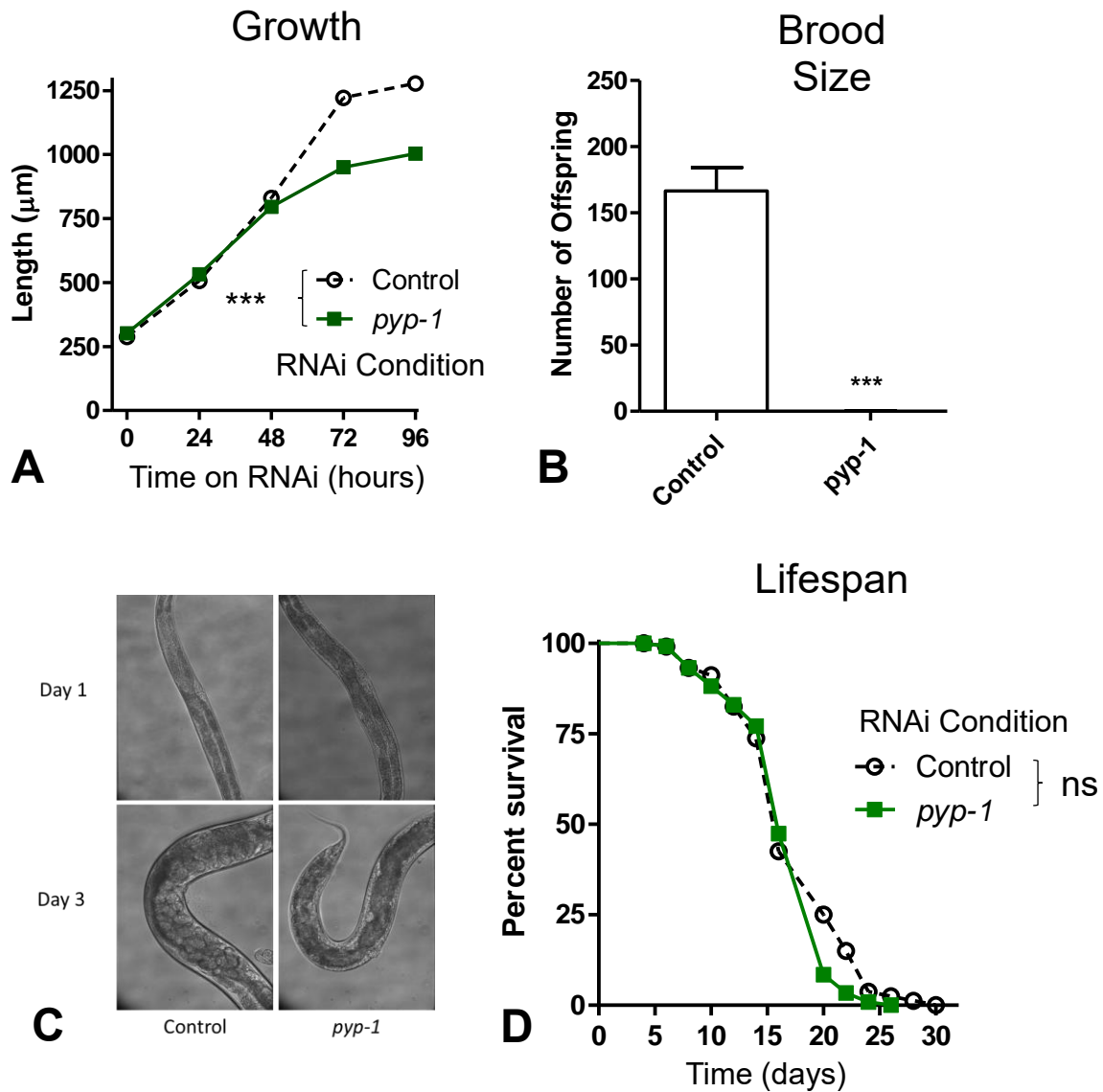


Figure 3.3 – *pyp-1* knockdown regulates growth and reproduction, but does not affect lifespan. (A) N2 worms were fed control or *pyp-1* knockdown from hatching and grown for four days. Worm lengths were measured along the midline and analyzed using GraphPad Prism. (***) indicates $p < 0.0001$. (B) N2 worms were fed control or *pyp-1* knockdown from hatching and moved to fresh plates as needed. Total live offspring was recorded as the number of offspring hatched for five total days post L4 then plotted and analyzed using GraphPad Prism (***) indicates $p < 0.0001$. (C) Brightfield images of N2 worms fed control or *pyp-1* knockdown from hatching either at L4 (Day 1) or two days later (Day 3). (D) N2 worms were fed control or *pyp-1* knockdown from hatching and moved to fresh plates as needed. Deaths were recorded as no response to gentle touch then plotted and analyzed using GraphPad Prism.

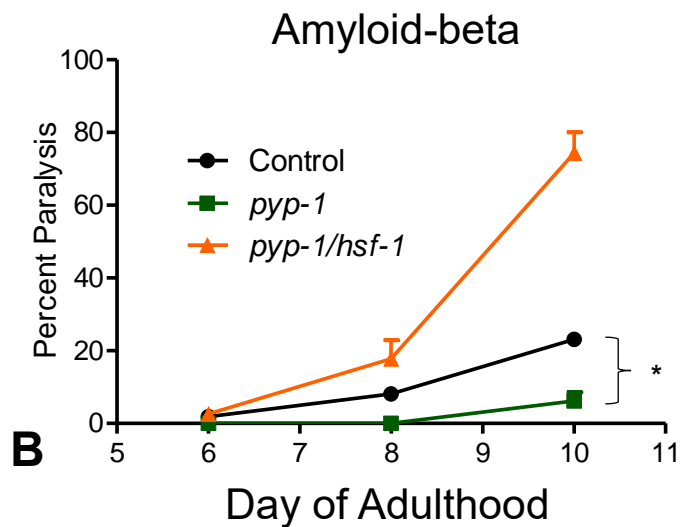
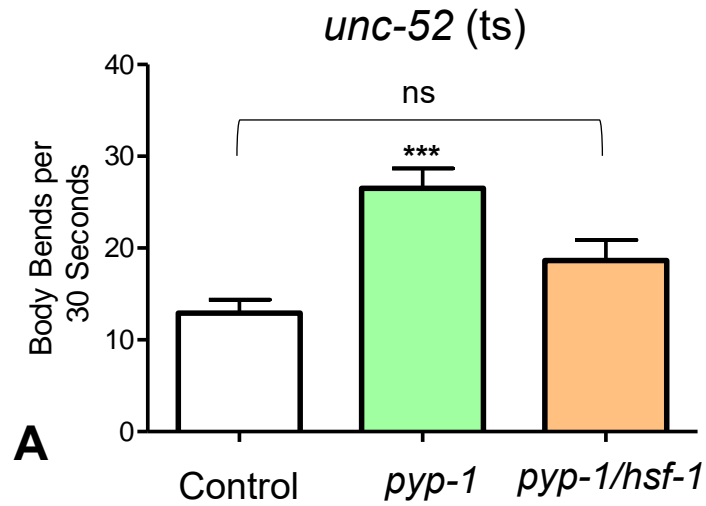
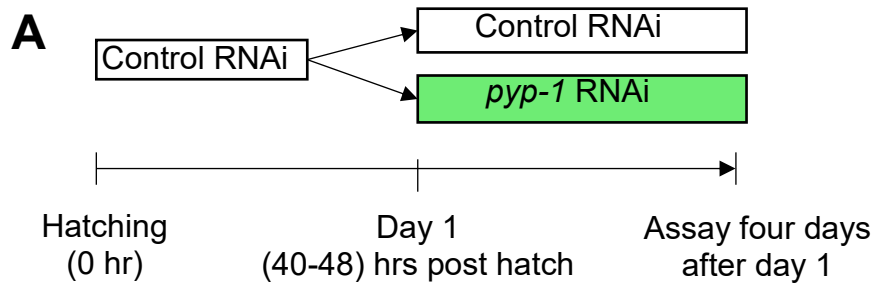
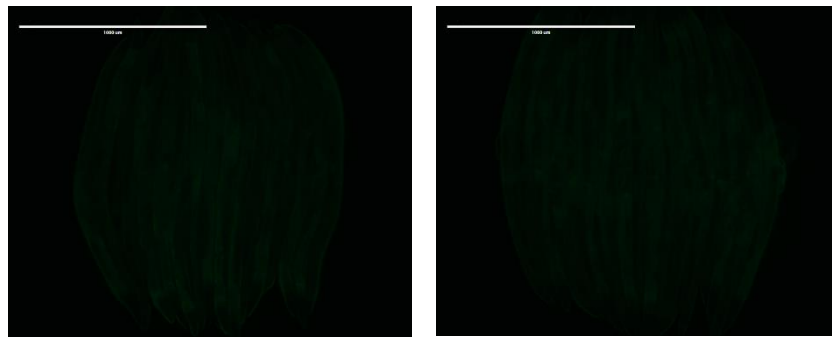


Figure 3.4 – *pyp-1* knockdown improved metastable protein folding and suppresses Amyloid-beta toxicity. (A) HE250 animals were fed control, *pyp-1*, or *pyp-1/hsf-1* RNAis from hatching and then shifted to 25C at day two of adulthood for 24 hours and then thrashing was assayed. Data was plotted and analyzed using GraphPad Prism. (***) indicates $p < 0.0001$. (B) CL2006 animals were fed control, *pyp-1*, or *pyp-1/hsf-1* RNAis from hatching and moved to fresh plates as needed. Non-motile worms were scored as paralyzed while motile animals were scored as non-paralyzed. Data was plotted and analyzed using GraphPad Prism. (*) indicates $p < 0.01$



phsp-70::GFP



B Control RNAi *pyp-1* RNAi

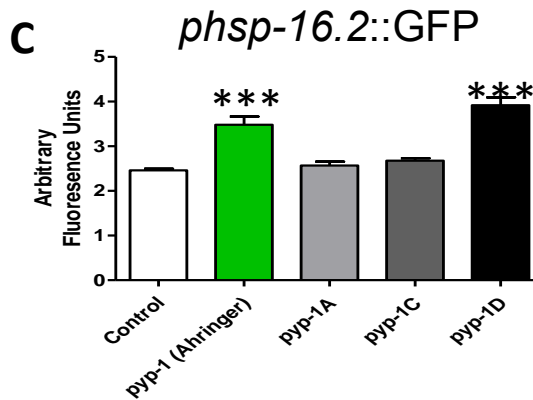


Figure 3.5 – Late *pyp-1* RNAi initiation is not sufficient to induce negative regulation of the HSR and knockdown of isoform *pyp-1C* is required. (A) Schematic diagram of late RNAi feeding schedule. Worms will receive the same total time on RNAi as previous experiments showing a *pyp-1* phenotype, but now RNAi is initiated at L4/YA. (B) AM446 animals fed with control or *pyp-1* RNAi using the late RNAi feeding schedule. (C) TJ375 were fed the indicated RNAis using the original RNAi feeding schedule. Day 3 worms were anesthetized using 10 mM Levamisole and mounted on agarose pads and imaged. Fluorescent images were analyzed using ImageJ and normalized to each days control RNAi sample and plotted using GraphPad Prism. Data was analyzed using a OneWay ANOVA. (***) indicates $p < 0.0001$

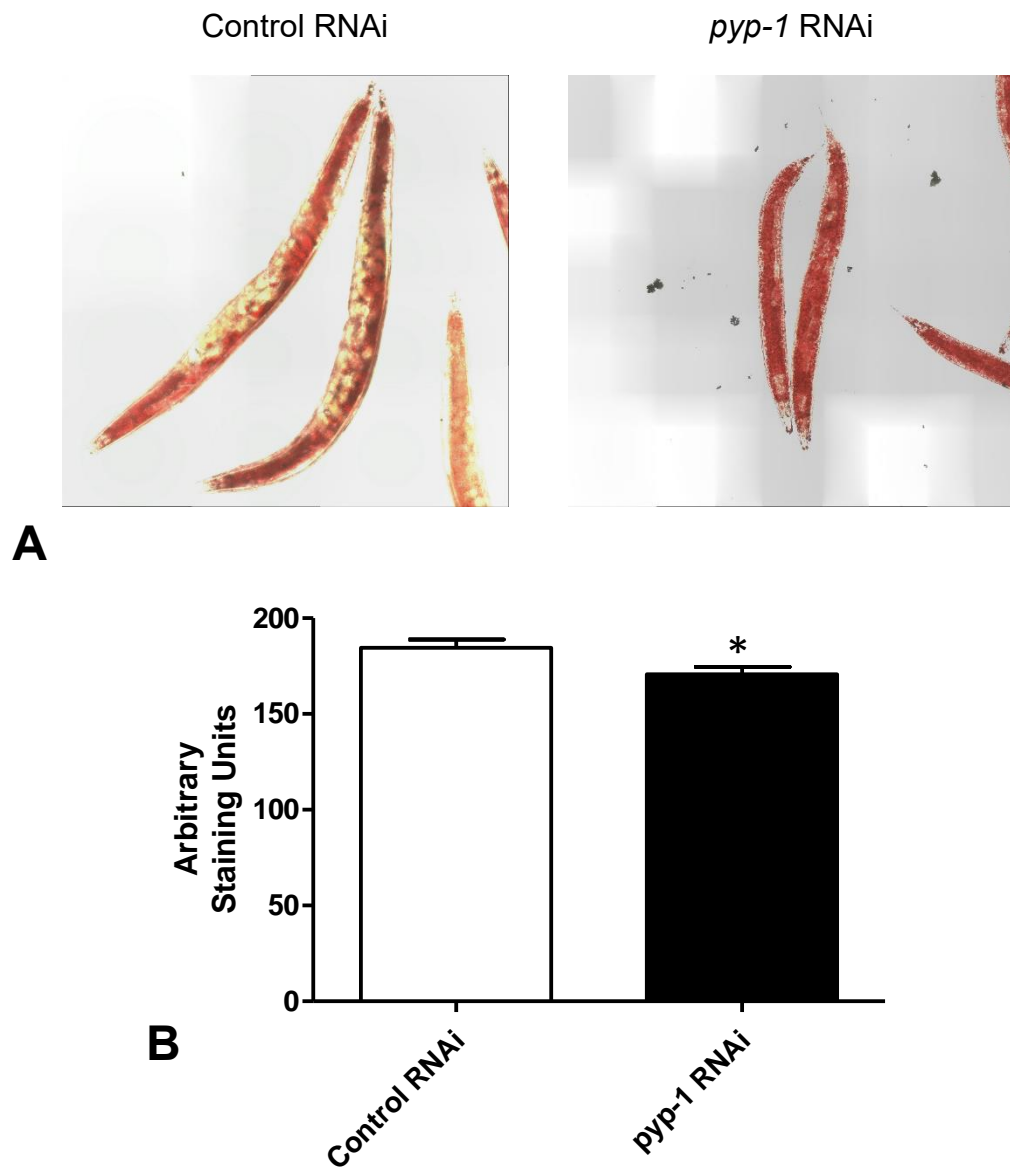


Figure 3.6 – *pyp-1* RNAi negatively regulates lipid staining. (A) N2 worms were fed the indicated RNAis using the original RNAi feeding schedule. Day 3 worms were then stained with Oil Red O and mounted on agarose pads and imaged. (B) Images were analyzed using ImageJ and plotted using GraphPad Prism. Data was analyzed using a Two tailed t-test. (*) indicates $p < 0.05$

Chapter 4

Modulation of the Heat Shock Response by O-GlcNAc in *C. elegans*

Introduction

Modification of proteins by O-linked β -N-acetylglucosamine (O-GlcNAc) is a dynamic, stress regulated post translational modification to serine and threonine residues that has been shown to modify cell signaling, apoptosis, and transcription [184-186]. Like phosphorylation, it is a reversible modification that can alter protein function. Because it can be added or removed from similar residues it may also compete with phosphorylation at these sites. Various human pathological conditions such as Diabetes, cancer, cell stress, and neurodegeneration have been shown to alter global O-GlcNAc cycling to cause both hyper and hypo-O-GlcNAcylation [187, 188]. Contrasted with phosphorylation, adding or removing O-GlcNAc groups can only be achieved with two proteins compared to the numerous kinase and phosphatase families. O-GlcNAc transferase (OGT-1) and O-GlcNAcase (OGA-1) can add or remove this modification to target substrates respectively. Both of these genes are essential in mammalian cells but are not in *C. elegans* [189-191].

Changes to overall cellular O-GlcNAcylation via Glutamine supplementation or oxidative stress via Arsenite treatment have been shown to regulate the expression of the HSF1 target gene HSP70 which suggests HSF1 involvement in some degree [33]. Reports of

mammalian HSF1 itself possibly being O-GlcNAcylated has been inconsistent in the literature. Two different studies, both using mouse embryonic fibroblasts (MEFs), have shown and not been able to demonstrate that HSF1 is modified by O-GlcNAc [34]. It has been reported to be found in lung homogenates from septic mice. These results could be explained in such that O-GlcNAcylation of HSF1 may be stress or cell type specific. Taken together we propose utilizing *C. elegans* to study O-GlcNAc cycling on the HSR would be an ideal tool to elucidate any conserved mechanisms relevant to human disease.

Materials and Methods

C. elegans strains. *C. elegans* strains were grown and maintained at 20°C unless otherwise noted [48]. Strains used in this study: wildtype Bristol N2, TJ375 [gpls1 (*phsp-16.2::GFP*)], SDW015 *hsf-1*(*asd002(hsf-1::GFP + unc-119(+))*), HE250 [*unc-52*(*e669su250*) II], AM140 [*rmls132* [*punc-54::Q35::YFP*], CL2006 [*dvls2* (*pCL12(unc-54/human Aβ peptide 1-42 minigene)*) + *pRF4*].SDW058 (*ogt-1(ok430)*), SDW061 (*oga-1(ok1207)*) Age synchronization was accomplished by standard hypochlorite treatment.

RNA interference. To perform RNAi animals were fed HT115(DE3) *E. coli* that are engineered to transcribe double-stranded RNA (dsRNA). Clones were obtained from the Ahringer RNAi feeding library (Geneservice, Cambridge, United Kingdom) and individual RNAi clones were obtained and sequenced verified prior to use. To induce dsRNA production NGM plates were supplemented with 0.2% β-lactose. RNAi was initiated at the L1 stage unless otherwise indicated.

Fluorescence analysis. TJ375 animals were grown to the indicated timepoints and anesthetized by picking individual worms to a drop of 10 mM levamisole on 1% agarose pads and then covered with a cover slip. Slides were imaged on an EVOS Fluorescence microscope. Fluorescent images analyzed using ImageJ (NIH) to quantify fluorescent intensity.

Thrashing analysis. HE250 animals were fed HT113(DE3) E. coli containing plasmids targeting *ogt-1*, *oga-1*, or non-targeting empty vector control. Animals were grown at 20°C until day 2 of adulthood and then shifted to 25°C for 24 hours and then motility was assayed. Length of trails were normalized to control RNAi.

SDW015 nuclear stress body formation assay. SDW015 animals were grown to L4 after being fed the indicated RNAis from hatching. Worms were anesthetized by picking individuals to a drop of 10 mM levamisole on 1% agarose pads and then covered with a cover slip and imaged on a Zeiss Axiovert 200M inverted confocal microscope (Jena, Germany) and a Zeiss LSM 700 laser scanning microscope (Jena, Germany). Nuclear stress body formation was quantified by assessing for the presence of nuclear foci containing HSF-1::GFP. After anesthetizing and placing the cover slip on top of the worms, they were imaged within 10-15 mins to avoid the spontaneous formation of nuclear stress bodies which may be due to hypoxia or other cytotoxic stress. Quantification was performed in GraphPad Prism (GraphPad Software, www.graphpad.com). A minimum of eight individual animals (n>8) were imaged per condition.

Polyglutamine analysis. AM140 animals were grown to the indicated timepoints and anesthetized by picking individual worms to a drop of 10 mM levamisole on 1% agarose

pads and then covered with a cover slip. Slides were imaged on an EVOS Fluorescence microscope. Worms were then assessed for the number of aggregates and analyzed using GraphPad Prism (GraphPad Software, www.graphpad.com). A minimum of eight individual animals ($n > 8$) were imaged per stress condition.

Thermotolerance. Worms were grown to the indicated timepoints at 20°C and then exposed to either 37°C for 2 hours or 35°C for 4 hours and then recovered for 24 hours at 20°C. Worms were then assessed for survival by visual analysis of movement. Data was then plotted using GraphPad Prism (GraphPad Software, www.graphpad.com). Approximately 120-160 individual animals were assessed per condition per trial.

mRNA expression analysis. N2, SDW058 (*ogt-1*), or SDW061 (*oga-1*) worms were grown to day 3 of adulthood on either control RNAi or *hsf-1* RNAi from hatching. Worms were then exposed to 33°C for one hour and then immediately washed clean of bacteria and snap frozen at -80°C. Worms were lysed in Trizol (Ambion) via sonication in Diagenode Bioruptor for 10 cycles of 30 seconds on and 30 seconds off on high power. RNA was extracted using the Zymo Direct-Zol RNA extraction kit and then equal amounts of RNA were reverse transcribed using the High Capacity cDNA synthesis kit (Invitrogen) according to manufacturer's instructions. RT-PCR was performed using a Applied Biosystems Stepone Plus real-time PCR machine using SYBR green chemistry and $\Delta\Delta C_t$ analysis. cDNA was amplified with primers for *hsp-16.2*, *hsp-70* (C12C8.1), or *cdc-42*. The resulting data was plotted and analyzed using GraphPad Prism (GraphPad Software, www.graphpad.com). All samples were compared to N2 no heat shock.

Results

Modulation of O-GlcNAc cycling transcriptionally regulates the HSR in *C. elegans*

To determine if O-GlcNAc cycling has any effect on the HSR we employed the transcriptional reporter model TJ375 which carries a integrated GFP reporter driven by the promotor for *hsp-16.2*. We examined two timepoints first at L4 which we refer to as day 1 and then two days later during adulthood. Day 1 animals showed that either *ogt-1* or *oga-1* knockdown lead to an increase in GFP induction after heat stress (Figure 4.1 A). In day 3 worms we showed an inverse relationship between *ogt-1* and *oga-1* RNAi which lead to a reduction and increase in reporter activity respectively compared to control knockdown (Figure 4.1 B). Thus, modulating the global O-GlcNAc levels in *C. elegans* can transcriptionally modulate the HSR.

Modulation of O-GlcNAc regulates a model of metastable protein folding

To determine if the transcriptional regulation we noted can have a functional benefit we utilized a *C. elegans* model of metastable protein folding. This worm carries an *unc-52* mutation which at the permissible temperature of 16°C allows for normal body movement, but at the non-permissible temperature of 25°C animals become paralyzed. We again employed *ogt-1* or *oga-1* RNAi from hatching and assessed for paralysis at day 1 and day 3 after being shifted to the non-permissible temperature for 24 hours. The day 1 data indicates that both RNAis are able to improve movement relative to control but but no statistically significant difference was found (Figure 4.2 A). However, day 3 data showed that *ogt-1* knockdown lead to slightly more paralysis and *oga-1* had a significant decrease in paralysis (Figure 4.2 B). Taken together, these results may

suggest that modulating O-GlcNAc can regulate metastable protein folding in *C. elegans*.

Modulating O-GlcNAc cycling affects the localization of intestinal HSF-1::GFP

Because we noted changes to the HSR and protein folding we hypothesized modulating O-GlcNAc cycling may affect HSF-1 localization and/or activity. To examine this, we utilized our CRISPR/Cas9 based HSF-1::GFP model to assess for changes to its localization with *ogt-1* or *oga-1* RNAi. Interestingly, we note that it appears that intestinal HSF-1::GFP undergoes a change in expression to display more foci like structures referred to nuclear stress bodies (nSBs) (Figure 4.3 A-D). Previous studies have implicated these structures as a hallmark of increased HSF-1 activity such as in response to thermal stress. We suggest that this result may indicate an increase the HSR previously noted in transcriptional reporter experiments but specific to the intestine of the worm.

***oga-1* knockdown suppresses Polyglutamine Aggregates in a Huntington's Disease model**

To further test if changes to global O-GlcNAc levels can regulate proteostasis in *C. elegans*, we next used *ogt-1* and *oga-1* RNAi in the Huntington's Disease model strain AM140. This strain carries 35 repeats of Glutamine fused to a YFP reporter which has been shown to mimic age-related aggregations similar to human disease samples. We found that at day 5 of adulthood lead to a significant decrease in the number of aggregates in *oga-1* knockdown compared to control RNAi (Figure 4.4). Thus,

knockdown of *oga-1*, which may globally increase O-GlcNAc levels, can improve a model of neurodegeneration in *C. elegans*.

Modulating O-GlcNAc levels regulates thermotolerance

Next, we tested whether *ogt-1* or *oga-1* knockdown can regulate thermotolerance at the same timepoints assessed above. N2 wildtype worms were fed the indicated RNAi and then exposed to 37°C for 2 hours and then recovered at 20°C for 24 before being assessed for survival. We found that both *ogt-1* and *oga-1* RNAi improve thermotolerance at day 1, but no difference was observed at day 3 of adulthood (Figure 4.5 A/B). We postulated the time and temperature may be too harsh for older worms which may mask any differences in survival. We then turned to utilizing *ogt-1* and *oga-1* mutant strains and performed control or *hsf-1* RNAi to check for thermotolerance effects dependent by *hsf-1*. Using a milder temperature of 35°C for 4 hrs at day 3 we reassessed thermotolerance. Interestingly, *ogt-1* mutant worms were much more stress resistant compared to *oga-1* mutant worms and this increase was dependent on *hsf-1* (Figure 4.5 C).

***ogt-1* mutants induce *hsf-1* target genes *hsp-70/hsp-16.2* more robustly *oga-1* mutants**

To follow up on our thermotolerance results, we hypothesized that *ogt-1* mutant worms should induce strong *hsf-1* target genes *hsp-70* and *hsp-16.2* more largely than *oga-1* mutants. To answer this, we exposed day 3 N2 wildtype animals, *ogt-1* mutants, and *oga-1* mutants either fed control or *hsf-1* RNAi to 33°C for 1 hr and then performed RT-PCR after RNA extraction and cDNA synthesis. In support of the thermotolerance

results, we found that *ogt-1* mutant worms did indeed induce larger changes to *hsp-16.2* (Figure 4.6 A) and *hsp-70* (Figure 4.6 B) compared to *oga-1* mutants which was dependent on *hsf-1*.

Discussion

Previous mammalian studies have shown that manipulations to global O-GlcNAc levels can regulate the HSR. Indeed, HSF1 itself has been shown to be O-GlcNAcylated, but the identity of which residues remains unknown. Our data in *C. elegans* also suggests that modulating global O-GlcNAc appears to alter the activity of the HSR and localization of HSF-1::GFP. This may indicate that the function of O-GlcNAc on the HSR is conserved in both systems. Our first studies utilized RNAi and made measurements at two timepoints, just prior to adulthood and roughly midway through reproduction. In these experiments we find a consistent effect of both *ogt-1* and *oga-1* in younger worms leading to activation of the HSR. We find this to be enigmatic as one may hypothesize that these two manipulations should display an inverse effect on the biological measurement. Indeed, it is only in the day 3 assessments that we find *oga-1* knockdown consistently improving the HSR while *ogt-1* knockdown displays a more muted effect. However, once we transitioned into mutant based studies we find a further inconsistency in effects. *ogt-1* mutants were vastly outperforming *oga-1* mutants in survival conflicting with the overall pattern observed in RNAi experiments. We hypothesize that perhaps the RNAis may be targeting other genes and confounding the data. To address these conflicts, future studies utilizing both *ogt-1* and *oga-1* mutants should be conducted to elucidate a common pattern of effects.

Because O-GlcNAc cycling is typically studied in the context of metabolic dysregulation we find it interesting that modulating it appears to affect the intestinal HSF-1::GFP more than the hypodermis. Localization changes in other tissues such as the neurons and body wall muscle should also be addressed, but given that the intestine is major metabolic regulator for the worm examining it further in that tissue should be performed. Previous studies have indicated that mammalian HSF1 itself can be O-GlcNAcylated [35, 36]. Data suggests that O-GlcNAcylation of HSF1 leads to increased HSP70 expression suggesting an upregulation of the HSR. One major question that remains however is that our data suggests older mutant hypo-O-GlcNAcylated worms are much more stress resistant than hyper-O-GlcNAcylated mutants suggesting an opposite phenotype than that described in mammalian cells. Furthermore, it is still unknown if worm HSF-1 is O-GlcNAcylated, and if so, in which tissues and which residues in the protein.

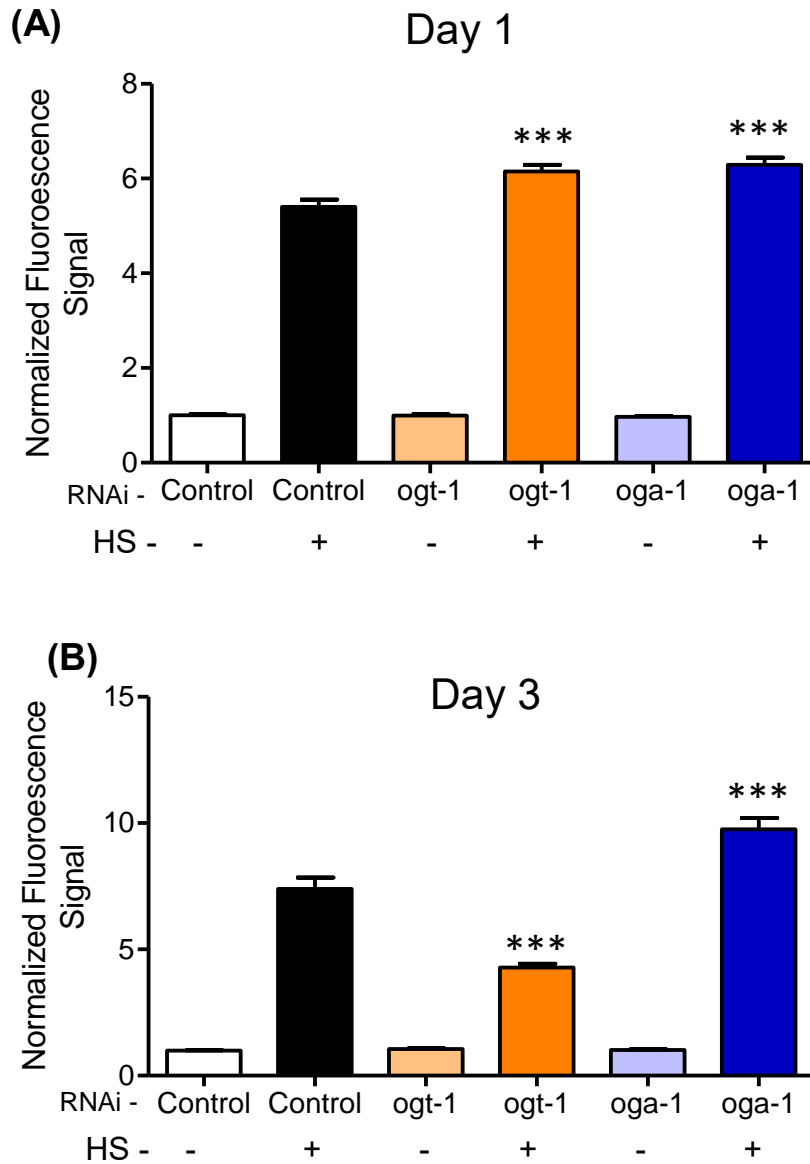


Figure 4.1 – Modulation of O-GlcNAc cycling transcriptionally regulates the HSR in *C. elegans*. (A) TJ375 animals were fed the indicated RNAis and then assessed at L4/YA (Day 1) or two days later (Day 3) (B). Worms were given no heat shock (-) or were exposed to 1 hour at 33°C and then recovered for 6 hours at 20°C (+). Fluorescent images were analyzed using ImageJ and plotted using GraphPad Prism. Data was analyzed using a OneWay ANOVA. (***) indicates $p < 0.0001$

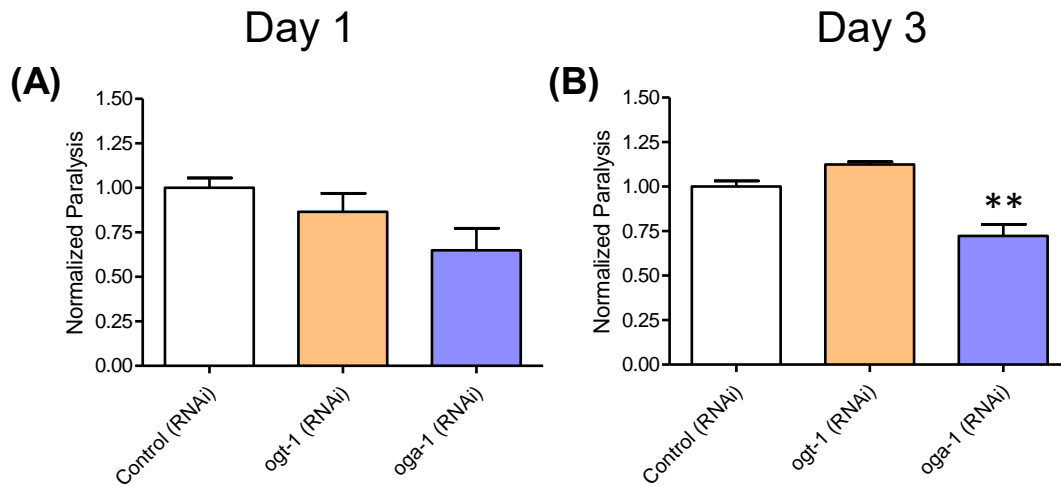


Figure 4.2 - Modulation of O-GlcNAc regulates a model of metastable protein folding. HE250 animals were fed control, *ogt-1*, or *oga-1* RNAis from hatching and then shifted to 25°C at day one (A) two days later (Day 3) (B) for 24 hours and then thrashing was assayed. Data was plotted and analyzed using GraphPad Prism. (**) indicates $p < 0.001$.

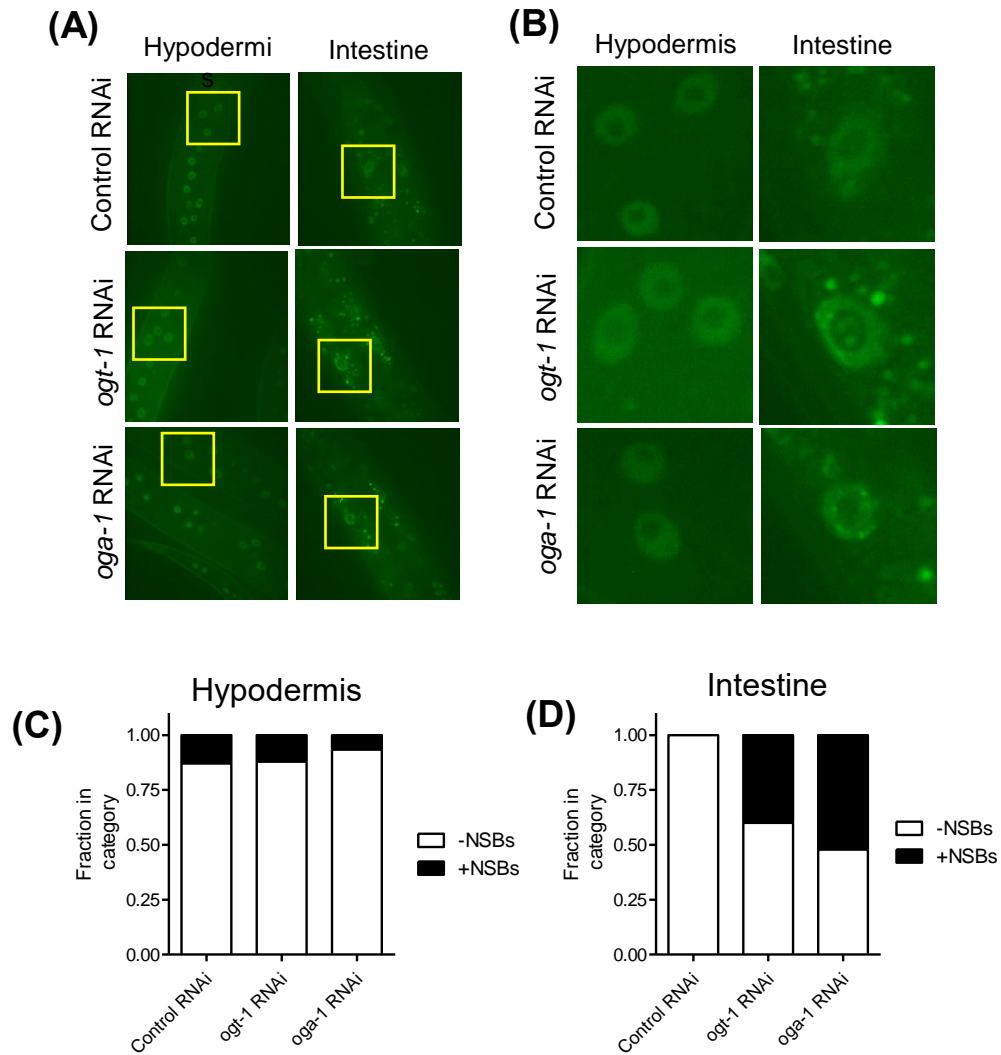


Figure 4.3 - Modulating O-GlcNAc cycling affects the localization of intestinal HSF-1::GFP. SDW015 worms were grown on indicated RNAis from hatching until L4 and then were anesthetized using 10 mM Levamisole and mounted on agarose pads and imaged. Yellow boxes in (A) represent the zoomed in areas in panel (B). The fraction of total hypodermal nuclei (C) or within the intestine (D) were scored as either containing no nSBs (-nSBs) or positive for nSBs (+nSBs) of HSF-1::GFP with and without HS for $n \geq 8$ worms and plotted using GraphPad Prism.

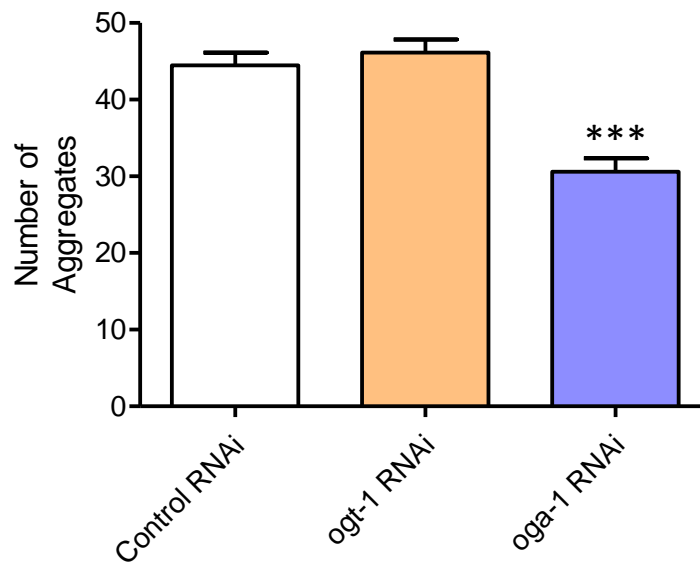


Figure 4.4 - *oga-1* knockdown suppresses Polyglutamine Aggregates in a Huntington's Disease model. AM140 animals were grown on indicated RNAis from hatching until L4 and then were anesthetized using 10 mM Levamisole and mounted on agarose pads and imaged. The number of Q35::YFP aggregates was counted and plotted using GraphPad Prism. Data was analyzed using a OneWay ANOVA. (***) indicates $p < 0.0001$

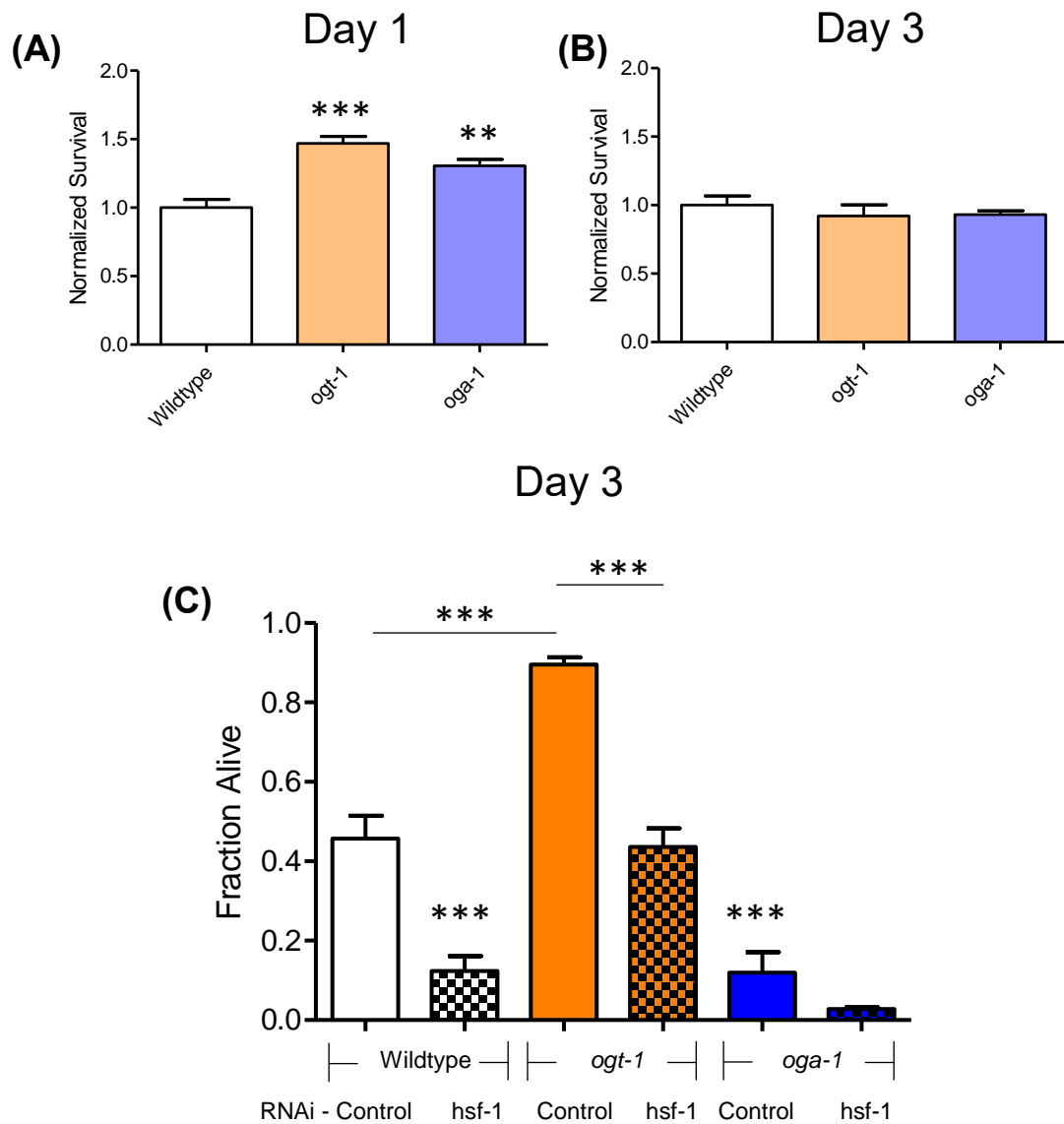


Figure 4.5 - Modulating O-GlcNAc levels regulates thermotolerance. (A/B) Wildtype, *ogt-1* (ok430), and *oga-1* (ok1207), worms were grown on OP50-1 until L4/YA (Day 1) or two days later (Day 3) and then exposed to 37°C for 2 hours and then left to recover at 20°C for 24 hrs before assessed for survival. (C) Wildtype, *ogt-1* (ok430), and *oga-1* (ok1207), worms were grown on indicated RNAis until Day 3 and then exposed to 35°C for 4 hours and then left to recover at 20°C for 24 hrs before assessed for survival. Survival was then plotted and analyzed using GraphPad Prism. (**) indicates $p < 0.001$. (***) indicates $p < 0.0001$. Comparisons made to Wildtype (A/B) or Wildtype (Control RNAi) (C) unless indicated otherwise with line.

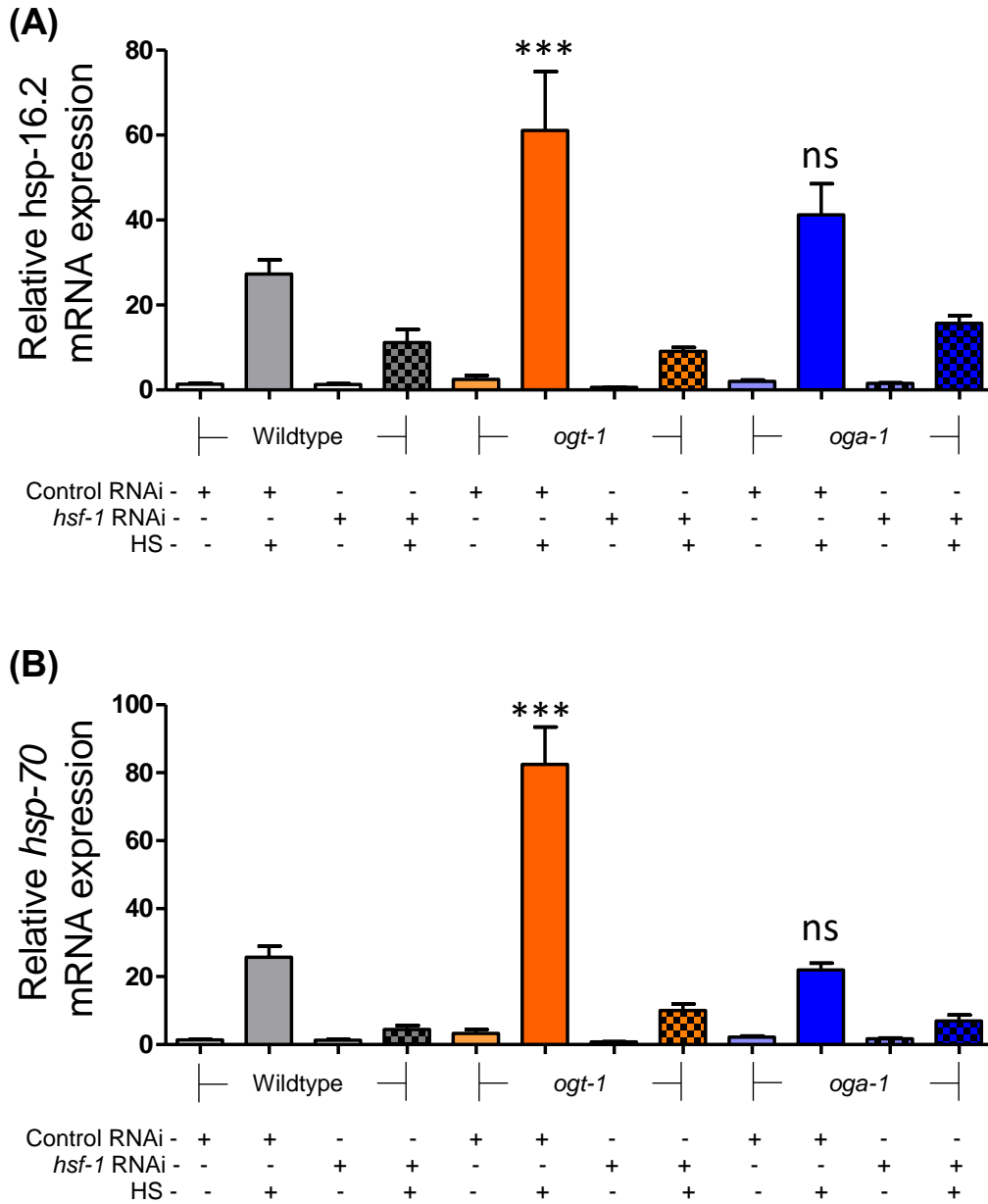


Figure 4.6 - *ogt-1* mutants induce *hsf-1* target genes *hsp-70/hsp-16.2* more robustly *oga-1* mutants. Wildtype, *ogt-1* (ok430), and *oga-1* (ok1207), worms were grown on indicated RNAis until Day 3 and then exposed to a heat shock (HS) of 33°C for 1 hour and then harvested for RNA extraction, cDNA synthesis, and RT-PCR for *hsp-16.2* (A) or *hsp-70* (B). Data was then plotted and analyzed using GraphPad Prism. (***) indicates $p < 0.0001$. Significance indicators are compared to wildtype control RNAi (+) HS.

Chapter 5

RNAi of Cuticle and Collagen Genes May Regulate the HSR

Introduction

The Heat Shock Response (HSR) is a highly conserved stress responsive pathway that serves to stabilize the proteome in response to diverse cytotoxic insults [183]. The master regulator of the HSR is heat shock factor 1 (HSF-1) which acts as a transcription factor to induce the expression of genes, most notably heat shock proteins (HSPs), to regulate global protein folding within the cell [70]. Specifically within *C. elegans*, data from our group has suggested that HSF-1 may regulate diverse families of genes including hsps, germline genes, and many cuticle/collagen related genes during non-stress and stress conditions [111]. Other groups have also identified the cytoskeleton, which include collagen genes, as key HSF-1 regulated genes as determinants of animal lifespan [58]. Because many of HSF-1 target genes, including HSPs, themselves are major regulators of stress and aging, we sought to identify cuticle and collagen genes that may regulate the HSR itself. We performed a non-biased RNAi screen of all available cuticle, collagen, and cuticle/collagen related genes using a transcriptional reporter of the HSR. Our results identify some novel HSR regulators which appear to enhance or suppress HSF-1 transcriptional activity.

Materials and Methods

C. elegans strains. *C. elegans* strains were grown and maintained at 20°C unless otherwise noted [48]. Strains used in this study: TJ375 [gpls1 (*phsp-16.2::GFP*)]

RNA interference. To perform RNAi animals were fed HT115(DE3) *E. coli* that are engineered to transcribe double-stranded RNA (dsRNA) [50, 163, 178]. Clones were obtained from the Ahringer RNAi feeding library (Geneservice, Cambridge, United Kingdom) and individual RNAi clones were obtained and sequenced verified prior to use. To induce dsRNA production NGM plates were supplemented with 0.2% β -lactose [179]. RNAi was initiated at the L1 stage unless otherwise indicated.

Fluorescence analysis. TJ375 animals were grown to L4 feeding on the indicated RNAis and then then exposed to 1 hour at 33°C and then recovered for 6 hours at 20°.

Approximately 20 worms were then anesthetized by picking individual worms to a drop of 10 mM levamisole on 1% agarose pads and then covered with a cover slip. Slides were imaged on an EVOS Fluorescence microscope. Fluorescent images analyzed using ImageJ (NIH) to quantify fluorescent intensity. Data was analyzed using GraphPad Prism with an OneWay ANOVA with Tukey comparisons of all conditions. Significance relative to control was noted.

Results

Cuticle and Collagen genes may regulate the HSR transcriptionally

To determine if collagen/cuticle genes and cuticle/collagen related genes regulate the HSR we performed the directed subscreen utilizing the transcriptional reporter model strain TJ375. This strain has the transgene containing the promotor for *hsp-16.2* driving

GFP expression and is integrated into the genome. Each candidate regulator was tested by RNAi by feeding from hatching until the last larval stage L4 and then changes to the GFP signal after thermal stressed was measured. Each portion of screen were tested on individual trials which necessitated the use of a biologically matched control sample for that round of testing. The results of our screen identified a total of 28 genes that can upregulate reporter activity and 28 genes that can suppress reporter activity relative to control after heat stress (Figure 5.1/2/3/4). Thus, modulation of cuticle and collagen genes may transcriptionally regulate the HSR.

Discussion

The worm cuticle is studied similarly to mammalian stratum corneum as a means of maintaining the internal function of the organism which can participate the regulation of temperature, block harmful pathogens or small molecules, and interpreting mechanosensation and chemosensation signals from the environment [192]. Although our data is very incomplete at this stage, it suggests that cuticle and collagen gene components may regulate the HSR itself. In contrast to the mammalian external barrier which is constantly being synthesized and renewed, the worm cuticle undergoes four distinct molts resulting in the adult cuticle for the rest of its lifespan. Previous work suggests that particular cuticle/collagen members or cuticle/collagen modifying genes are regulated at specific spatiotemporal points corresponding to the appropriate molt of the animal [135, 192, 193]. Our data suggests that some of these collagen/cuticle genes may also modulate the HSR as measured through a transcriptional reporter. The candidate regulators were broken up into five major classes of genes.

Acs genes

In *C. elegans*, Fatty acid CoA synthetase genes (*acs*) are a twenty two member family of genes that function to synthesize fatty acyl-CoA. They are not well studied, however two members have been shown to play a role in regulating the the cuticle of the worm. *acs-20/22* have been shown to regulate the cuticle resulting in a hyper-permeable barrier when suppressed [194]. Mutation of these genes regulates COL-19::GFP expression and appropriate alae formation. Our data suggests that *acs-5/11/15* and *acs-4/19* increased and decreased the GFP signal in response to heat shock respectively. Our reporter system is exquisitely sensitive to the transcriptional activity of HSF-1, and it remains unclear how these members may regulate HSF-1 activity which may act through regulating cuticle permeability.

Bli genes

Mutations that lead to changes in the morphology in the worm cuticle may lead to fluid filled blisters and those genes responsible are termed bli (BLIstered). The bli family of genes consists of six members in *C. elegans*. The two bli genes that altered our transcriptional reporter are *bli-3* and *bli-5*. BLI-3 is an ortholog of human DUOX1 (dual oxidase 1) and DUOX2 (dual oxidase 2) which functions as an NADPH oxidase [195]. BLI-3 has been reported to regulate oxidative stress, lifespan, and fungal pathogenesis acting through SKN-1/WDR-23 dependent mechanism [196]. BLI-5 is an ortholog of the human genes AMBP1 (alpha-microglobulin/bikunin precursor; LRP11 (LDL receptor protein 11); and SPINT1 (serine peptidase inhibitor, Kunitz type 1) which exhibits serine type endopeptidase activity. BLI-5 is not well studied, but mutations in *bli-5* have been shown disrupt COL-19::GFP distribution, dorso/ventral and lateral alae formation, and is

expressed in both the larval and adult hypodermis [195]. Conversely, overexpression of BLI-5 leads to a disruption of molting, and cuticle and vulval defects. Oxidative stress has been reported to modulate the HSR, but it remains unclear specifically how changes to NADPH oxidase activity may regulate HSF-1 activity.

Col genes

Collagens by far were the largest group identified in our screen. Interestingly, collagens were shown to lead to both increased and decreased GFP signals. The cellular role of collagens are very diverse in *C. elegans*. Beyond their structural role they also may participate in regulating cell stress pathways. Changes in cytoplasmic osmolarity result can result in decreased cell volume, mechanical stress on the cell and cell connections, and dysfunction of proteins and DNA. In response to high osmolarity cells can accumulate osmolites to encourage water retention to restore cellular function. In *C. elegans*, it has been described that specific collagen genes when disrupted lead to similar cellular conditions that mimic osmotic stress [138]. Previous research identified *dpy-10*, when mutated, increase intracellular glycerol similar to being exposed to a high osmotic stress environment. Within our data, we identified the knockdown of *dpy-10* as a candidate regulator of the HSR. It may suggest that increased cytoplasmic osmolites regulate HSF-1 transcriptional activity. The suppression of collagen/cuticle genes can also lead to the coactivation of oxidative stress mediated by *skn-1* [140]. Suppressing morphological changes to the alae and furrows in the worm cuticle leads to the activation of accumulation of osmolites as previously described, but also activates *skn-1* and cellular detoxification programs. Previous data from our lab implicated *hsf-1* as a regulator of cuticle and collagens [111]. The current data may also suggest that cuticle

and collagen components may act upstream of *hsf-1* as well. Further investigation into whether or not the collagen genes identified regulate *hsf-1* target gene expression will be important to confirm true HSR regulation.

Dpy genes

Genes that result in shorter worms when mutated lead to the dpy (DumPY) phenotype in *C. elegans*. Our screen identified six dpy genes that regulated transcriptional reporter activity. DPY-18 is an ortholog of human P4HA1 (prolyl 4-hydroxylase subunit alpha 1) and P4HA2 (prolyl 4-hydroxylase subunit alpha 2) which exhibits procollagen-proline 4-dioxygenase activity. *dpy-18* plays a major role in axon guidance by modifying ECM components to guide the ventral nerve cord in the worm [197]. *dpy-6* has been reported to have calmodulin binding activity, but is not well studied. *dpy-19* is an ortholog of human DPY19L1 (dpy-19 like C-mannosyltransferase 1), and is reported to glycosylate Thrombospondin type 1 repeats which are involved in cell adhesion and signaling [198]. Dpy-28 is an ortholog of human NCAPD2 (non-SMC condensing I complex subunit D2) which has chromatin binding activity and histone binding activity. DPY-28 is important for regulating X chromosome dosage by controlling transcript levels as well as meiotic crossover [199-202]. Because the function of dpy genes is very diverse it remains unclear how each particular gene may modify HSF-1 transcriptional activity.

Sqt genes

In *C. elegans*, genes that result in shorter, fatter appearing worms were given the phenotypic description of SQuaT. The *sqt* family of genes consists of three members *sqt-1/2/3*. The majority of literature related to this family revolves around *sqt-1*. SQT-1 is

an ortholog of human METTL24 (methyltransferase like 24) and SCARA3 (scavenger receptor class A member 3). At the present moment, data regarding changes to the function of these genes describe morphological changes to the worm cuticle. For example, *sqt-1* is the most well studied with mutations in this locus resulting in a variety of changes to the worm cuticle including helical, long or short, and right or left handed rollers [133, 203-206]. Both *sqt-1* and *sqt-2* identified in our screen resulted in decreased signal after heat shock. It remains unclear how changes to cuticle patterning may regulate the activity of the HSR.

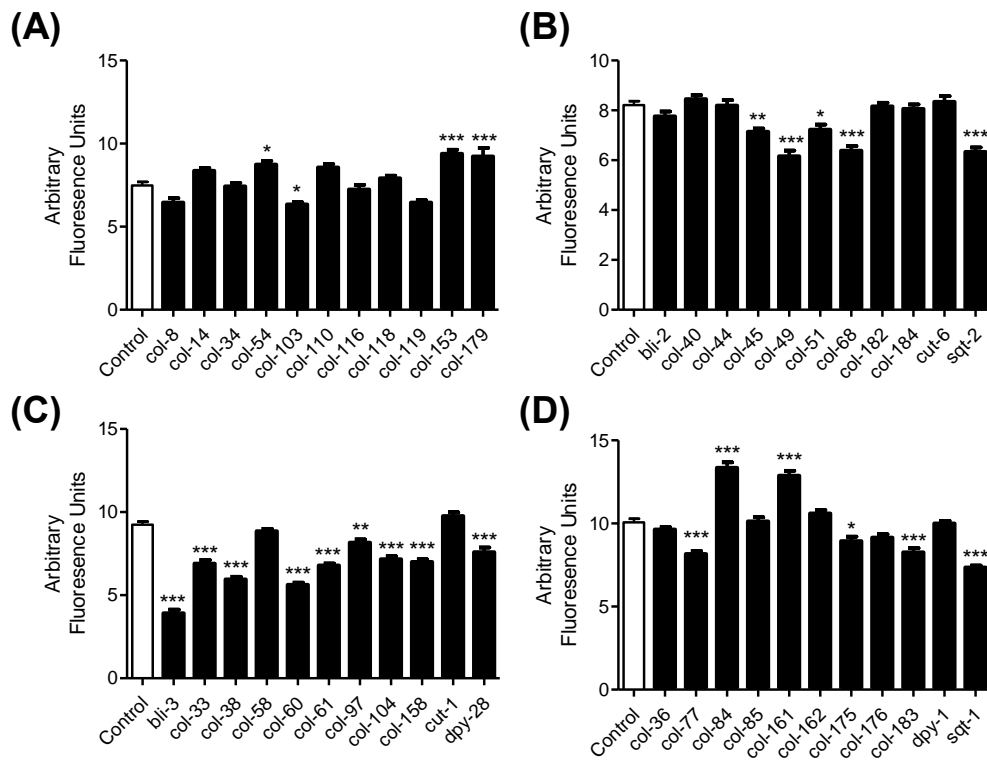


Figure 5.1 - RNAi of Cuticle and Collagen Related Genes Identified with Increased or Decreased GFP Intensity. (A-D) TJ375 (*phsp-16.2::GFP*) animals were grown with the indicated RNAis and then exposed to 1 hour at 33°C and then recovered for 6 hours at 20°. Approximately 20 worms were then anesthetized with 10 mM levamisole, imaged, and analyzed with ImageJ. Data was analyzed using GraphPad Prism with a OneWay ANOVA with Tukey comparisons of all conditions. Significance relative to control was noted.

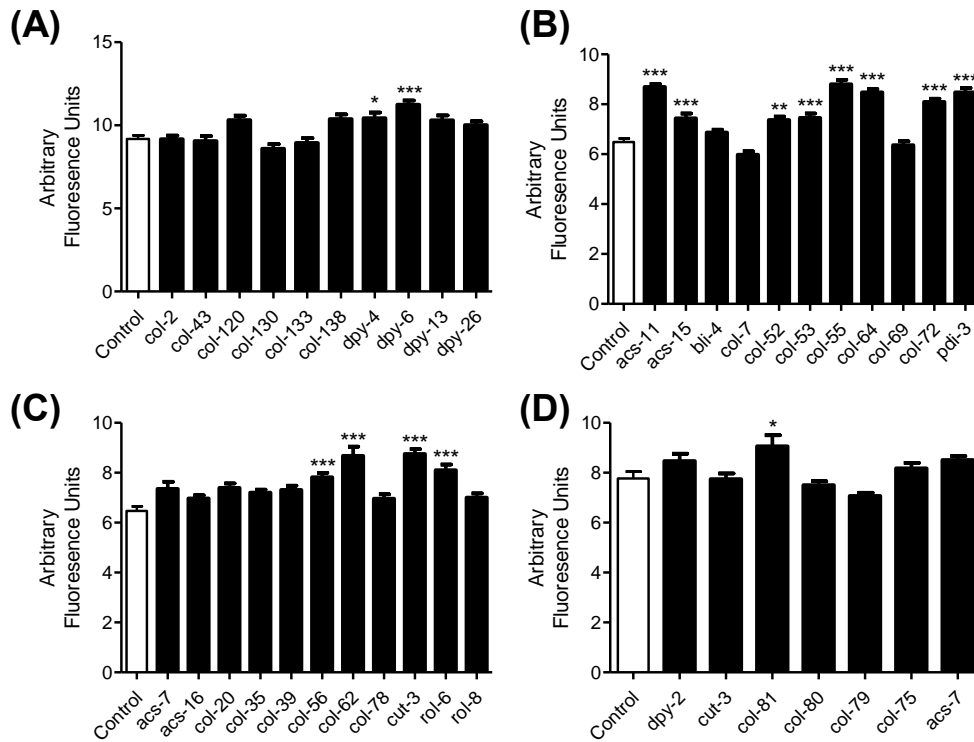


Figure 5.2 - RNAi of Cuticle and Collagen Related Genes Identified with Increased or Decreased GFP Intensity. (A-D) TJ375 (*phsp-16.2::GFP*) animals were grown with the indicated RNAis and then exposed to 1 hour at 33°C and then recovered for 6 hours at 20°. Approximately 20 worms were then anesthetized with 10 mM levamisole, imaged, and analyzed with ImageJ. Data was analyzed using GraphPad Prism with a OneWay ANOVA with Tukey comparisons of all conditions. Significance relative to control was noted.

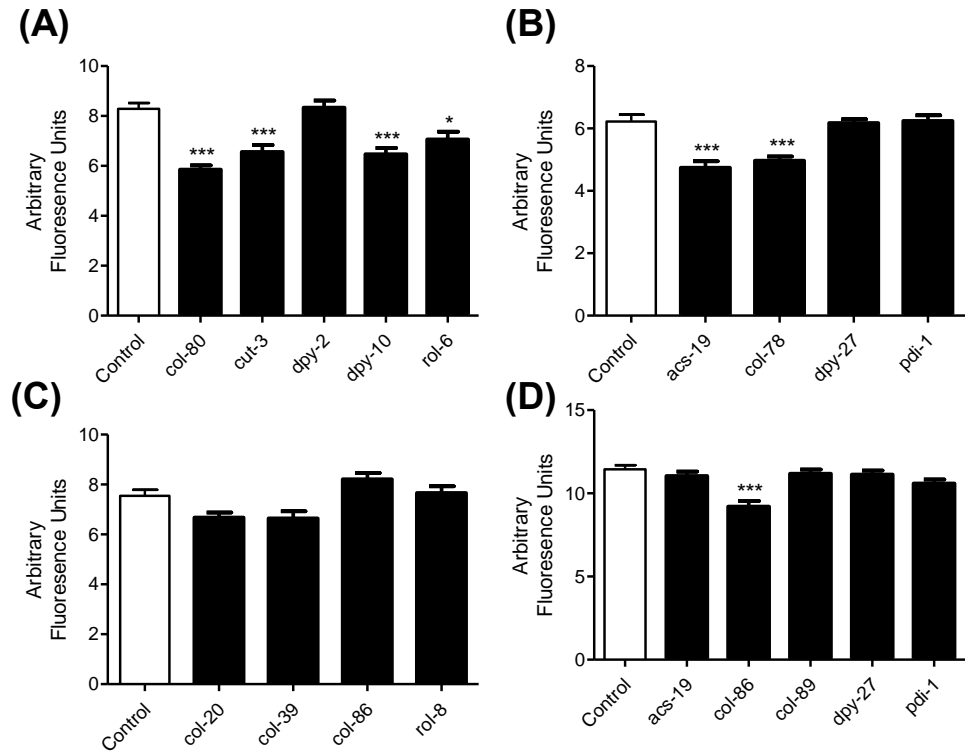


Figure 5.3 - RNAi of Cuticle and Collagen Related Genes Identified with Increased or Decreased GFP Intensity. (A-D) TJ375 (*phsp-16.2::GFP*) animals were grown with the indicated RNAis and then exposed to 1 hour at 33°C and then recovered for 6 hours at 20°. Approximately 20 worms were then anesthetized with 10 mM levamisole, imaged, and analyzed with ImageJ. Data was analyzed using GraphPad Prism with a OneWay ANOVA with Tukey comparisons of all conditions. Significance relative to control was noted.

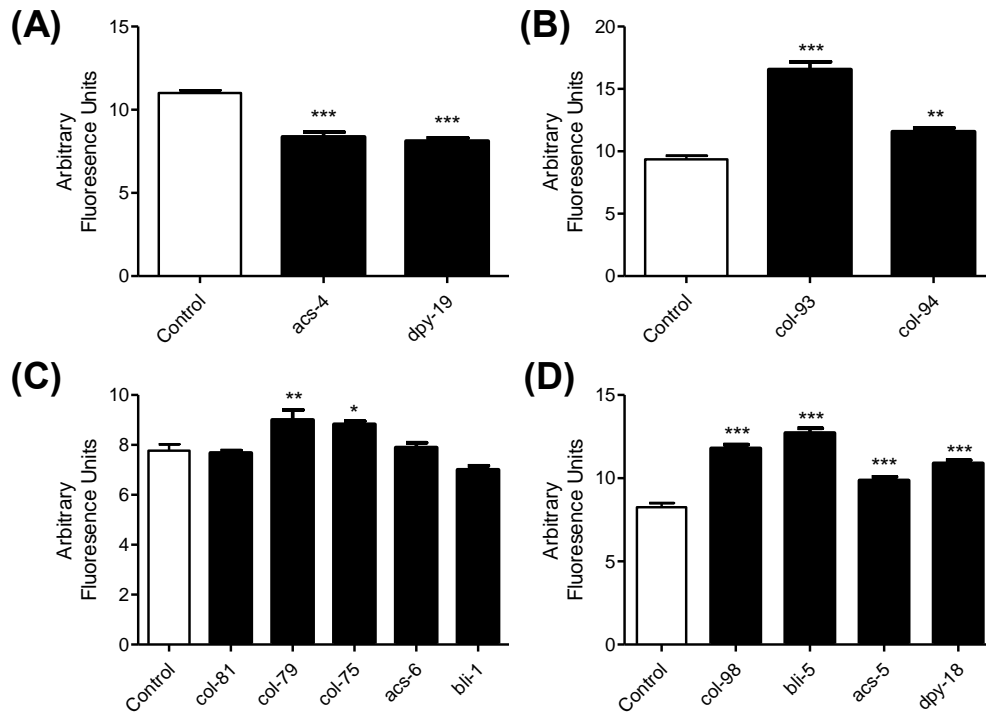


Figure 5.4 - RNAi of Cuticle and Collagen Related Genes Identified with Increased or Decreased GFP Intensity. (A-D) TJ375 (*phsp-16.2::GFP*) animals were grown with the indicated RNAis and then exposed to 1 hour at 33°C and then recovered for 6 hours at 20°. Approximately 20 worms were then anesthetized with 10 mM levamisole, imaged, and analyzed with ImageJ. Data was analyzed using GraphPad Prism with a OneWay ANOVA with Tukey comparisons of all conditions. Significance relative to control was noted.

Chapter 6

Analysis of Genetic Regulation of HSF-1 Nuclear Stress Bodies

Introduction

In the previous studies it was shown that our CRISPR/Cas9 based model reflected phenotypes of HSF-1::GFP nuclear stress bodies (nSBs) previously reported in MosSci based models and expanded upon changes to HSF-1::GFP localization in stress conditions as well as during early aging. Recent evidence suggests that the physical state of HSF-1 in the cell ties strongly with its transcriptional activity and thus the overall activity of the HSR. Thus, understanding what stress conditions, pathological conditions, or genetic backgrounds regulate HSF-1 localization may be essential to discern the mechanisms of disease states as well as designing novel therapeutic interventions. Using this now validated model we examined how the formation of HSF-1::GFP nuclear stress bodies can be genetically regulated in by cell stress responsive pathways.

One of the most well conserved pathways from worm to human is p38 MAPK signaling. In the worm this pathway responds to a diversity of upstream inputs including pathogenic infection, oxidative stress, and calcium signaling. In *C. elegans* this cascade is mediated by three genes *nsy-1* (MAPKKK), *sek-1* (MAPKK), and *pmk-1* (MAPK). It has been shown that *pmk-1* is required for thermotolerance and during heat stress it

can relocalize in the nucleus for its kinase activity. In human cells, it has been shown that HSF1 is a substrate for p38 MAPK activity, but it remains undescribed how this activity may regulate HSF1 localization including HSF-1::GFP nSBs. Here we show evidence suggesting that p38 MAPK activity is required for the suppression of HSF-1::GFP nSBs upon the transition to adulthood in animals with genetic ablation of the germline. This suggests that there may be increased p38 MAPK activity in animals lacking a germline to promote HSF-1::GFP to remain distributed in the nucleus which may increase HSR activity.

The Sirtuin *sir-2.1* has been previously shown to strongly regulate *C. elegans* lifespan, and stress resistance [84, 86]. Previous research on the effect of SIRT1 on HSF-1 in mammalian cells shows that HSF-1 is a substrate of SIRT1 and deacetylation of HSF-1 by SIRT1 can promote more robust HSR [31]. Here we show data suggesting the SIR-2.1 overexpression is sufficient to suppress the formation of HSF-1::GFP nSBs upon the transition to adulthood and that requires *jmjd-3.1*. This may suggest that SIR-2.1 overexpression enhances *jmjd-3.1* expression or activity which is able to promote diffuse HSF-1::GFP nuclear localization and an increased HSR through the transition to adulthood. This result suggests a novel mechanism whereby *sir-2.1* may support increased stress resistance and longevity shown by my previous groups by maintaining a youthful HSF-1 localization.

One of the most widely verified mechanisms to extend *C. elegans* longevity is a disruption to the insulin/insulin like (IIS) signaling pathway. When dysregulated, it has been reported that worms may have a doubling of lifespan relative to wildtype. The major components of this pathway are the receptor *daf-2* and a conserved kinase

cascade signaling pathway including the genes *age-1*, *pdk-1*, and *akt-1/2* [207]. The lifespan extension conferred by IIS dysregulation has been shown to require multiple stress responsive transcription factors including *daf-16*, *hsf-1*, and *skn-1* [69, 208, 209]. However, the role of IIS on regulating the localization of HSF-1 is still unknown.

Lastly, we investigated how *hsb-1* may regulate HSF-1::GFP localization and give more insights into the mechanism of *hsb-1* mediated lifespan extension and stress resistance. It was previously reported in mammalian cells that Heat Shock Factor Binding Protein 1 (HSBP1) can interact with active trimeric HSF1 to negatively regulate the HSR [66]. Next, a study in *C. elegans* confirmed the worm homolog of HSBP1 also functions to negatively regulate the HSR, and this effect may function through the insulin/insulin-like signaling pathway [69]. However, it is still unknown in what cells HSB-1 is expressed in or how its localization may change during cell stress or aging at the organismal level. This is especially concerning given the dynamic nature of HSF-1::GFP localization changes during aging across multiple tissue types in the worm. We find that manipulating *hsb-1* expression regulates HSF-1::GFP nSB formation as well as may regulate the HSR via modulating the expression of a lysine demethylase *jmjd-3.1*. Interestingly, the effect of increased HSF-1::GFP nSBs may not be surprising given that *hsb-1* is already shown to function as a negative regulator of the HSR, but combined with recent literature suggesting prolonged HSF1 nSBs are detrimental to cell survival it presents an interesting conflict to be further resolved.

Materials and Methods

Worm strains

C. elegans strains and maintenance. *C. elegans* strains were grown and maintained at 20°C on NGM plates with *Escherichia coli* OP50-1, unless otherwise noted. Bristol N2 was used as the wild-type strain for these studies. Additional strains used were, SDW015 *hsf-1(asd002(hsf-1::GFP + unc-119(+))*), SDW050 *hsf-1(asd002(hsf-1::GFP + unc-119(+))*); *glp-1(e2144)*, SDW122 *hsf-1(asd002(hsf-1::GFP + unc-119(+)*; SIR-2.1 OE)); (SDW123 *hsf-1(asd002(hsf-1::GFP + unc-119(+))*); *glp-1(e2144)*; *pmk-1(km25)*; SDW130 *hsf-1(asd002(hsf-1::GFP + unc-119(+))*; *daf-2(e1370)*, CH116 (*hsb-1(cg116)*), WS2170 (*opls110 [lim-7p::YFP::actin + unc-119(+)]* IV. Age synchronization was accomplished by standard hypochlorite treatment.

Heat shock

Worms were grown on OP50-1 plates to L4 and then subjected to a 35°C HS for 2 hrs and then immediately recovered at 20°C. Animals were imaged after 2, 3, and 4 hours of recovery at 20°C.

RNA interference (RNAi). To perform RNAi, animals were fed HT115(DE3) *E.*

coli transformed with the indicated RNAi vectors (J. Ahringer, University of Cambridge, Cambridge, U.K.) as previously described [163]. Individual RNAi clones were sequence-verified prior to use. To induce dsRNA production, NGM plates were supplemented with 1 mM IPTG and inoculated plates were left to mature overnight at room temperature.

RNAi feeding was initiated at the L1 developmental stage unless otherwise noted.

Fluorescence imaging. Animals were picked free of bacteria and anesthetized with 10 mM levamisole. Nuclear stress body formation was quantified by assessing for the presence of nuclear foci containing HSF-1::GFP. After anesthetizing and placing the cover slip on top of the worms, they were imaged within 10-15 mins to avoid the spontaneous formation of nuclear stress bodies which may be due to hypoxia or other cytotoxic stress. Quantification was performed in GraphPad Prism (GraphPad Software, www.graphpad.com). A minimum of eight individual animals ($n > 8$) were imaged per condition.

Brood Size Analysis. Animals were grown on OP50-1 plates until L4 and then individual worms were transferred to 6-well plates. Parental worms were transferred to fresh plates daily for 6 days and total live offspring were counted per worm. Brood assay data reflects three biologically independent trials with 4-6 replicate animals per condition. Significance was determined by conducting a two-tailed t-test using GraphPad Prism (GraphPad Software, www.graphpad.com).

Embryogenesis defect assay. Animals were synchronized using standard hypochlorite treatment and the resulting eggs were deposited into replicate drops on an unseeded NGM plate with the outline of each droplet outlined. Eggs were allowed to hatch overnight and then each droplet was assessed for the number of unhatched eggs present within the droplet outline.

Germline corpse assay. WS2170 animals were grown on either control L4440 RNAi or *hsb-1* RNAi for 3 days after hatching. Worms were then anesthetized and imaged on a Keyence Fluorescence Microscope and the germlines for 14 biological replicate animals were assessed for the number of germline corpses. Data was collected and analyzed

using a two-tailed t-test using GraphPad Prism (GraphPad Software, www.graphpad.com).

Growth assay. Wildtype or *hsb-1*(cg116) mutant animals were grown on OP50-1 plates and 50 replicate animals were imaged each day for four days until gravid adulthood was reached. Images were analyzed using ImageJ to measure the length of the worms measured along the centerline of the body from pharynx to tail tip. Data was collected and analyzed using a two-tailed t-test using GraphPad Prism (GraphPad Software, www.graphpad.com).

qPCR analysis. Approximately 250-300 animals were grown on OP50-1 plates until L4 and then subjected to either a 1 hr HS at 33°C or left at 20°C. Following HS, all plates were washed twice with NGM buffer and worms were washed clean of bacteria before immediately being snap frozen at -80°C. Trizol was added to the frozen worm pellet prior to sonication for 10 cycles of 30 seconds on/off in a Bioruptor sonicator (Diagenode, Inc., Denville, NJ). RNA was extracted via Direct-Zol RNA Miniprep kit (Zymo Research, Irvine, CA) and reverse transcribed into cDNA via the High Capacity cDNA Reverse Transcription Kit (Thermo Fisher Scientific, Waltham, MA) according to manufacturer's instructions. Expression levels for *hsp-70* (C12C8.1), *hsp-16.2* (Y46H3A.3), *jmjd-3.1*(F18E9.5) were analyzed via qPCR using the Step-One Plus Real-time PCR machine (Applied Biosystems, Waltham, MA) using the the $\Delta\Delta C_t$ method. The housekeeping gene *cdc-42* (R07G3.1) was used for normalization. qPCR analysis reflect three biologically replicate trials. Significance was determined by conducting a One-Way ANOVA using GraphPad Prism (GraphPad Software, www.graphpad.com) followed by a Tukey post-hoc test comparisons of all columns.

Results

p38 MAPK Signaling

In our previous studies we show that HSF-1::GFP nSBs may be regulated by the presence of the germline. Specifically, animals that had the germline genetically removed via the *glp-1* (e2144) mutant background displayed HSF-1::GFP diffusely throughout hypodermal cells during the transition to adulthood. Whereas in worms with the wildtype *glp-1* background these cells displayed an increase in nSBs suggesting a disruption of proteostasis. To identify genetic interactors that may support the *glp-1*(e2144) mediated phenotype, we first examined the role of p38 MAPK signaling. We found that when HSF-1::GFP; *glp-1*(e2144) animals were crossed to mutants for *pmk-1* (km25) this suppressed the effect of *glp-1*(e2144) on HSF-1::GFP localization (Figure 6.1). In these double mutants we observed an increase in cells displaying HSF-1::GFP nSBs during the transition to adulthood. This suggests that p38 MAPK signaling may regulate HSF-1 localization in *C. elegans*.

SIR-2.1 Overexpression may support diffuse nuclear HSF-1::GFP during the transition to adulthood which requires *jmjd-3.1*

Previous literature has suggested that sirtuins may play important roles in regulating cell survival, longevity, pathogen resistance, and abiotic stress resistance. In *C. elegans*, it has been demonstrated that SIR-2.1 overexpression can extend worm lifespan relative to wildtype and promote increases stress resistance. In this study we crossed our HSF-1::GFP CRISPR/Cas9 model animals to an integrated SIR-2.1 overexpression strain and monitored for the presence or absence of HSF-1::GFP nSBs in hypodermal cells

across the transition to adulthood. We find that SIR-2.1 overexpression is able to suppress the formation of HSF-1::GFP nSBs during the this time period and that this may require *jmjd-3.1* expression (Figure 6.2).

Insulin Signaling may regulate HSF-1::GFP localization during the transition to adulthood

Disruptions to insulin/insulin-like signaling is one of the most well studied and verified mechanisms to extend lifespan and stress resistance in *C. elegans*. The HSR has already been shown to be regulated by IIS, but how this may alter HSF-1 localization is still unknown. To modulate IIS, we crossed the *daf-2(e1370)* mutant into our CRISPR/Cas9 HSF-1::GFP model. In this mutant background the key IIS receptor is functionally null which is thought to disrupt a downstream kinase cascade. We compared this mutant background to wildtype *daf-2* and monitored for the presence or absence of HSF-1::GFP nSBs in hypodermal cells across the transition to adulthood. Interestingly, we find that *daf-2* mutants do have a decreased amount of HSF-1::GFP nSBs relative to wildtype, but also do not completely retain the more youthful phenotype (Figure 6.3).

HSB-1 negatively regulates HSF-1::GFP nSBs

hsb-1 has been reported to negatively regulate the HSR by binding to active trimeric HSF-1 [66]. We tested how *hsb-1* or other genes, all *hsps*, that may potentially interact with HSF-1::GFP and regulate HSF-1::GFP localization and found that only *hsb-1* knockdown lead to an increase in cells with nSBs present (Figure 6.4. Next, we examined how HSF-1::GFP localization is altered during the recovery phase of a

thermal stress with or without a *hsb-1* mutant background. Interestingly, we find that *hsb-1* mutants show a delay in the speed of recovery as well as displaying an increased number of cells exhibiting HSF-1::GFP nSBs relative to wildtype in the non-stressed condition (Figure 6.5).

This presented an interesting result as previous data suggests prolonged HSF-1 nSBs reduces HSR induction and as a result is detrimental for cell survival. We were able to find negative effects on *C. elegans* growth and reproduction. Growth in the *hsb-1* mutant background measured along the longitudinal midline was modestly reduced, but found to be statistically significant (Figure 6.6). We also observed an increase in the number of apoptotic germline cells utilizing an YFP::ACT-5 reporter strain (Figure 6.7A-D) and a significantly reduced brood size (Figure 6.7E) [210, 211]. Lastly in reproduction, in the *hsb-1* mutant, we also observed the appearance of dead eggs after a standard hypochlorite synchronization and overnight hatch which could not be found in the wildtype genetic background (Figure 6.8).

However, previous analysis of *hsb-1* mutants in *C. elegans* have reported increased HSF-1 target *hsp* induction relative to wildtype in the non-stressed conditions which we also confirmed (Figure 6.9 A/B). Given this information, we suspected that there may be compensatory gene expression that allows for a more robust HSR despite the presence of HSF-1 nSBs. We find that in the *hsb-1* mutant background there is a higher expression of *jmjd-3.1* (Figure 6.9 C) which is conserved lysine demethylase previously shown to regulate the HSR in *C. elegans* [61]. This increase in *hsp* expression also was found to be dependent on *jmjd-3.1* (Figure 6.9D)

Discussion

Our data presents multiple genetic pathways converging to regulate HSF-1::GFP nSBs during the transition to adulthood. This timepoint in early *C. elegans* aging is becoming a focal point of understanding what gene expression changes may set the determination of longevity at the whole-organism level [212]. Given this important time point we sought to examine the contribution of different longevity mediating pathways on their ability to regulate HSF-1::GFP nSBs during the transition to adulthood. In our previous study, the data suggested that during normal aging there is an increase in the presence of HSF-1::GFP nSBs between the L4 stage to gravid adults. This coincides with a dramatic decline in the robustness of induction of the HSR and a collapse in proteostasis reported by multiple groups. The genetic mutant *glp-1* (e2144) has been shown to rescue proteostasis during this timepoint through the use of metastable protein folding reporters [90]. Indeed, we show that in the *glp-1* mutant background HSF-1::GFP animals did not display an increase in nSBs relative to wildtype *glp-1* individuals. This suggested that genetic loss of the germline may regulate HSF-1::GFP to keep it diffuse and hypothetically more active. This posed the next question as to what molecular signaling may be supporting this result? We examined the contribution of the conserved p38 MAPK pathway by introducing a *pmk-1* (MAPK) mutation into the HSF-1::GFP; *glp-1* (e2144) animals and examining if the protection conferred by the *glp-1* mutation was lost. We found that *pmk-1* was required for *glp-1* mediated protection as these double mutants displayed an increased level of HSF-1::GFP nSBs. The mammalian literature suggests that HSF1 is a substrate of p38 MAPK signaling so one interpretation of our result may indicate that there may be increase HSF-1 phosphorylation by p38 MAPK

signaling in the *glp-1* mutant background which enables it to remain diffuse in the nucleus and support the HSR and proteostasis [27].

Sirtuin signaling is a well conserved pathway to enhance longevity in many metazoan species. It has been shown to be required in dietary restriction as a means to enhance healthy aging in many species including *C. elegans*, *Drosophila*, and *S. cerevisiae* [213]. Sirtuin substrates include histone proteins, but many non-histone proteins including centrosome protein Plk2 and DNA methyltransferase DNMT1, and importantly HSF-1 [31, 214, 215]. In the worm, SIR-2.1 expression can be upregulated by dietary restriction and SIR-2.1 mediated longevity requires stress responsive transcription factors including HSF-1 [84]. We hypothesized that this enhancement of longevity may be reflected in the localization of HSF-1. When SIR-2.1 overexpression mutants were crossed to our HSF-1:GFP model we found that across the transition to adulthood hypodermal cells were not significantly changed in the appearance of HSF-1::GFP nSBs relative to wildtype. Interestingly, this suppression of nSBs required the lysine demethylase *jmjd-3.1*. It was reported that in a wildtype animals *jmjd-3.1* expression normally decreases across this period [61]. Our data may suggest that SIR-2.1 overexpression is able to maintain sufficient *jmjd-3.1* expression to support proteostasis and lifespan. Further research is required to examine this relationship as a novel mechanism of lifespan regulation in *C. elegans*.

Disruptions to IIS has been one method to improve *C. elegans* lifespan and stress resistance that has been confirmed by many independent research groups [73, 208]. It has been shown that in mutants that have a non-functional IIS receptor or null mutants in the downstream signaling cascade stress pathways are enhanced and confer

increased stress resistance and longevity to *C. elegans*. In particular, multiple *hsf-1* dependent *hsps* are enhanced which led us to hypothesize whether or not there would be any observable differences in HSF-1::GFP localization. As stated above, the transition to adulthood is a critical point in the worm lifespan so we utilized the *daf-2* mutant to examine if in this genetic background HSF-1::GFP localization can be regulated across the transition. We found that *daf-2* (e1370) does indeed decrease the prevalence of hypodermal cells displaying HSF-1::GFP nSBs, but it was not able to completely retain the more youthful phenotype. This result may suggest other parallel mechanisms to regulate HSF-1::GFP localization and requires further investigation.

The literature suggests that HSB-1 or its mammalian homolog HSBP-1 bind to and suppress HSF-1 activity only during its active trimeric phase. We found it interesting that knockdown of *hsb-1* or within a mutant *hsb-1* (ch116) background HSF-1::GFP was found to have increased nSBs when it may be thought that this is only found in stressed cells. This result throws into question the function, if any, that HSF-1 nSBs may have when present in the cell. We observed that HSF-1::GFP animals carrying the mutant *hsb-1* (cg116) also had a delay in restoring HSF-1::GFP back to its diffuse non-stressed appearance. Recently, cells displaying prolonged HSF-1 nSBs were suggested to be more susceptible to stress, yet it has already been reported that *hsb-1* mutant worms are more stress resistant and have an increased lifespan [45, 70]. We hypothesized that there may be an underlying mechanism(s) to circumvent and deleterious effects of prolonged HSF-1::GFP nSBs in *C. elegans*. We found that the expression of *jmjd-3.1* was significantly upregulated in the *hsb-1* mutant background. The literature suggests that this gene normally decreases in expression in wildtype animals, and can

specifically regulate the expression of *hsf-1* dependent *hsps* [61]. Taken together, this may suggest that while there are increased HSF-1::GFP nSBs the increased expression of *jmjd-3.1* allows for an enhanced HSR that supports the increased stress resistance and longevity previously reported. However, one area that remains to be addressed is what factors may be regulating *jmjd-3.1* expression itself. Elucidating this genetic regulation may shed insights into novel mechanisms of the regulation of stress resistance and aging in *C. elegans*

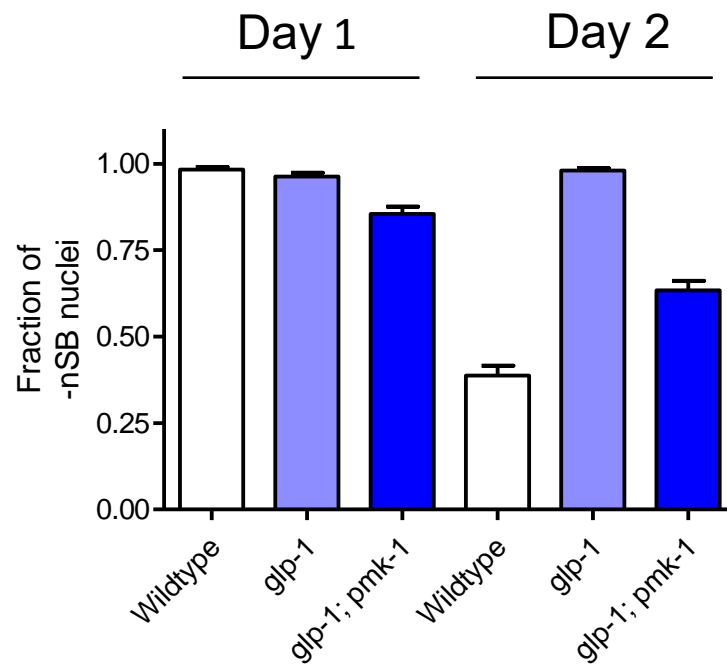


Figure 6.1 - p38 MAPK Signaling May Support the HSR in Germline Lacking *C. elegans*. Hypodermal nuclei from SDW015 (HSF-1::GFP), SDW050 (HSF-1::GFP; *glp-1*(e2144)), and SDW123 ((HSF-1::GFP; *glp-1*(e2144); *pmk-1* (km25)) were scored for the appearance of nSBs in at day 1 (L4) and gravid adult (day 2) the fraction of those containing no nSBs was calculated and plotted in GraphPad Prism for n≥8 replicate worms.

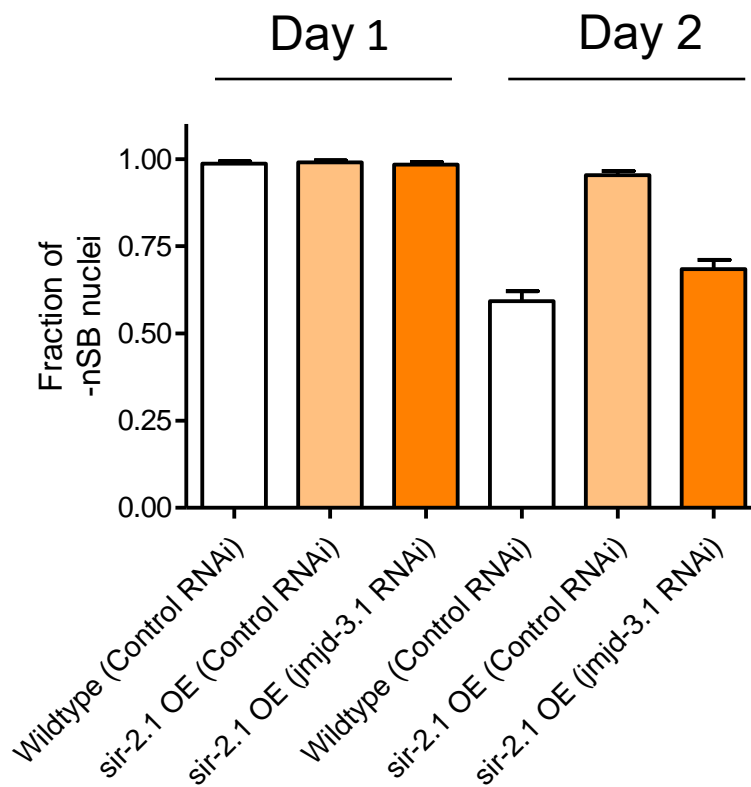


Figure 6.2 – SIR-2.1 Overexpression May Support Diffuse Nuclear HSF-1::GFP During the Transition to Adulthood Which Requires *jmid-3.1*. Hypodermal nuclei from SDW015 (HSF-1::GFP) and SDW122 (HSF-1::GFP; SIR-2.1 OE) with control RNAi or *jmid-3.1* RNAi were scored for the appearance of nSBs in at day 1 (L4) and gravid adult (day 2) the fraction of those containing no nSBs was calculated and plotted in GraphPad Prism for n≥8 replicate worms.

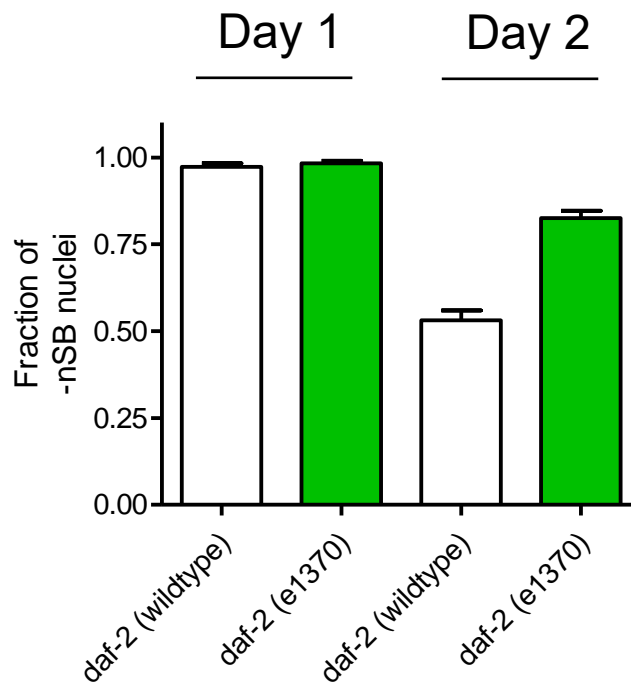


Figure 6.3 – Insulin Signaling May Regulate HSF-1::GFP ILocalization During the Transition to Adulthood. Hypodermal nuclei from SDW015 (HSF-1::GFP) and SDW130(HSF-1::GFP; *daf-2*(e1370)) were scored for the appearance of nSBs in at day 1 (L4) and gravid adult (day 2) the fraction of those containing no nSBs was calculated and plotted in GraphPad Prism for n≥8 replicate worms.

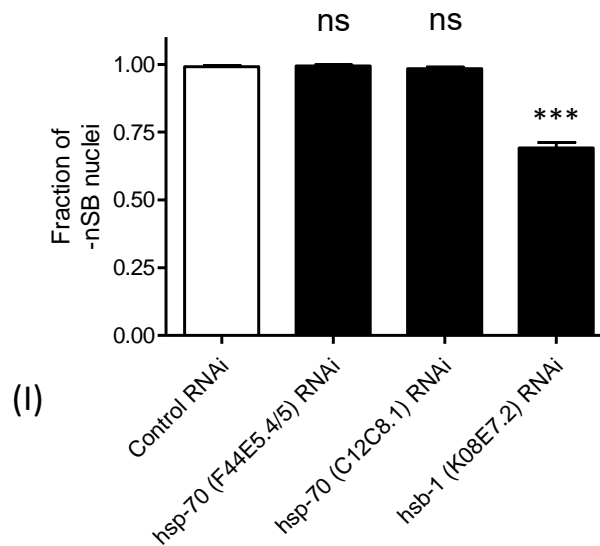
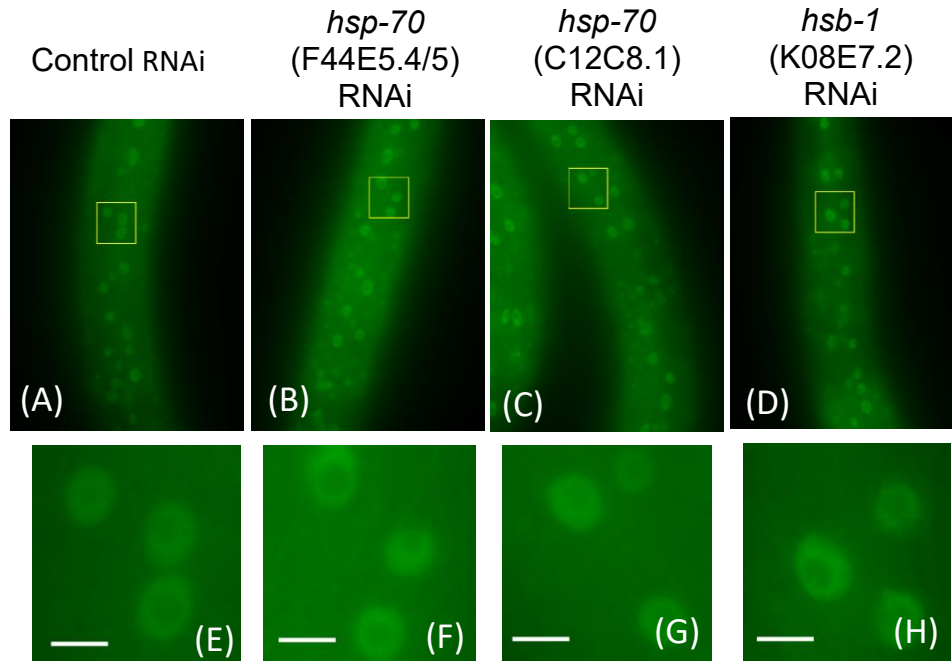


Figure 6.4 – *hsb-1* Negatively Regulates HSF-1::GFP nSBs. SDW015 (HSF-1::GFP) animals were grown with control RNAi (A/E), *hsp-70* (F44E5.4/5) RNAi (B/F), *hsp-70* (C12C8.1) RNAi (C/G), or *hsb-1* (K08E7.2) RNAi (D/H) from L1 to L4 and then hypodermal nuclei from were scored for the appearance of nSBs and the fraction of those containing no nSBs was calculated and plotted in GraphPad Prism (I). for $n \geq 8$ replicate worms. Scale bar in zoomed images (E-H) represent 5 microns. Statistical significance was assessed by comparing all conditions to control RNAi, “***” represents $p < 0.0001$

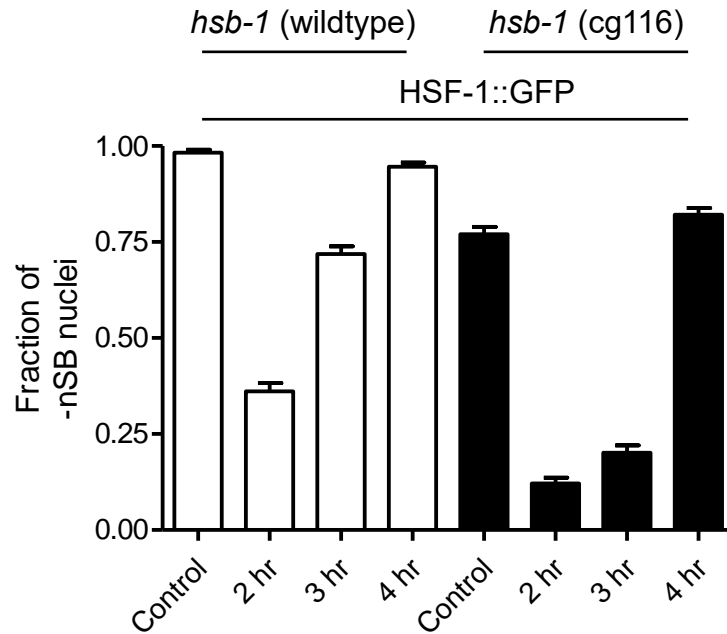
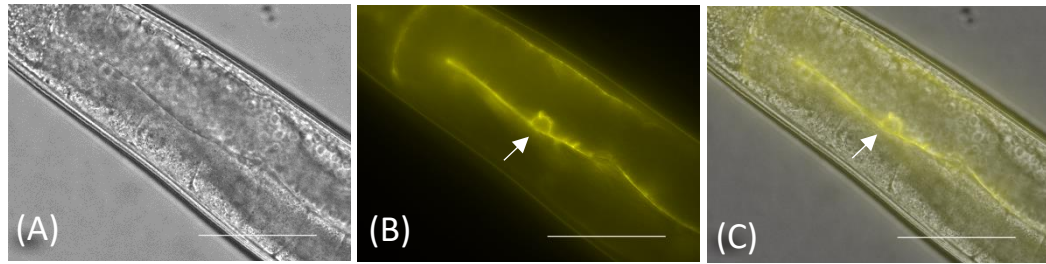


Figure 6.5 – *hsb-1* delays full recovery of HSF-1::GFP nSBs Following Heat Shock. SDW015 (HSF-1::GFP) and SDW101 (HSF-1::GFP; *hsb-1* (cg116)) animals were subjected to a 35°C HS for 2 hours and then immediately recovered at 20°C. Animals were imaged after 2, 3, and 4 hours of recovery at 20°C. Hypodermal nuclei from were scored for the appearance of nSBs and the fraction of those containing no nSBs was calculated and plotted in GraphPad Prism.



lim-7p::YFP::act-5 (Actin)

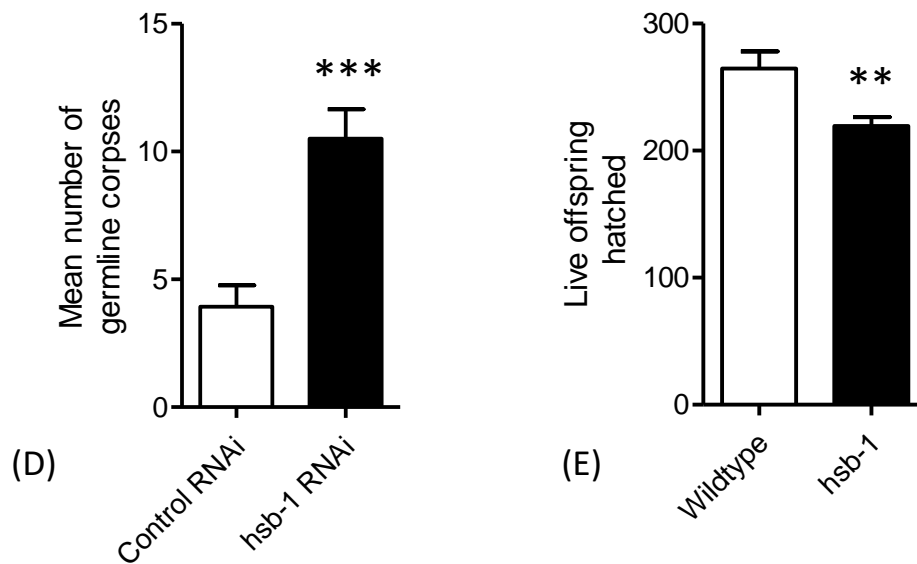


Figure 6.7 – *hsb-1* Regulates Germline Apoptosis and Brood Size. (A/B/C) Brightfield, fluorescence, and merged images of WS2170 (*opls110* [*lim-7p::YFP::actin* + *unc-119(+)*] IV.) in control conditions display the presence of germline cells undergoing apoptosis (white arrow) following engulfment by YFP::ACT-5. Scale bar represents 50 microns. (D) WS2170 animals were grown for 3 days from L1 in control RNAi or *hsb-1* RNAi, the number of germline corpses was then counted for n=14 replicate animals per condition. Total number of germline corpses were plotted using GraphPad Prism and analyzed with a t-test, “***” indicates p<0.0001. (E) Wildtype or *hsb-1* (*cg116*) animals were grown on OP50-1 plates to L4 and then a single worm was assessed for the number of hatched offspring produced for the next 5 days of adulthood, n=12 per condition. Hatched offspring totals were then plotted in GraphPad Prism and analyzed with a t-test, “***” indicates p<0.001.

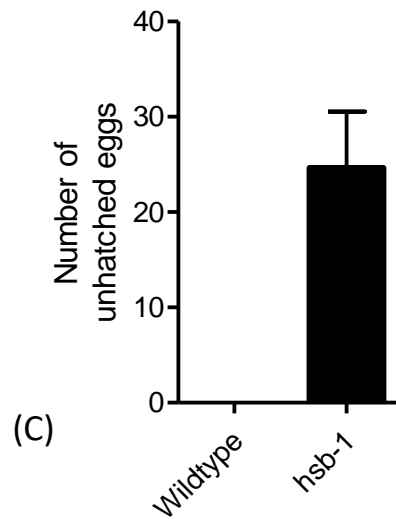
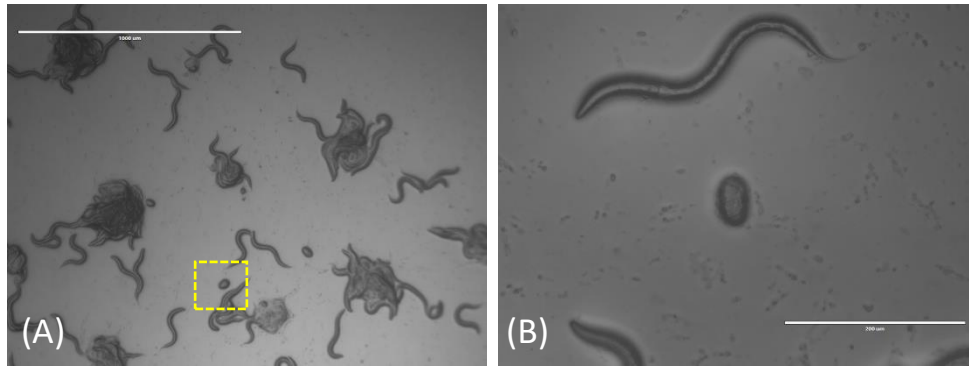


Figure 6.8 – *hsb-1* May Regulate Embryogenesis in *C.elegans*. (A/B) Brightfield images of *hsb-1*(cg116) animals following a standard hypochlorite synchronization and overnight hatching show the presence of un-hatched eggs. Scale bar in A represents 1000 microns, scale bar in B represents 400 microns. No un-hatched eggs were visible on wildtype plates following synchronization to be imaged. (C) Wildtype or *hsb-1* (cg116) animals were synchronized by standard hypochlorite treatment and washed eggs were deposited on an unseeded NGM plate and left to hatch overnight. Three replicate drops of eggs were outlined prior to hatching and the number of un-hatched eggs the following day were counted and plotted in GraphPad Prism.

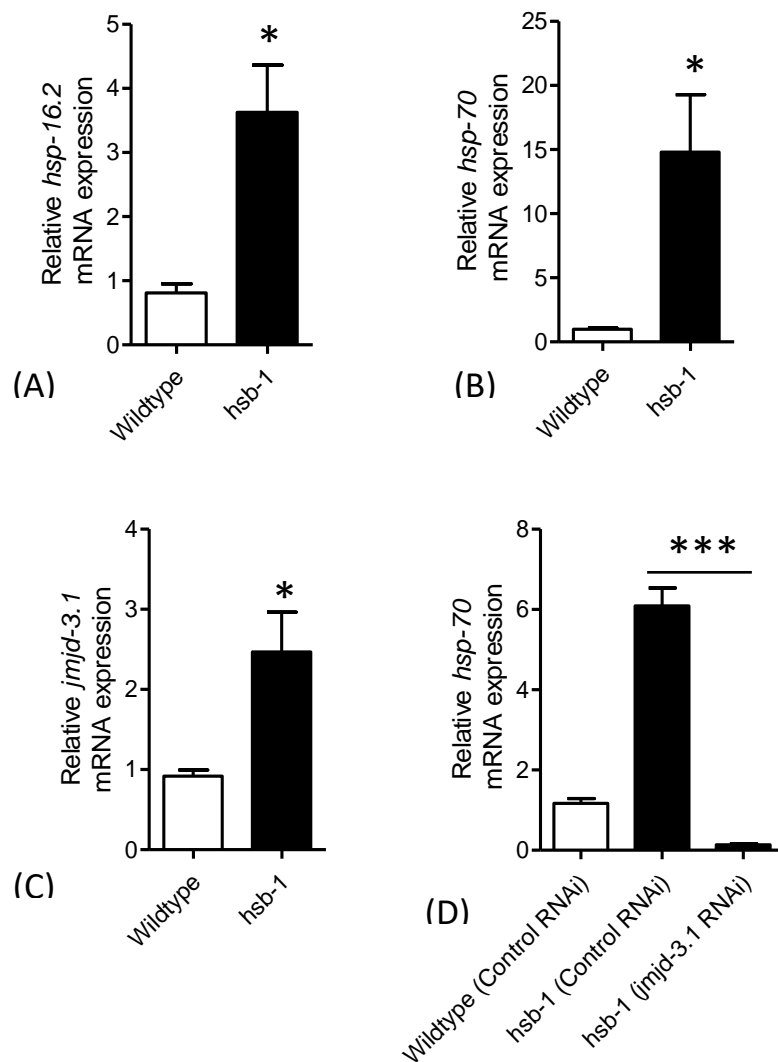


Figure 6.9 – *hsb-1* Negatively Regulates *hsf-1* Target *hsp* Expression Dependent on *jmjd-3.1*. (A/B/C) Wildtype or *hsb-1*(cg116) mutant animals were grown on OP50-1 plates to the L4/YA stage and then subjected to RNA extraction for qRT-PCR analysis of *hsp-16.2*, *hsp-70* (C12C8.1), and *jmjd-3.1* mRNA expression, significance was calculated using a t-test in GraphPad Prism and is indicated relative to wildtype, "*" indicates $p < 0.05$. (D) Wildtype or *hsb-1*(cg116) mutant animals were grown on control RNAi or *jmjd-3.1* RNAi where indicated and then subjected to RNA extraction for qRT-PCR analysis of *hsp-70* (C12C8.1) mRNA expression, significance was calculated using a One-Way ANOVA followed by a Tukey post-hoc test of all comparisons, significance between *hsb-1* (cg116) mutants in control RNAi and *jmjd-3.1* RNAi is indicated, "****" $p < 0.0001$.

Chapter 7

Implications and Future Directions

HSF-1 localization in *C. elegans*

Our data suggests that HSF-1 in *C. elegans* undergoes distinct changes in localization very early in adulthood. However, there are many unresolved questions that remain. For example, the appearance of nSBs may indicate the collapse in proteostasis, but what is the physical state of HSF-1 in *C. elegans* cells at this timepoint? Because recent data suggests that HSF-1::GFP in nSBs may represent a liquid-solid phase transition in the cell, it would be pertinent to examine what state HSF-1::GFP is in during the transition to adulthood [216]. Additionally, we also observe that HSF-1::GFP remains predominantly in nSBs during aging. Is HSF-1::GFP in these cells also trapped as solid aggregates which do not function in the HSR? Fluorescence microscopy utilizing Fluorescent recovery after photobleaching (FRAP) will be key to understand these questions. FRAP is a microscopy technique that allows you to examine the physical state of fluorophores by first using laser light to eliminate any fluorescence from the protein (photobleaching). If the protein is capable of being restored to function, in this case still functional in the liquid phase of the cell, it can recovery its fluorescent

properties and be imaged again. Using this technique at multiple timepoints in aging or stress conditions may be able to confirm what physical state or how functional HSF-1::GFP may be.

Understanding what elicits nSBs themselves is also an outstanding question in the literature. For example, we have also observed the appearance of HSF-1::GFP nSBs within the germline in the mitotic region. Because HSF-1 nSBs are usually associated with increases in HSF-1 activity, does mitosis require increased HSF-1 activity? Or is the HSR responding to a stress induced by mitosis? Further probing of HSF-1 target genes in these cells with standard gene expression approaches including gene knockdown via RNAi, mutant analysis, and overexpression coupled to mRNA expression analysis may give insight into these questions.

Beyond these unanswered questions, our CRISPR/Cas9-based model indicates that HSF-1::GFP is expressed in all cell types examined, highlighting the importance of HSF-1 to cellular function. Because of the various functions of each cell type, it is unlikely that HSF-1 regulation is similar in each one. Our work already demonstrates that one tissue type appears to react differently than another very early in aging. The data suggests that, in *C. elegans*, neurons do not exhibit any HSF-1::GFP nSBs during the transition to adulthood. But they may be induced during this timepoint with a thermal stress. This may suggest that neurons are not undergoing age-related changes similar to other tissues like the hypodermis, intestine, and germline at this timepoint. This may be addressed with tissue-specific analysis to identify the differences in each cell type and elucidate novel mechanisms of aging.

Previous literature has already confirmed the existence of both cell autonomous and non-cell autonomous regulation of HSR activity [55, 217, 218]. For example, neuronal activation via heat stress or optogenetic methods is capable of signaling to the germline and causing the induction of HSF-1 nSBs in developing germ cells [55]. In the worm, it was also found that the thermosensory neurons are required to mount a full induction of the HSR [219]. Furthermore, neuroendocrine signals may also regulate the HSR. It was shown that, in Wistar rats, higher levels of the stress hormone cortisol show increased expression of active trimeric HSF1 and HSP70 expression levels in adrenal glands [220]. The worm is well suited for tissue-specific aging studies to address these questions. There may be age-related or disease specific changes to these tissues or organs which then lead to systemic dysregulation of the HSR at the organismal level. Further research to understand how these mechanisms act on HSF-1's activity or localization will yield valuable insights into how the HSR is regulated.

PYP-1 as a Regulator of the HSR

The data we have collected suggests that *pyp-1* does regulate the HSR, but needs to be suppressed prior to the transition to adulthood to manifest its effects. In our first experiments, we show that knockdown from L1 leads to the upregulation of HSF-1 dependent transcriptional reporters assessed during the first day of adulthood. If the knockdown is given for the same length of time starting at the first day of adulthood, we do not observe a similar negative regulation in the transcriptional reporter. This suggests that temporal regulation of the HSR may be critical. This is a unique situation among those HSR regulators described in the literature thus far. PYP-1 is a component of the NuRF complex which regulates many cellular processes. It may also suggest a

larger implication that particular genes may regulate the HSR within a particular temporal point in aging. The worm is very amenable to genetic screening approaches and has been used to screen for proteostasis regulators in disease models as well as other HSR regulator candidates.

Our results hint at a possibility that some of these genes may be regulating the HSR depending on the specifics of how each screen was conducted such as the timing of RNAi or developmental stage when scored. Some data already suggests a tissue-specific network of HSR regulators and it may also be possible to sort genetic regulators by developmental stage as well [221]. How might the lack of sufficient PYP-1 expression lead to the activation of HSF-1? To address these questions some preliminary experiments may be insightful to refine the understanding of *pyp-1*'s effect on the HSR. Does *pyp-1* expression normally change during the transition to adulthood? Because we noted the effect across the transition to adulthood, is there a change in expression of *pyp-1* during this timepoint that we perturbed in our experiments which led to an increase in HSF-1 activity? Measuring *pyp-1* expression with standard techniques may resolve this question. Additionally, in what tissues is *pyp-1* acting to regulate the HSR? We may address where is *pyp-1* normally expressed using CRISPR/Cas9 fluorescent tagging. Knocking in a fluorescent tag would provide the insight to its expression *in vivo* as well as give the ability to track its expression across the transition to adulthood.

Another area of interest that arose in this project was the contribution of lipids to potentially regulating the HSR. One area that this has already been studied in is the composition of membrane lipids in regulating the HSR in plants, cyanobacteria, and

yeast. It has been shown that alterations leading to the increase in saturated fatty acids enhances regulates mRNA expression changes during heat shock in *S. cerevisiae* [222]. Relatedly, modulating the composition of plant membrane lipid compositions has also been shown to regulate *hsp* expression. In particular, the composition of one particular class of lipid, phosphatidylglycerol, is thought to manipulate membrane fluidity and affect temperature sensing [223]. These changes to membrane lipid composition may also be an adaptive mechanism to tolerate high temperatures as it was shown that chronic stress alters membrane lipid composition, but not necessarily from the result of an acute thermal shock [224]. In *C. elegans*, it has been shown that long-lived mutants alter the ratio of polyunsaturated fatty acids to monounsaturated fatty acids which is thought to lead to less oxidative stress prolonging lifespan [225, 226]. This oxidative metric can be quantified and is termed the peroxidizability index (PI) and refers to the number of unsaturated bonds in the lipids present [227]. Having a low PI has been shown to be present in long-lived animals including natural variants of wildtype rats, naked mole rats, and many other mammalian species [228-230]. It remains unknown whether or not *pyp-1* may regulate these processes as an indirect method to regulate the HSR in *C. elegans*. Furthermore, our data suggests that while *pyp-1* knockdown was sufficient to induce HSF-1 dependent transcriptional reporter activity, the lack of any apparent lifespan extension conferred by this regulation raises the question of whether other mechanisms of HSF-1 activation are present in *pyp-1* deficient animals.

O-GlcNAc Cycling as a Regulator of the HSR

Our data so far indicates that modulating global O-GlcNAc cycling regulates HSF-1 activity, but how and in which tissues remains incomplete. We have shown that in L4

animals intestinal HSF-1 appears to have localization changes compared to the hypodermis, but it may also be important to assess other tissues. Examining HSF-1::GFP expression in the neuronal cells, body wall muscle, and other cells may give insight into how O-GlcNAc cycling is regulating the HSR. One important question to address is whether or not *C. elegans*' HSF-1 is itself O-GlcNAcylated. To address this, employing immunoprecipitation followed by western blotting with O-GlcNAc antibodies or mass spectrometry could resolve this question. HSF-1 is an extensively phosphorylated protein which has been shown to regulate its activity. If O-GlcNAc modifications are competing for similar serine or threonine residues it raises important questions as to how O-GlcNAc modification at those sites regulate HSF-1 activity [32]. We also noted a general pattern of young worms showing increases in the HSR with both global hyper and hypo-O-GlcNAcylation whereas older worms had reciprocal effects. How might young cells generally activate HSF-1 in this manner? One interpretation of these results could suggest additional layers of regulation indicating O-GlcNAc regulating other HSF-1 modifying genes in youth vs adulthood. To examine this it may be insightful to examine upstream HSF-1 regulators such as kinase and acetylation modifying enzymes for O-GlcNAcylation.

Collagen and the Cuticle as a Regulator of the HSR

Our data suggests that similarly to regulating osmotic stress and oxidative stress collagen/cuticle gene expression may also regulate the HSR [138, 140]. The exact mechanism of each regulator may be very distinct. As described the different effects of each gene can range from leading to morphological changes in the cuticle, cuticle permeability, chromatin changes, and oxidative changes [194, 196, 199, 231]. For

example, within the genes that when disrupted lead to loss of cuticle furrows or changes in alae morphology, is this morphological change itself sufficient to regulate *hsf-1* activity? The epidermis and cuticle of the worm which is composed of over 150 collagen genes serves as the essential barrier to protect the animal. It has been reported that defects to this barrier function may compromise osmotic balance, pathogen resistance, and neuronal function [232]. Osmotic stress has been shown to lead to changes in intracellular osomolyte concentrations where namely glycerol expression is enhanced [233]. Our previous data shows that the HSR may indeed respond to osmotic changes as shown by the formation of HSF-1::GFP nSBs during osmotic stress. Next, genetic changes to the cuticle composition have been shown to alter the worm's ability to resist pathogens [234]. While we have not used a specific human related pathogen, it is thought that even the laboratory strain of *E. coli* OP50 worm research commonly uses can act as a pathogen. Our candidate regulators may function to compromise the worm cuticle and initiate a mild pathogen response which the HSR is known to regulate in *C. elegans* [146, 156]. Specific worm neurons become embedded in the cuticle during development including the mechanosensory neurons ALM and PLM [235]. Changes to the structure of the cuticle may then regulate neuronal function and this could be transmitted to distal tissues through already established mechanisms of non-cell autonomous signaling in the HSR [56, 217]. It is important to recognize that this data is still very preliminary. The data from our subscreen indicates that these candidate regulator components of the worm cuticle may regulate the HSR as measured through a transcriptional reporter system. It will be extremely important to verify these candidate regulators act through *hsf-1* as some regulators have already

been described in the literature to act through alternative cell stress pathways. Nevertheless, those candidates can be readily verified with the use of *hsf-1* RNAi or through an *hsf-1* mutant background. For those genes that appeared to enhance *hsf-1* activity it would be interesting to determine if HSP expression is also upregulated. If so, it would suggest that modulation of cuticle/collagens may be an untapped avenue to enhance proteostasis and longevity.

HSB-1 as a Regulator of the HSR

Our data suggests that *hsb-1* may regulate the expression of a known chromatin regulator of the HSR *jmjd-3.1*. Other studies have indicated that enhanced *jmjd-3.1* expression through exogenous transgenic models is able to suppress the decline in proteostasis during early aging in *C. elegans*. This increase in expression may represent a novel mechanism of action in *hsb-1* mediated lifespan regulation and potential therapeutic avenues to enhance longevity through *hsb-1* suppression. The worm is an excellent genetic model to identify candidate regulators of the increased *jmjd-3.1* expression. This may shed novel insights into other genetic regulators of aging. However, *hsb-1* and its mammalian counterpart HSBP-1 are still understudied genes in the literature. The relationship between HSB-1 and HSF-1 during stress and aging still warrants further investigation. For example, during conditions in which HSF-1 is activated such as thermal stress or other disruptions to proteostasis HSF-1 may form nSBs that in some species represent fully active trimeric HSF-1. Given that the constituents of these nSBs are not well defined, and previous research suggests that HSBP-1 interacts with active trimeric HSF-1 it would be pertinent to examine if HSBP-1/HSB-1 are part of these structures to further understand the regulation of HSF-1

localization. Furthermore, our data suggests that cells deficient of HSB-1 contain HSF-1::GFP nSBs in the absence of stress, and experience a delay in recovery of HSF-1::GFP nSBs after thermal stress. This increased presence of HSF-1::GFP nSBs may suggest an overall less active HSR given the data involving HSF-1 solid/liquid phase transitions, but it has been reported that *hsb-1* mutant worms have increased stress resistance and longevity dependent on *hsf-1* [45, 69]. This conflict suggests that further research be performed to identify the components of the HSF-1 nSBs in these genetic mutant backgrounds to further understand the regulation of the HSR. Lastly, we show that hypodermal cells deficient of *hsb-1* exhibit increased HSF-1::GFP nSBs. Our previous data with aging HSF-1::GFP animals in an otherwise wildtype genetic background suggest that different tissues display a tissue-specific pattern of HSF-1::GFP nSBs upon the transition to adulthood. Many other studies have indicated that this early aging timepoint is associated with a diverse array of gene expression changes. It may be informative to investigate *hsb-1* expression across the worm's tissues to potentially reveal a novel mechanism of age-related HSF-1 nSBs regulation.

References

1. De Maio, A., et al., *Ferruccio Ritossa's scientific legacy 50 years after his discovery of the heat shock response: a new view of biology, a new society, and a new journal*. Cell Stress and Chaperones, 2012. **17**(2): p. 139-143.
2. Ritossa, F., *A new puffing pattern induced by temperature shock and DNP in Drosophila*. Experientia, 1962. **18**(12): p. 571-573.
3. Georgopoulos, C. and W. Welch, *Role of the major heat shock proteins as molecular chaperones*. Annual review of cell biology, 1993. **9**(1): p. 601-634.
4. Ohtsuka, K. and M. Hata, *Molecular chaperone function of mammalian Hsp70 and Hsp40-a review*. International Journal of Hyperthermia, 2000. **16**(3): p. 231-245.
5. Parker, C.S. and J. Topol, *A Drosophila RNA polymerase II transcription factor binds to the regulatory site of an hsp 70 gene*. Cell, 1984. **37**(1): p. 273-283.
6. Wiederrecht, G., et al., *The Saccharomyces and Drosophila heat shock transcription factors are identical in size and DNA binding properties*. Cell, 1987. **48**(3): p. 507-515.

7. Goldenberg, C., et al., *Purified human factor activates heat shock promoter in a HeLa cell-free transcription system*. *Journal of Biological Chemistry*, 1988. **263**(36): p. 19734-19739.
8. Eggers, D.K., W. Welch, and W. Hansen, *Complexes between nascent polypeptides and their molecular chaperones in the cytosol of mammalian cells*. *Molecular biology of the cell*, 1997. **8**(8): p. 1559-1573.
9. Frydman, J., et al., *Folding of nascent polypeptide chains in a high molecular mass assembly with molecular chaperones*. *Nature*, 1994. **370**(6485): p. 111-117.
10. Schmitt, M., W. Neupert, and T. Langer, *The molecular chaperone Hsp78 confers compartment-specific thermotolerance to mitochondria*. *The Journal of cell biology*, 1996. **134**(6): p. 1375-1386.
11. Jackson, S.E., *Hsp90: structure and function*, in *Molecular chaperones*. 2012, Springer. p. 155-240.
12. Fan, C.-Y., S. Lee, and D.M. Cyr, *Mechanisms for regulation of Hsp70 function by Hsp40*. *Cell stress & chaperones*, 2003. **8**(4): p. 309.
13. Neudegger, T., et al., *Structure of human heat-shock transcription factor 1 in complex with DNA*. *Nature structural & molecular biology*, 2016. **23**(2): p. 140.
14. Damberger, F.F., et al., *Solution structure of the DNA-binding domain of the heat shock transcription factor determined by multidimensional heteronuclear magnetic resonance spectroscopy*. *Protein Science*, 1994. **3**(10): p. 1806-1821.

15. Harrison, C.J., A.A. Bohm, and H. Nelson, *Crystal structure of the DNA binding domain of the heat shock transcription factor*. Science, 1994. **263**(5144): p. 224-227.
16. Vuister, G.W., et al., *Solution structure of the DNA-binding domain of Drosophila heat shock transcription factor*. Nature structural biology, 1994. **1**(9): p. 605-614.
17. Peteranderl, R. and H.C. Nelson, *Trimerization of the heat shock transcription factor by a triple-stranded. alpha.-helical coiled-coil*. Biochemistry, 1992. **31**(48): p. 12272-12276.
18. Rabindran, S.K., et al., *Regulation of heat shock factor trimer formation: role of a conserved leucine zipper*. Science, 1993. **259**(5092): p. 230-234.
19. Westwood, J.T. and C. Wu, *Activation of Drosophila heat shock factor: conformational change associated with a monomer-to-trimer transition*. Molecular and Cellular Biology, 1993. **13**(6): p. 3481-3486.
20. Björk, J.K. and L. Sistonen, *Regulation of the members of the mammalian heat shock factor family*. The FEBS journal, 2010. **277**(20): p. 4126-4139.
21. Mathew, A., et al., *Analysis of the mammalian heat-shock response*, in *Stress Response*. 2000, Springer. p. 217-255.
22. Sandqvist, A., et al., *Heterotrimerization of heat-shock factors 1 and 2 provides a transcriptional switch in response to distinct stimuli*. Molecular biology of the cell, 2009. **20**(5): p. 1340-1347.
23. Korfanty, J., et al., *Crosstalk between HSF1 and HSF2 during the heat shock response in mouse testes*. The international journal of biochemistry & cell biology, 2014. **57**: p. 76-83.

24. Soncin, F., et al., *Transcriptional activity and DNA binding of heat shock factor-1 involve phosphorylation on threonine 142 by CK2*. Biochemical and biophysical research communications, 2003. **303**(2): p. 700-706.
25. Murshid, A., et al., *Protein kinase A binds and activates heat shock factor 1*. PloS one, 2010. **5**(11).
26. Holmberg, C.I., et al., *Phosphorylation of serine 230 promotes inducible transcriptional activity of heat shock factor 1*. The EMBO journal, 2001. **20**(14): p. 3800-3810.
27. Naidu, S.D., et al., *Heat shock factor 1 is a substrate for p38 mitogen-activated protein kinases*. Molecular and cellular biology, 2016. **36**(18): p. 2403-2417.
28. Kim, S.-A., et al., *Polo-like kinase 1 phosphorylates heat shock transcription factor 1 and mediates its nuclear translocation during heat stress*. Journal of Biological Chemistry, 2005. **280**(13): p. 12653-12657.
29. Wang, X., et al., *Phosphorylation of HSF1 by MAPK-activated protein kinase 2 on serine 121, inhibits transcriptional activity and promotes HSP90 binding*. Journal of Biological Chemistry, 2006. **281**(2): p. 782-791.
30. Xavier, I.J., et al., *Glycogen synthase kinase 3 β negatively regulates both DNA-binding and transcriptional activities of heat shock factor 1*. Journal of Biological Chemistry, 2000. **275**(37): p. 29147-29152.
31. Westerheide, S.D., et al., *Stress-inducible regulation of heat shock factor 1 by the deacetylase SIRT1*. Science, 2009. **323**(5917): p. 1063-6.
32. Love, D.C. and J.A. Hanover, *The hexosamine signaling pathway: deciphering the "O-GlcNAc code"*. Sci. Stke, 2005. **2005**(312): p. re13-re13.

33. Miura, Y., et al., *Hyper-O-GlcNAcylation inhibits the induction of heat shock protein 70 (Hsp 70) by sodium arsenite in HeLa cells*. *Biological and Pharmaceutical Bulletin*, 2014. **37**(8): p. 1308-1314.
34. Singleton, K.D. and P.E. Wischmeyer, *Glutamine induces heat shock protein expression via O-glycosylation and phosphorylation of HSF-1 and Sp1*. *Journal of Parenteral and Enteral Nutrition*, 2008. **32**(4): p. 371-376.
35. Hamiel, C.R., et al., *Glutamine enhances heat shock protein 70 expression via increased hexosamine biosynthetic pathway activity*. *American Journal of Physiology-Cell Physiology*, 2009. **297**(6): p. C1509-C1519.
36. Gong, J. and L. Jing, *Glutamine induces heat shock protein 70 expression via O-GlcNAc modification and subsequent increased expression and transcriptional activity of heat shock factor-1*. *Minerva anesthesiologica*, 2011. **77**(5): p. 488-495.
37. Zou, J., et al., *Repression of heat shock transcription factor HSF1 activation by HSP90 (HSP90 complex) that forms a stress-sensitive complex with HSF1*. *Cell*, 1998. **94**(4): p. 471-480.
38. Bharadwaj, S., A. Ali, and N. Ovsenek, *Multiple components of the HSP90 chaperone complex function in regulation of heat shock factor 1 in vivo*. *Molecular and cellular biology*, 1999. **19**(12): p. 8033-8041.
39. Ali, A., et al., *HSP90 interacts with and regulates the activity of heat shock factor 1 in Xenopus oocytes*. *Molecular and cellular biology*, 1998. **18**(9): p. 4949-4960.
40. Jolly, C., Y. Usson, and R.I. Morimoto, *Rapid and reversible relocalization of heat shock factor 1 within seconds to nuclear stress granules*. *Proc Natl Acad Sci U S A*, 1999. **96**(12): p. 6769-74.

41. Jolly, C., et al., *HSF1 transcription factor concentrates in nuclear foci during heat shock: relationship with transcription sites*. Journal of cell science, 1997. **110**(23): p. 2935-2941.
42. Cotto, J., S. Fox, and R. Morimoto, *HSF1 granules: a novel stress-induced nuclear compartment of human cells*. Journal of cell science, 1997. **110**(23): p. 2925-2934.
43. Biamonti, G. and C. Vourc'h, *Nuclear stress bodies*. Cold Spring Harbor perspectives in biology, 2010. **2**(6): p. a000695.
44. Jolly, C., et al., *Stress-induced transcription of satellite III repeats*. J Cell Biol, 2004. **164**(1): p. 25-33.
45. Gaglia, G., et al., *HSF1 phase transition mediates stress adaptation and cell fate decisions*. Nat Cell Biol, 2020. **22**(2): p. 151-158.
46. Dai, C. and S.B. Sampson, *HSF1: guardian of proteostasis in cancer*. Trends in cell biology, 2016. **26**(1): p. 17-28.
47. Anckar, J. and L. Sistonen, *Regulation of HSF1 function in the heat stress response: implications in aging and disease*. Annual review of biochemistry, 2011. **80**: p. 1089-1115.
48. Brenner, S., *The genetics of Caenorhabditis elegans*. Genetics, 1974. **77**(1): p. 71-94.
49. Tabara, H., et al., *The rde-1 gene, RNA interference, and transposon silencing in C. elegans*. Cell, 1999. **99**(2): p. 123-132.

50. Kamath, R.S., et al., *Effectiveness of specific RNA-mediated interference through ingested double-stranded RNA in Caenorhabditis elegans*. *Genome biology*, 2000. **2**(1): p. 1.
51. The, C. and R.K. Wilson, *How the worm was won: the C. elegans genome sequencing project*. *Trends in Genetics*, 1999. **15**(2): p. 51-58.
52. Morton, E.A. and T. Lamitina, *Caenorhabditis elegans HSF-1 is an essential nuclear protein that forms stress granule-like structures following heat shock*. *Aging Cell*, 2013. **12**(1): p. 112-20.
53. Tatum, M.C., et al., *Neuronal serotonin release triggers the heat shock response in C. elegans in the absence of temperature increase*. *Current Biology*, 2015. **25**(2): p. 163-174.
54. Nussbaum-Krammer, C.I. and R.I. Morimoto, *Caenorhabditis elegans as a model system for studying non-cell-autonomous mechanisms in protein-misfolding diseases*. *Disease models & mechanisms*, 2014. **7**(1): p. 31-39.
55. Prahlad, V., T. Cornelius, and R.I. Morimoto, *Regulation of the cellular heat shock response in Caenorhabditis elegans by thermosensory neurons*. *Science*, 2008. **320**(5877): p. 811-814.
56. Prahlad, V. and R.I. Morimoto, *Neuronal circuitry regulates the response of Caenorhabditis elegans to misfolded proteins*. *Proceedings of the National Academy of Sciences*, 2011. **108**(34): p. 14204-14209.
57. Hsu, A.L., C.T. Murphy, and C. Kenyon, *Regulation of aging and age-related disease by DAF-16 and heat-shock factor*. *Science*, 2003. **300**(5622): p. 1142-5.

58. Baird, N.A., et al., *HSF-1–mediated cytoskeletal integrity determines thermotolerance and life span*. *Science*, 2014. **346**(6207): p. 360-363.
59. Arantes-Oliveira, N., et al., *Regulation of life-span by germ-line stem cells in *Caenorhabditis elegans**. *Science*, 2002. **295**(5554): p. 502-505.
60. Pinkston, J.M., et al., *Mutations that increase the life span of *C. elegans* inhibit tumor growth*. *Science*, 2006. **313**(5789): p. 971-975.
61. Labbadia, J. and R.I. Morimoto, *Repression of the heat shock response is a programmed event at the onset of reproduction*. *Molecular cell*, 2015. **59**(4): p. 639-650.
62. Labbadia, J., et al., *Mitochondrial stress restores the heat shock response and prevents proteostasis collapse during aging*. *Cell reports*, 2017. **21**(6): p. 1481-1494.
63. Kumsta, C. and M. Hansen, *Hormetic heat shock and HSF-1 overexpression improve *C. elegans* survival and proteostasis by inducing autophagy*. *Autophagy*, 2017. **13**(6): p. 1076-1077.
64. Salmand, P.A., et al., *Mouse heat-shock factor 1 (HSF1) is involved in testicular response to genotoxic stress induced by doxorubicin*. *Biology of reproduction*, 2008. **79**(6): p. 1092-1101.
65. Zhou, L., et al., *Histone acetylation promotes long-lasting defense responses and longevity following early life heat stress*. *PLoS genetics*, 2019. **15**(4): p. e1008122.
66. Satyal, S.H., et al., *Negative regulation of the heat shock transcriptional response by HSBP1*. *Genes & development*, 1998. **12**(13): p. 1962-1974.

67. Tai, L.-J., et al., *Structure-function analysis of the heat shock factor-binding protein reveals a protein composed solely of a highly conserved and dynamic coiled-coil trimerization domain*. Journal of Biological Chemistry, 2002. **277**(1): p. 735-745.
68. Cotto, J.J. and R.I. Morimoto. *Stress-induced activation of the heat-shock response: cell and molecular biology of heat-shock factors*. in *Biochemical Society Symposium*. 1999.
69. Chiang, W.C., et al., *HSF-1 regulators DDL-1/2 link insulin-like signaling to heat-shock responses and modulation of longevity*. Cell, 2012. **148**(1-2): p. 322-34.
70. Sural, S., et al., *HSB-1 inhibition and HSF-1 overexpression trigger overlapping transcriptional changes to promote longevity in Caenorhabditis elegans*. G3: Genes, Genomes, Genetics, 2019. **9**(5): p. 1679-1692.
71. Murphy, C.T. and P.J. Hu, *Insulin/insulin-like growth factor signaling in C. elegans*, in *WormBook: The Online Review of C. elegans Biology [Internet]*. 2018, WormBook.
72. Tissenbaum, H.A., *DAF-16: FOXO in the context of C. elegans*, in *Current topics in developmental biology*. 2018, Elsevier. p. 1-21.
73. Kimura, K.D., et al., *daf-2, an insulin receptor-like gene that regulates longevity and diapause in Caenorhabditis elegans*. Science, 1997. **277**(5328): p. 942-946.
74. Zheng, S., et al., *A functional study of all 40 Caenorhabditis elegans insulin-like peptides*. Journal of Biological Chemistry, 2018. **293**(43): p. 16912-16922.

75. Hua, Q.-x., et al., *A divergent INS protein in Caenorhabditis elegans structurally resembles human insulin and activates the human insulin receptor*. *Genes & development*, 2003. **17**(7): p. 826-831.
76. Kenyon, C., et al., *A C. elegans mutant that lives twice as long as wild type*. *Nature*, 1993. **366**(6454): p. 461-464.
77. Taniguchi, C.M., B. Emanuelli, and C.R. Kahn, *Critical nodes in signalling pathways: insights into insulin action*. *Nature reviews Molecular cell biology*, 2006. **7**(2): p. 85-96.
78. Morley, J.F. and R.I. Morimoto, *Regulation of longevity in Caenorhabditis elegans by heat shock factor and molecular chaperones*. *Mol Biol Cell*, 2004. **15**(2): p. 657-64.
79. An, J.H., et al., *Regulation of the Caenorhabditis elegans oxidative stress defense protein SKN-1 by glycogen synthase kinase-3*. *Proceedings of the National Academy of Sciences*, 2005. **102**(45): p. 16275-16280.
80. Morris, J.Z., H.A. Tissenbaum, and G. Ruvkun, *A phosphatidylinositol-3-OH kinase family member regulating longevity and diapause in Caenorhabditis elegans*. *Nature*, 1996. **382**(6591): p. 536-539.
81. Padmanabhan, S., et al., *A PP2A regulatory subunit regulates C. elegans insulin/IGF-1 signaling by modulating AKT-1 phosphorylation*. *Cell*, 2009. **136**(5): p. 939-951.
82. Toker, A. and A.C. Newton, *Cellular signaling: pivoting around PDK-1*. *Cell*, 2000. **103**(2): p. 185-188.

83. Brunet, A., et al., *Akt promotes cell survival by phosphorylating and inhibiting a Forkhead transcription factor*. *cell*, 1999. **96**(6): p. 857-868.
84. Bamps, S., et al., *The Caenorhabditis elegans sirtuin gene, sir-2.1, is widely expressed and induced upon caloric restriction*. *Mechanisms of ageing and development*, 2009. **130**(11): p. 762-770.
85. Gräff, J., et al., *A dietary regimen of caloric restriction or pharmacological activation of SIRT1 to delay the onset of neurodegeneration*. *The Journal of Neuroscience*, 2013. **33**(21): p. 8951-8960.
86. Wang, Y., et al., *C. elegans 14-3-3 proteins regulate life span and interact with SIR-2.1 and DAF-16/FOXO*. *Mechanisms of ageing and development*, 2006. **127**(9): p. 741-747.
87. Viswanathan, M. and H.A. Tissenbaum, *C. elegans Sirtuins*, in *Sirtuins*. 2013, Springer. p. 39-56.
88. Westerheide, S.D., et al., *Stress-inducible regulation of heat shock factor 1 by the deacetylase SIRT1*. *Science*, 2009. **323**(5917): p. 1063-1066.
89. Brunquell, J., et al., *CCAR-1 is a negative regulator of the heat-shock response in Caenorhabditis elegans*. *Aging cell*, 2018. **17**(5): p. e12813.
90. Ben-Zvi, A., E.A. Miller, and R.I. Morimoto, *Collapse of proteostasis represents an early molecular event in Caenorhabditis elegans aging*. *Proceedings of the National Academy of Sciences*, 2009. **106**(35): p. 14914-14919.
91. Hsin, H. and C. Kenyon, *Signals from the reproductive system regulate the lifespan of C. elegans*. *Nature*, 1999. **399**(6734): p. 362-366.

92. Wood, A.J., et al., *Targeted genome editing across species using ZFNs and TALENs*. Science, 2011. **333**(6040): p. 307-307.
93. Joung, J.K. and J.D. Sander, *TALENs: a widely applicable technology for targeted genome editing*. Nature reviews Molecular cell biology, 2013. **14**(1): p. 49-55.
94. Gupta, R.M. and K. Musunuru, *Expanding the genetic editing tool kit: ZFNs, TALENs, and CRISPR-Cas9*. The Journal of clinical investigation, 2014. **124**(10): p. 4154-4161.
95. Doudna, J.A. and E.J. Sontheimer, *The Use of CRISPR/cas9, ZFNs, TALENs in Generating Site-Specific Genome Alterations*. 2014: Academic Press.
96. Mello, C.C., et al., *Efficient gene transfer in C. elegans: extrachromosomal maintenance and integration of transforming sequences*. The EMBO journal, 1991. **10**(12): p. 3959-3970.
97. Frøkjær-Jensen, C., et al., *Single-copy insertion of transgenes in Caenorhabditis elegans*. Nature genetics, 2008. **40**(11): p. 1375.
98. Merritt, C., et al., *3' UTRs are the primary regulators of gene expression in the C. elegans germline*. Current Biology, 2008. **18**(19): p. 1476-1482.
99. Gilbert, L.A., et al., *CRISPR-mediated modular RNA-guided regulation of transcription in eukaryotes*. Cell, 2013. **154**(2): p. 442-451.
100. Barrangou, R., et al., *CRISPR provides acquired resistance against viruses in prokaryotes*. Science, 2007. **315**(5819): p. 1709-1712.

101. Ishino, Y., M. Krupovic, and P. Forterre, *History of CRISPR-Cas from encounter with a mysterious repeated sequence to genome editing technology*. Journal of bacteriology, 2018. **200**(7): p. e00580-17.
102. Olsen, A., M.C. Vantipalli, and G.J. Lithgow, *Lifespan extension of *Caenorhabditis elegans* following repeated mild hormetic heat treatments*. Biogerontology, 2006. **7**(4): p. 221.
103. Grunstein, M., *Histone acetylation in chromatin structure and transcription*. Nature, 1997. **389**(6649): p. 349-352.
104. Matilainen, O., et al., *The chromatin remodeling factor ISW-1 integrates organismal responses against nuclear and mitochondrial stress*. Nature communications, 2017. **8**(1): p. 1-11.
105. Shivaswamy, S. and V.R. Iyer, *Stress-dependent dynamics of global chromatin remodeling in yeast: dual role for SWI/SNF in the heat shock stress response*. Molecular and cellular biology, 2008. **28**(7): p. 2221-2234.
106. Erkina, T.Y., et al., *Functional interplay between chromatin remodeling complexes RSC, SWI/SNF and ISWI in regulation of yeast heat shock genes*. Nucleic acids research, 2010. **38**(5): p. 1441-1449.
107. Yamada, K., et al., *Cytosolic HSP90 regulates the heat shock response that is responsible for heat acclimation in *Arabidopsis thaliana**. Journal of Biological Chemistry, 2007. **282**(52): p. 37794-37804.
108. Trinklein, N.D., et al., *The role of heat shock transcription factor 1 in the genome-wide regulation of the mammalian heat shock response*. Molecular biology of the cell, 2004. **15**(3): p. 1254-1261.

109. Helmann, J.D., et al., *Global transcriptional response of Bacillus subtilis to heat shock*. Journal of Bacteriology, 2001. **183**(24): p. 7318-7328.
110. Mendillo, M.L., et al., *HSF1 drives a transcriptional program distinct from heat shock to support highly malignant human cancers*. Cell, 2012. **150**(3): p. 549-562.
111. Brunquell, J., et al., *The genome-wide role of HSF-1 in the regulation of gene expression in Caenorhabditis elegans*. BMC genomics, 2016. **17**(1): p. 559.
112. Fritah, S., et al., *Heat-shock factor 1 controls genome-wide acetylation in heat-shocked cells*. Molecular biology of the cell, 2009. **20**(23): p. 4976-4984.
113. Labbé, R.M., A. Holowatyj, and Z.-Q. Yang, *Histone lysine demethylase (KDM) subfamily 4: structures, functions and therapeutic potential*. American journal of translational research, 2014. **6**(1): p. 1.
114. Valgardsdottir, R., et al., *Structural and functional characterization of noncoding repetitive RNAs transcribed in stressed human cells*. Molecular biology of the cell, 2005. **16**(6): p. 2597-2604.
115. Biamonti, G., *Nuclear stress bodies: a heterochromatin affair?* Nat Rev Mol Cell Biol, 2004. **5**(6): p. 493-8.
116. Kawaguchi, T., et al., *SWI/SNF chromatin-remodeling complexes function in noncoding RNA-dependent assembly of nuclear bodies*. Proceedings of the National Academy of Sciences, 2015. **112**(14): p. 4304-4309.
117. Kawaguchi, T. and T. Hirose, *Chromatin remodeling complexes in the assembly of long noncoding RNA-dependent nuclear bodies*. Nucleus, 2015. **6**(6): p. 462-467.

118. Ko, K.M., et al., *PYP-1, inorganic pyrophosphatase, is required for larval development and intestinal function in C. elegans*. FEBS letters, 2007. **581**(28): p. 5445-5453.
119. Kornberg, A., *On the metabolic significance of phosphorolytic and pyrophosphorolytic reactions*. Horizons in biochemistry, 1962: p. 251-264.
120. Lahti, R., *Microbial inorganic pyrophosphatases*. Microbiological reviews, 1983. **47**(2): p. 169.
121. Islam, M.K., et al., *Inorganic pyrophosphatase in the roundworm Ascaris and its role in the development and molting process of the larval stage parasites*. European journal of biochemistry, 2003. **270**(13): p. 2814-2826.
122. Cooperman, B.S., A.A. Baykov, and R. Lahti, *Evolutionary conservation of the active site of soluble inorganic pyrophosphatase*. Trends in biochemical sciences, 1992. **17**(7): p. 262-266.
123. Sonnewald, U., *Expression of E. coli inorganic pyrophosphatase in transgenic plants alters photoassimilate partitioning*. The Plant Journal, 1992. **2**(4): p. 571-581.
124. Gdula, D.A., et al., *Inorganic pyrophosphatase is a component of the Drosophila nucleosome remodeling factor complex*. Genes & development, 1998. **12**(20): p. 3206-3216.
125. Verghese, S. and T.T. Su, *STAT, Wingless, and Nurf-38 determine the accuracy of regeneration after radiation damage in Drosophila*. PLoS genetics, 2017. **13**(10): p. e1007055.

126. Badenhorst, P., et al., *The Drosophila nucleosome remodeling factor NURF is required for Ecdysteroid signaling and metamorphosis*. Genes & development, 2005. **19**(21): p. 2540-2545.
127. Cherry, C.M. and E.L. Matunis, *Epigenetic regulation of stem cell maintenance in the Drosophila testis via the nucleosome-remodeling factor NURF*. Cell stem cell, 2010. **6**(6): p. 557-567.
128. Darby, C., *Interactions with microbial pathogens*, in *WormBook: The Online Review of C. elegans Biology [Internet]*. 2005, WormBook.
129. Burns, A.R., et al., *A predictive model for drug bioaccumulation and bioactivity in Caenorhabditis elegans*. Nature chemical biology, 2010. **6**(7): p. 549.
130. Hresko, M.C., B.D. Williams, and R.H. Waterston, *Assembly of body wall muscle and muscle cell attachment structures in Caenorhabditis elegans*. The Journal of cell biology, 1994. **124**(4): p. 491-506.
131. Francis, R. and R.H. Waterston, *Muscle cell attachment in Caenorhabditis elegans*. The Journal of cell biology, 1991. **114**(3): p. 465-479.
132. Page, A.P. and I. Johnstone, *The cuticle*. WormBook, 2007.
133. Yang, J. and J.M. Kramer, *Proteolytic Processing of Caenorhabditis elegans SQT-1 Cuticle Collagen Is Inhibited in Right Roller Mutants whereas Cross-linking Is Inhibited in Left Roller Mutants*. Journal of Biological Chemistry, 1999. **274**(46): p. 32744-32749.
134. Cox, G.N., et al., *Temporal regulation of cuticle synthesis during development of Caenorhabditis elegans*. Developmental biology, 1981. **84**(2): p. 277-285.

135. Johnstone, I.L. and J.D. Barry, *Temporal reiteration of a precise gene expression pattern during nematode development*. The EMBO journal, 1996. **15**(14): p. 3633-3639.
136. Ranga, A., N. Gjorevski, and M.P. Lutolf, *Drug discovery through stem cell-based organoid models*. Advanced drug delivery reviews, 2014. **69**: p. 19-28.
137. Dedhia, P.H., et al., *Organoid models of human gastrointestinal development and disease*. Gastroenterology, 2016. **150**(5): p. 1098-1112.
138. Wheeler, J.M. and J.H. Thomas, *Identification of a novel gene family involved in osmotic stress response in Caenorhabditis elegans*. Genetics, 2006. **174**(3): p. 1327-1336.
139. Burkewitz, K., et al., *Characterization of the proteostasis roles of glycerol accumulation, protein degradation and protein synthesis during osmotic stress in C. elegans*. PLoS One, 2012. **7**(3): p. e34153.
140. Dodd, W., et al., *A damage sensor associated with the cuticle coordinates three core environmental stress responses in Caenorhabditis elegans*. Genetics, 2018. **208**(4): p. 1467-1482.
141. Ewald, C.Y., et al., *Dauer-independent insulin/IGF-1-signalling implicates collagen remodelling in longevity*. Nature, 2015. **519**(7541): p. 97-101.
142. Joutsen, J. and L. Sistonen, *Tailoring of Proteostasis Networks with Heat Shock Factors*. Cold Spring Harb Perspect Biol, 2019. **11**(4).
143. Hartl, F.U., A. Bracher, and M. Hayer-Hartl, *Molecular chaperones in protein folding and proteostasis*. Nature, 2011. **475**(7356): p. 324-32.

144. Gomez-Pastor, R., E.T. Burchfiel, and D.J. Thiele, *Regulation of heat shock transcription factors and their roles in physiology and disease*. Nat Rev Mol Cell Biol, 2017.
145. Hsu, A.-L., C.T. Murphy, and C. Kenyon, *Regulation of aging and age-related disease by DAF-16 and heat-shock factor*. Science, 2003. **300**(5622): p. 1142-1145.
146. Singh, V. and A. Aballay, *Heat-shock transcription factor (HSF)-1 pathway required for Caenorhabditis elegans immunity*. Proc Natl Acad Sci U S A, 2006. **103**(35): p. 13092-7.
147. Li, J., et al., *E2F coregulates an essential HSF developmental program that is distinct from the heat-shock response*. Genes Dev, 2016. **30**(18): p. 2062-2075.
148. Biamonti, G. and C. Vourc'h, *Nuclear stress bodies*. Cold Spring Harb Perspect Biol, 2010. **2**(6): p. a000695.
149. Sulston, J.E. and J. Hodgkin, *Methods*. In: *The Nematode Caenorhabditis elegans*, ed Wood WB. Cold Spring Harbor Laboratory Press, Cold Spring Harbor, NY, 1988: p. 587–606.
150. Berman, J.R. and C. Kenyon, *Germ-cell loss extends C. elegans life span through regulation of DAF-16 by kri-1 and lipophilic-hormone signaling*. Cell, 2006. **124**(5): p. 1055-1068.
151. Shemesh, N., N. Shai, and A. Ben-Zvi, *Germline stem cell arrest inhibits the collapse of somatic proteostasis early in Caenorhabditis elegans adulthood*. Aging cell, 2013. **12**(5): p. 814-822.

152. Chalfie, M. and J. Sulston, *Developmental genetics of the mechanosensory neurons of Caenorhabditis elegans*. Dev Biol, 1981. **82**(2): p. 358-70.
153. Voellmy, R. and F. Boellmann, *Chaperone regulation of the heat shock protein response*. Adv Exp Med Biol, 2007. **594**: p. 89-99.
154. Martinez-Balbas, M.A., et al., *Displacement of sequence-specific transcription factors from mitotic chromatin*. Cell, 1995. **83**(1): p. 29-38.
155. Mercier, P.A., N.A. Winegarden, and J.T. Westwood, *Human heat shock factor 1 is predominantly a nuclear protein before and after heat stress*. J Cell Sci, 1999. **112 (Pt 16)**: p. 2765-74.
156. Ooi, F.K. and V. Prahlad, *Olfactory experience primes the heat shock transcription factor HSF-1 to enhance the expression of molecular chaperones in C. elegans*. Sci Signal, 2017. **10**(501).
157. Bohnert, K.A. and C. Kenyon, *A lysosomal switch triggers proteostasis renewal in the immortal C. elegans germ lineage*. Nature, 2017. **551**(7682): p. 629.
158. Burkewitz, K., K. Choe, and K. Strange, *Hypertonic stress induces rapid and widespread protein damage in C. elegans*. Am J Physiol Cell Physiol, 2011. **301**(3): p. C566-76.
159. Ahn, S.G. and D.J. Thiele, *Redox regulation of mammalian heat shock factor 1 is essential for Hsp gene activation and protection from stress*. Genes Dev, 2003. **17**(4): p. 516-28.
160. Trott, A., et al., *Activation of heat shock and antioxidant responses by the natural product celastrol: transcriptional signatures of a thiol-targeted molecule*. Molecular biology of the cell, 2008. **19**(3): p. 1104-12.

161. Erkekoglu, P. and T. Baydar, *Acrylamide neurotoxicity*. *Nutr Neurosci*, 2014. **17**(2): p. 49-57.
162. Dickinson, D.J., et al., *Engineering the Caenorhabditis elegans genome using Cas9-triggered homologous recombination*. *Nature methods*, 2013. **10**(10): p. 1028-1034.
163. Kamath, R.S., et al., *Systematic functional analysis of the Caenorhabditis elegans genome using RNAi*. *Nature*, 2003. **421**(6920): p. 231.
164. Morimoto, R.I., et al., *The heat-shock response: regulation and function of heat-shock proteins and molecular chaperones*. *Essays in biochemistry*, 1997. **32**: p. 17-29.
165. Trepel, J., et al., *Targeting the dynamic HSP90 complex in cancer*. *Nature reviews cancer*, 2010. **10**(8): p. 537-549.
166. Wandinger, S.K., K. Richter, and J. Buchner, *The Hsp90 chaperone machinery*. *Journal of Biological Chemistry*, 2008. **283**(27): p. 18473-18477.
167. Whitesell, L. and S.L. Lindquist, *HSP90 and the chaperoning of cancer*. *Nature Reviews Cancer*, 2005. **5**(10): p. 761-772.
168. Hendrick, J.P. and F.-U. Hartl, *Molecular chaperone functions of heat-shock proteins*. *Annual review of biochemistry*, 1993. **62**(1): p. 349-384.
169. Parsell, D. and S. Lindquist, *The function of heat-shock proteins in stress tolerance: degradation and reactivation of damaged proteins*. *Annual review of genetics*, 1993. **27**(1): p. 437-496.

170. Pierce, A., et al., *A Novel mouse model of enhanced proteostasis: Full-length human heat shock factor 1 transgenic mice*. Biochemical and biophysical research communications, 2010. **402**(1): p. 59-65.
171. Mizuguchi, G., et al., *Role of nucleosome remodeling factor NURF in transcriptional activation of chromatin*. Molecular cell, 1997. **1**(1): p. 141-150.
172. Hamiche, A., et al., *Histone tails modulate nucleosome mobility and regulate ATP-dependent nucleosome sliding by NURF*. Proceedings of the National Academy of Sciences, 2001. **98**(25): p. 14316-14321.
173. Xiao, H., et al., *Dual functions of largest NURF subunit NURF301 in nucleosome sliding and transcription factor interactions*. Molecular cell, 2001. **8**(3): p. 531-543.
174. Kang, J.G., A. Hamiche, and C. Wu, *GAL4 directs nucleosome sliding induced by NURF*. The EMBO journal, 2002. **21**(6): p. 1406-1413.
175. Hamiche, A., et al., *ATP-dependent histone octamer sliding mediated by the chromatin remodeling complex NURF*. Cell, 1999. **97**(7): p. 833-842.
176. Badenhorst, P., et al., *Biological functions of the ISWI chromatin remodeling complex NURF*. Genes & development, 2002. **16**(24): p. 3186-3198.
177. Landry, J.W., et al., *Chromatin remodeling complex NURF regulates thymocyte maturation*. Genes & development, 2011. **25**(3): p. 275-286.
178. Ahringer, J., *Reverse genetics*. 2006.
179. Choe, K.P., A.J. Przybysz, and K. Strange, *The WD40 repeat protein WDR-23 functions with the CUL4/DDB1 ubiquitin ligase to regulate nuclear abundance*

- and activity of SKN-1 in Caenorhabditis elegans*. Molecular and cellular biology, 2009. **29**(10): p. 2704-2715.
180. Abràmoff, M.D., P.J. Magalhães, and S.J. Ram, *Image processing with ImageJ*. Biophotonics international, 2004. **11**(7): p. 36-42.
181. Escorcía, W., et al., *Quantification of lipid abundance and evaluation of lipid distribution in Caenorhabditis elegans by Nile red and Oil Red O staining*. JoVE (Journal of Visualized Experiments), 2018(133): p. e57352.
182. Hansen, D., E.J.A. Hubbard, and T. Schedl, *Multi-pathway control of the proliferation versus meiotic development decision in the Caenorhabditis elegans germline*. Developmental biology, 2004. **268**(2): p. 342-357.
183. Vihervaara, A. and L. Sistonen, *HSF1 at a glance*. Journal of cell science, 2014. **127**(2): p. 261-266.
184. Bond, M.R. and J.A. Hanover, *A little sugar goes a long way: the cell biology of O-GlcNAc*. Journal of Cell Biology, 2015. **208**(7): p. 869-880.
185. Hanover, J.A., *Epigenetics gets sweeter: O-GlcNAc joins the "histone code"*. Chemistry & biology, 2010. **17**(12): p. 1272-1274.
186. Hanover, J.A., M.W. Krause, and D.C. Love, *The hexosamine signaling pathway: O-GlcNAc cycling in feast or famine*. Biochimica et Biophysica Acta (BBA)-General Subjects, 2010. **1800**(2): p. 80-95.
187. Hanover, J.A., M.W. Krause, and D.C. Love, *Linking metabolism to epigenetics through O-GlcNAcylation*. Nature reviews Molecular cell biology, 2012. **13**(5): p. 312-321.

188. Lazarus, B.D., D.C. Love, and J.A. Hanover, *O-GlcNAc cycling: implications for neurodegenerative disorders*. The international journal of biochemistry & cell biology, 2009. **41**(11): p. 2134-2146.
189. Love, D.C., et al., *Dynamic O-GlcNAc cycling at promoters of Caenorhabditis elegans genes regulating longevity, stress, and immunity*. Proceedings of the National Academy of Sciences, 2010. **107**(16): p. 7413-7418.
190. Forsythe, M.E., et al., *Caenorhabditis elegans ortholog of a diabetes susceptibility locus: oga-1 (O-GlcNAcase) knockout impacts O-GlcNAc cycling, metabolism, and dauer*. Proceedings of the National Academy of Sciences, 2006. **103**(32): p. 11952-11957.
191. Wang, P., et al., *O-GlcNAc cycling mutants modulate proteotoxicity in Caenorhabditis elegans models of human neurodegenerative diseases*. Proceedings of the National Academy of Sciences, 2012. **109**(43): p. 17669-17674.
192. Cox, G.N., M. Kusch, and R.S. Edgar, *Cuticle of Caenorhabditis elegans: its isolation and partial characterization*. The Journal of cell biology, 1981. **90**(1): p. 7-17.
193. Johnstone, I.L., *Cuticle collagen genes: expression in Caenorhabditis elegans*. Trends in Genetics, 2000. **16**(1): p. 21-27.
194. Kage-Nakadai, E., et al., *Two very long chain fatty acid acyl-CoA synthetase genes, acs-20 and acs-22, have roles in the cuticle surface barrier in Caenorhabditis elegans*. PloS one, 2010. **5**(1).

195. Page, A.P., G. McCormack, and A.J. Birnie, *Biosynthesis and enzymology of the Caenorhabditis elegans cuticle: identification and characterization of a novel serine protease inhibitor*. International journal for parasitology, 2006. **36**(6): p. 681-689.
196. Xu, Z., et al., *WDR-23 and SKN-1/Nrf2 coordinate with the BLI-3 dual oxidase in response to iodide-triggered oxidative stress*. G3: Genes, Genomes, Genetics, 2018. **8**(11): p. 3515-3527.
197. Torpe, N. and R. Pocock, *Regulation of axonal midline guidance by prolyl 4-hydroxylation in Caenorhabditis elegans*. Journal of Neuroscience, 2014. **34**(49): p. 16348-16357.
198. Shcherbakova, A., et al., *Distinct C-mannosylation of netrin receptor thrombospondin type 1 repeats by mammalian DPY19L1 and DPY19L3*. Proceedings of the National Academy of Sciences, 2017. **114**(10): p. 2574-2579.
199. Hsu, D.R. and B.J. Meyer, *The dpy-30 gene encodes an essential component of the Caenorhabditis elegans dosage compensation machinery*. Genetics, 1994. **137**(4): p. 999-1018.
200. Tsai, C.J., et al., *Meiotic crossover number and distribution are regulated by a dosage compensation protein that resembles a condensin subunit*. Genes & development, 2008. **22**(2): p. 194-211.
201. Plenefisch, J.D., L. DeLong, and B.J. Meyer, *Genes that implement the hermaphrodite mode of dosage compensation in Caenorhabditis elegans*. Genetics, 1989. **121**(1): p. 57-76.

202. Meyer, B.J. and L.P. Casson, *Caenorhabditis elegans* compensates for the difference in X chromosome dosage between the sexes by regulating transcript levels. *Cell*, 1986. **47**(6): p. 871-881.
203. Park, Y.-S. and J.M. Kramer, *The C. elegans sqt-1 and rol-6 collagen genes are coordinately expressed during development, but not at all stages that display mutant phenotypes*. *Developmental biology*, 1994. **163**(1): p. 112-124.
204. Kramer, J.M. and J.J. Johnson, *Analysis of mutations in the sqt-1 and rol-6 collagen genes of Caenorhabditis elegans*. *Genetics*, 1993. **135**(4): p. 1035-1045.
205. Kramer, J.M., et al., *The sqt-1 gene of C. elegans encodes a collagen critical for organismal morphogenesis*. *Cell*, 1988. **55**(4): p. 555-565.
206. Kramer, J.M., et al., *The Caenorhabditis elegans rol-6 gene, which interacts with the sqt-1 collagen gene to determine organismal morphology, encodes a collagen*. *Molecular and cellular biology*, 1990. **10**(5): p. 2081-2089.
207. Altintas, O., S. Park, and S.-J.V. Lee, *The role of insulin/IGF-1 signaling in the longevity of model invertebrates, C. elegans and D. melanogaster*. *BMB reports*, 2016. **49**(2): p. 81.
208. Lee, R.Y., J. Hench, and G. Ruvkun, *Regulation of C. elegans DAF-16 and its human ortholog FKHL1 by the daf-2 insulin-like signaling pathway*. *Current Biology*, 2001. **11**(24): p. 1950-1957.
209. Tullet, J.M., et al., *Direct inhibition of the longevity-promoting factor SKN-1 by insulin-like signaling in C. elegans*. *Cell*, 2008. **132**(6): p. 1025-1038.

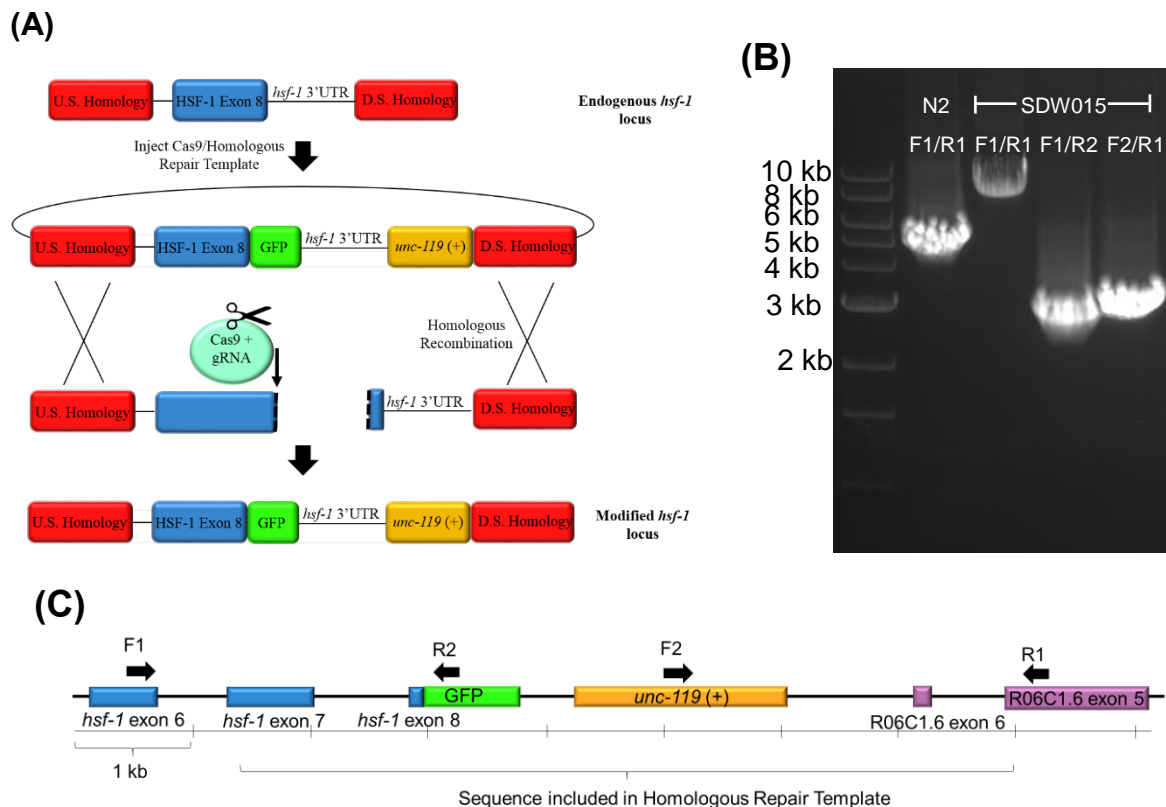
210. Lant, B. and W.B. Derry, *Methods for detection and analysis of apoptosis signaling in the C. elegans germline*. *Methods*, 2013. **61**(2): p. 174-182.
211. Lant, B. and W.B. Derry, *Fluorescent visualization of germline apoptosis in living Caenorhabditis elegans*. *Cold Spring Harbor protocols*, 2014. **2014**(4): p. pdb.prot080226.
212. Booth, L.N. and A. Brunet, *Shockingly early: chromatin-mediated loss of the heat shock response*. *Molecular cell*, 2015. **59**(4): p. 515-516.
213. Kapahi, P., M. Kaeberlein, and M. Hansen, *Dietary restriction and lifespan: lessons from invertebrate models*. *Ageing research reviews*, 2017. **39**: p. 3-14.
214. Ling, H., et al., *Histone deacetylase SIRT1 targets Plk2 to regulate centriole duplication*. *Cell reports*, 2018. **25**(10): p. 2851-2865. e3.
215. Peng, L., et al., *SIRT1 deacetylates the DNA methyltransferase 1 (DNMT1) protein and alters its activities*. *Molecular and cellular biology*, 2011. **31**(23): p. 4720-4734.
216. Gaglia, G., et al., *HSF1 phase transition mediates stress adaptation and cell fate decisions*. *Nature Cell Biology*, 2020. **22**(2): p. 151-158.
217. Douglas, P.M., et al., *Heterotypic signals from neural HSF-1 separate thermotolerance from longevity*. *Cell reports*, 2015. **12**(7): p. 1196-1204.
218. Taylor, R.C., K.M. Berendzen, and A. Dillin, *Systemic stress signalling: understanding the cell non-autonomous control of proteostasis*. *Nature reviews Molecular cell biology*, 2014. **15**(3): p. 211.

219. Åkerfelt, M., R.I. Morimoto, and L. Sistonen, *Heat shock factors: integrators of cell stress, development and lifespan*. Nature reviews Molecular cell biology, 2010. **11**(8): p. 545-555.
220. Fawcett, T.W., et al., *Effects of neurohormonal stress and aging on the activation of mammalian heat shock factor 1*. Journal of Biological Chemistry, 1994. **269**(51): p. 32272-32278.
221. Guisbert, E., et al., *Identification of a tissue-selective heat shock response regulatory network*. PLoS Genet, 2013. **9**(4): p. e1003466.
222. Carratù, L., et al., *Membrane lipid perturbation modifies the set point of the temperature of heat shock response in yeast*. Proceedings of the National Academy of Sciences, 1996. **93**(9): p. 3870-3875.
223. Vigh, L., et al., *The primary signal in the biological perception of temperature: Pd-catalyzed hydrogenation of membrane lipids stimulated the expression of the desA gene in Synechocystis PCC6803*. Proceedings of the National Academy of Sciences, 1993. **90**(19): p. 9090-9094.
224. Saidi, Y., et al., *Membrane lipid composition affects plant heat sensing and modulates Ca²⁺-dependent heat shock response*. Plant signaling & behavior, 2010. **5**(12): p. 1530-1533.
225. Bielski, B., R.L. Arudi, and M.W. Sutherland, *A study of the reactivity of HO₂/O₂- with unsaturated fatty acids*. Journal of Biological Chemistry, 1983. **258**(8): p. 4759-4761.
226. Papsdorf, K. and A. Brunet, *Linking lipid metabolism to chromatin regulation in aging*. Trends in cell biology, 2019. **29**(2): p. 97-116.

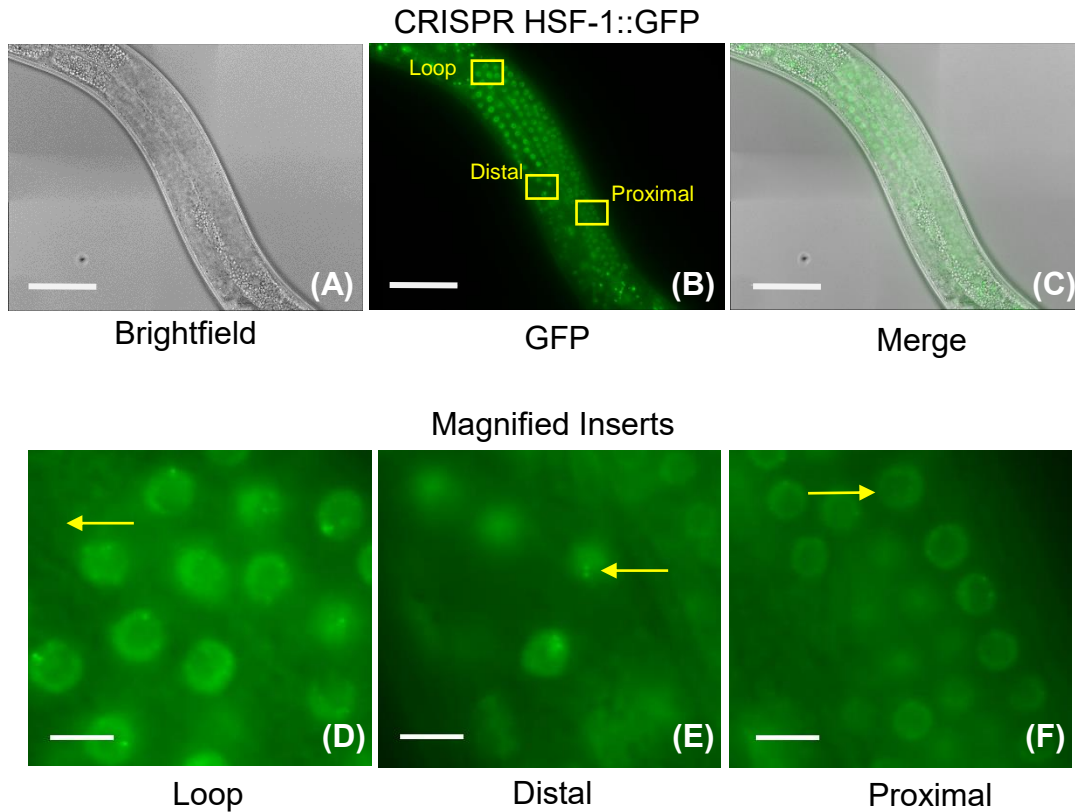
227. Pamplona, R., *Membrane phospholipids, lipoxidative damage and molecular integrity: a causal role in aging and longevity*. *Biochimica et Biophysica Acta (BBA)-Bioenergetics*, 2008. **1777**(10): p. 1249-1262.
228. Hulbert, A., et al., *Extended longevity of wild-derived mice is associated with peroxidation-resistant membranes*. *Mechanisms of ageing and development*, 2006. **127**(8): p. 653-657.
229. Mitchell, T.W., R. Buffenstein, and A. Hulbert, *Membrane phospholipid composition may contribute to exceptional longevity of the naked mole-rat (*Heterocephalus glaber*): a comparative study using shotgun lipidomics*. *Experimental gerontology*, 2007. **42**(11): p. 1053-1062.
230. Jové, M., et al., *Plasma long-chain free fatty acids predict mammalian longevity*. *Scientific reports*, 2013. **3**: p. 3346.
231. Weimar, J.D., et al., *Functional Role of Fatty Acyl-Coenzyme A Synthetase in the Transmembrane Movement and Activation of Exogenous Long-chain Fatty Acids* **AMINO ACID RESIDUES WITHIN THE ATP/AMP SIGNATURE MOTIF OF ESCHERICHIA COLI FadD ARE REQUIRED FOR ENZYME ACTIVITY AND FATTY ACID TRANSPORT**. *Journal of Biological Chemistry*, 2002. **277**(33): p. 29369-29376.
232. Chisholm, A.D. and S. Xu, *The *Caenorhabditis elegans* epidermis as a model skin. II: differentiation and physiological roles*. *Wiley Interdisciplinary Reviews: Developmental Biology*, 2012. **1**(6): p. 879-902.

233. Lamitina, S.T., et al., *Adaptation of the nematode Caenorhabditis elegans to extreme osmotic stress*. American Journal of Physiology-Cell Physiology, 2004. **286**(4): p. C785-C791.
234. Parsons, L.M., et al., *Caenorhabditis elegans bacterial pathogen resistant bus-4 mutants produce altered mucins*. PloS one, 2014. **9**(10): p. e107250.
235. Emtage, L., et al., *Extracellular proteins organize the mechanosensory channel complex in C. elegans touch receptor neurons*. Neuron, 2004. **44**(5): p. 795-807.

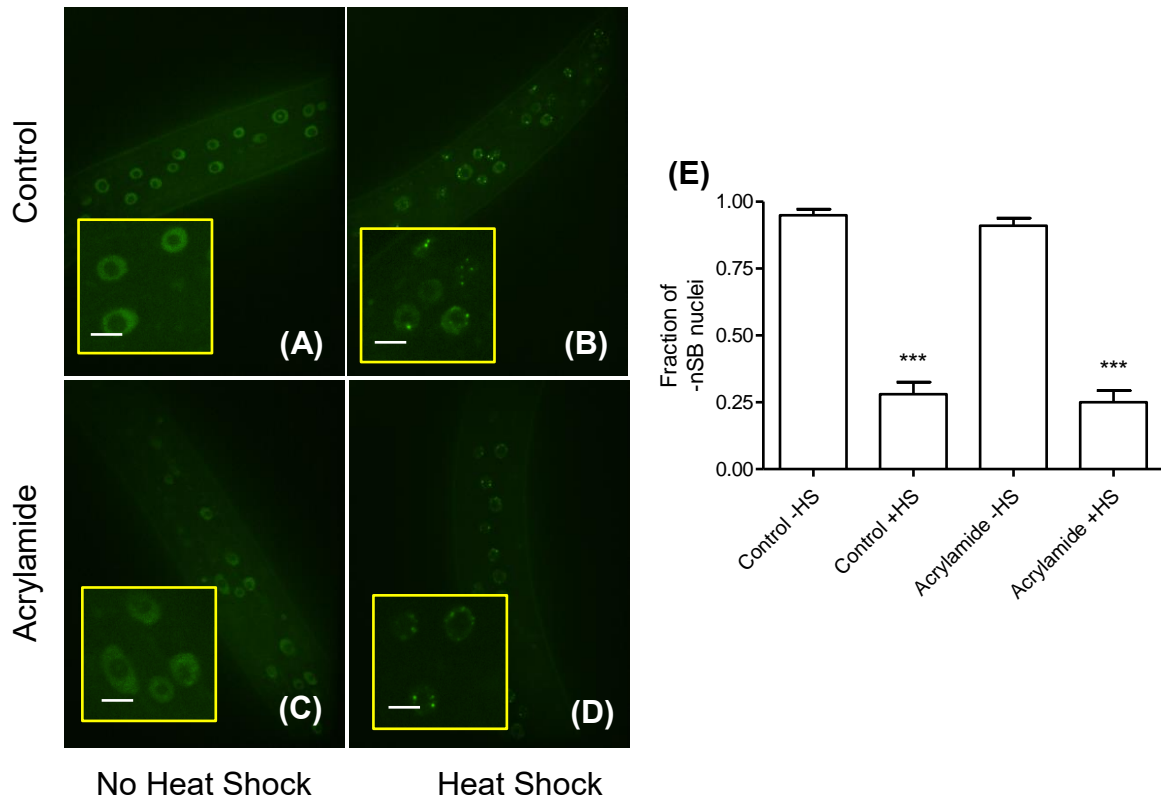
Appendix A: Supporting Figures for Chapter 2 CRISPR-Cas9 Tagging and Characterization of HSF-1 *C. elegans* model



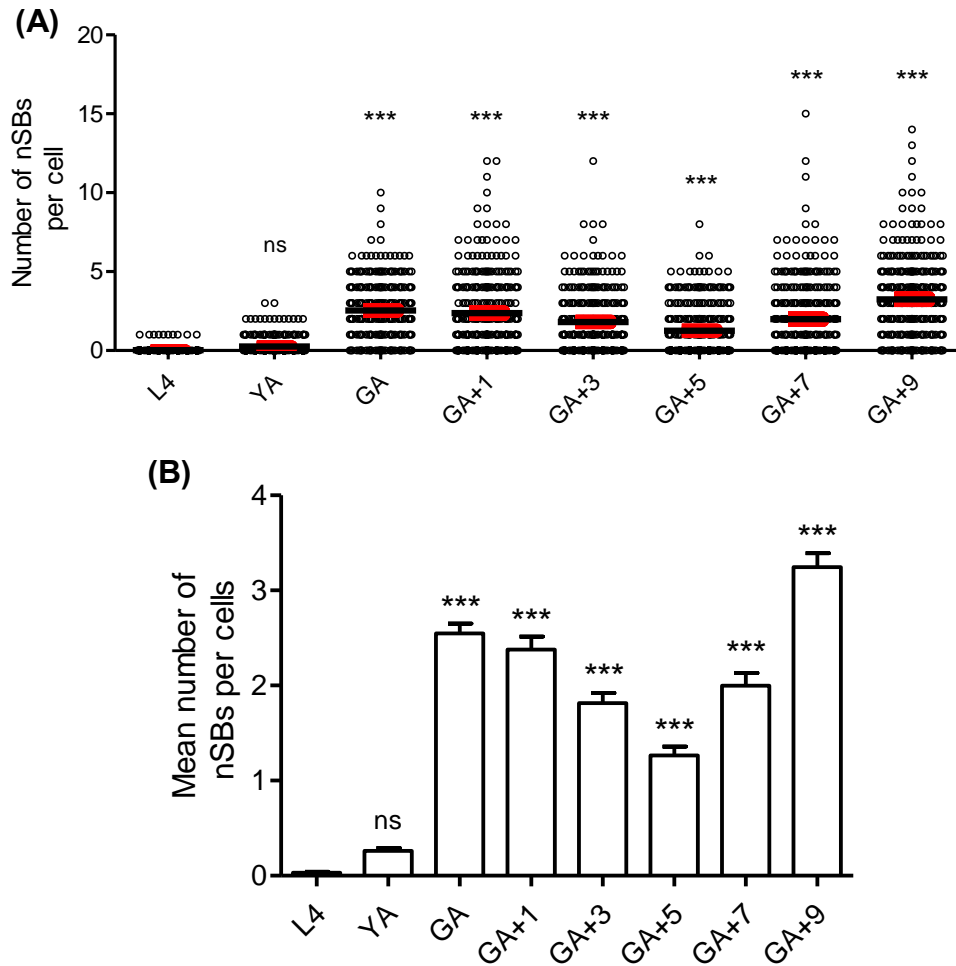
Appendix A1 - CRISPR/Cas9-mediated transgenesis of the endogenous *hsf-1* locus in *C. elegans* to include a C-terminal GFP tag. (A) Cas9 was programmed with a guiding RNA (gRNA) to create a double-strand break upstream of the translational stop site in exon eight of HSF-1. This break was then repaired via homologous recombination utilizing *unc-119 (+)* as a non-fluorescent marker of repair. Green fluorescent protein (GFP) was cloned in a direct fusion to exon eight and 286 bp of the *hsf-1* 3' UTR was retained following the translational stop site of GFP. Upstream and downstream homology arms (U.S. and D.S. homology) of 2.0 kb flank the targeted double strand break location. (B) PCR verification of insertion of Homologous Repair Template (HRT) into endogenous HSF-1 genomic locus. Whole worm lysate was used to genotype for the appropriate CRISPR/Cas9 mediated knock-in compared to N2 (wildtype) and CRISPR strain SDW015 (HSF-1::GFP). (C) Approximate schematic cartoon model of modified HSF-1 locus with location of genotyping primers.



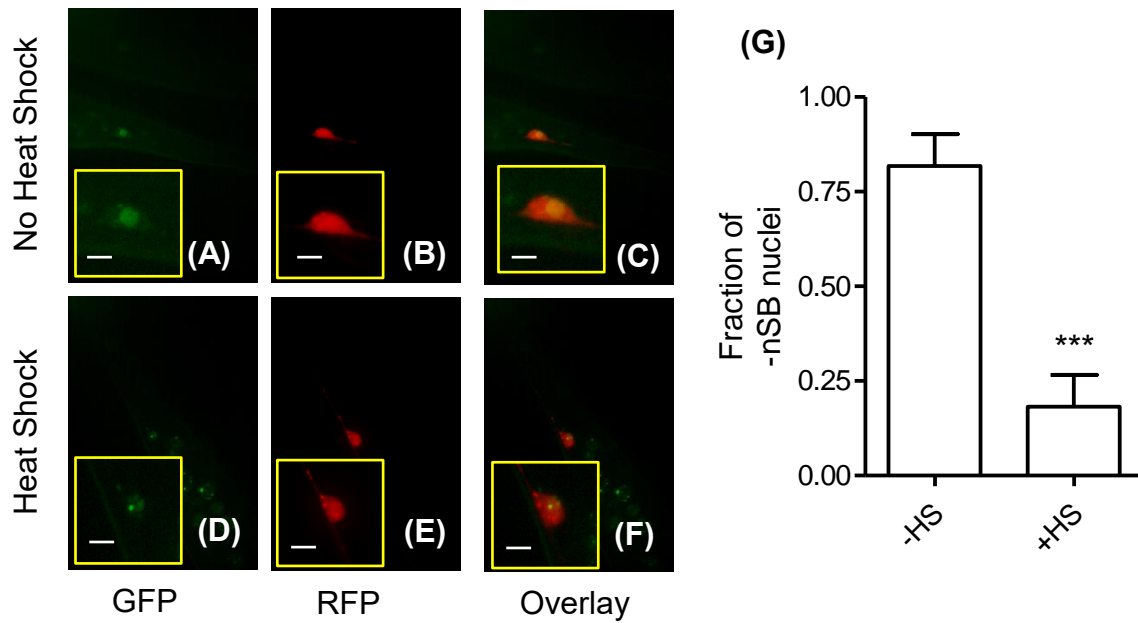
Appendix A2 HSF-1::GFP Nuclear Stress Bodies Can Form throughout the *C. elegans* Germline. Digitally stitched brightfield and fluorescence images of the germline of L4 CRISPR HSF-1::GFP (SDW015) are shown. Magnified inserts in three regions the loop, distal, and proximal end of the germline display germ cells displaying the presence of HSF-1::GFP nSBs in the absence of any exogenous stressors. Yellow arrows indicate HSF-1::GFP nSBs. Scale bar in (A-C) represents 45 microns in (D-F) scale represents 5 microns.



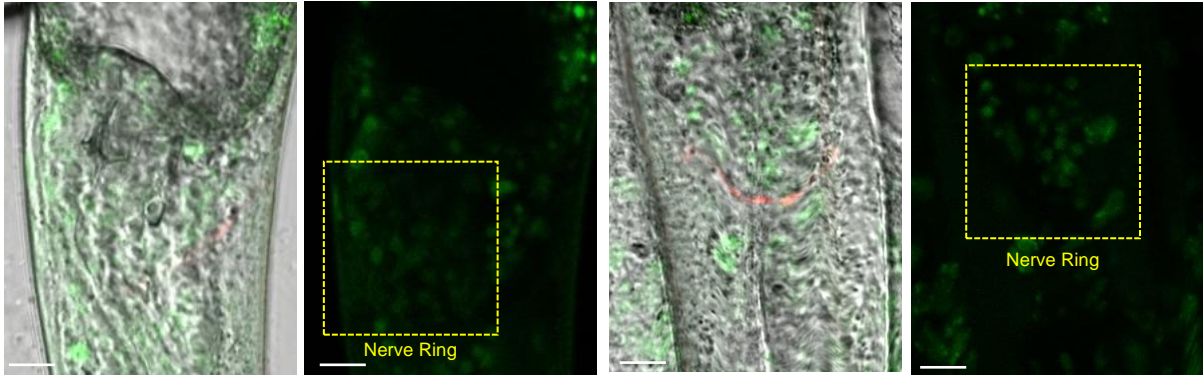
Appendix A3 HSF-1::GFP forms nuclear stress bodies upon heat shock after exposure to acrylamide. (A-D) Confocal brightfield images of SDW015 shows expression of HSF-1::GFP during control conditions or upon exposure to acrylamide (7 mM) with or without heat shock (HS). (E) Nuclear stress body formation was quantified and graphed in GraphPad Prism with $n > 8$ (n = number of animals assessed). All conditions were compared to Control -HS. (F) CL2166 (*pgst-4::GFP*) animals before and after a 5 hour exposure to 7 mM acrylamide shows that acrylamide induces the expected oxidative stress response. Scale bar in A-D presents 5 microns, scale bar in F represents 1000 microns.



Appendix A4 SDW015 displays numbers of HSF-1::GFP nSBs throughout aging. (A) SDW015 animals were grown without heat shock and assessed for the number of nSBs within individual hypodermal nuclei beginning at the last larval-increased stage (L4), in young adult (YA), fully gravid adults (GA) and then for the indicated number of days (+n) post GA. The number of nSBs per cell assessed was plotted in (A) with the mean number of nSBs per cell plotted using GraphPad Prism in (B). The red bar in (A) represents the mean number of nSBs present per cell. Approximately 300 individual cells were assessed across n=8 individual animals per condition. Significance was determined with a One-way ANOVA followed by a Tukey Post-Hoc test of all comparisons. *** indicates p<0.0001. All conditions were compared to L4.



Appendix A5 PLM neurons form HSF-1 nuclear stress bodies in response to heat shock. Confocal fluorescence images of HSF-1::GFP CRISPR; *p_{mec-17}::RFP* worms (SDW077) are shown without heat shock (A-C) and with heat shock (D-F). PLM neurons are marked by RFP. (G) The fraction of PLM nuclei scored as negative for nSBs or positive for nSBs for $n \geq 8$ worms with or without heat shock was quantified and graphed in GraphPad Prism for images (A-F). Significance indicated compares -HS to +HS, *** indicates $p < 0.0001$. Scale bar represents 5 microns



GFP + RFP + DIC

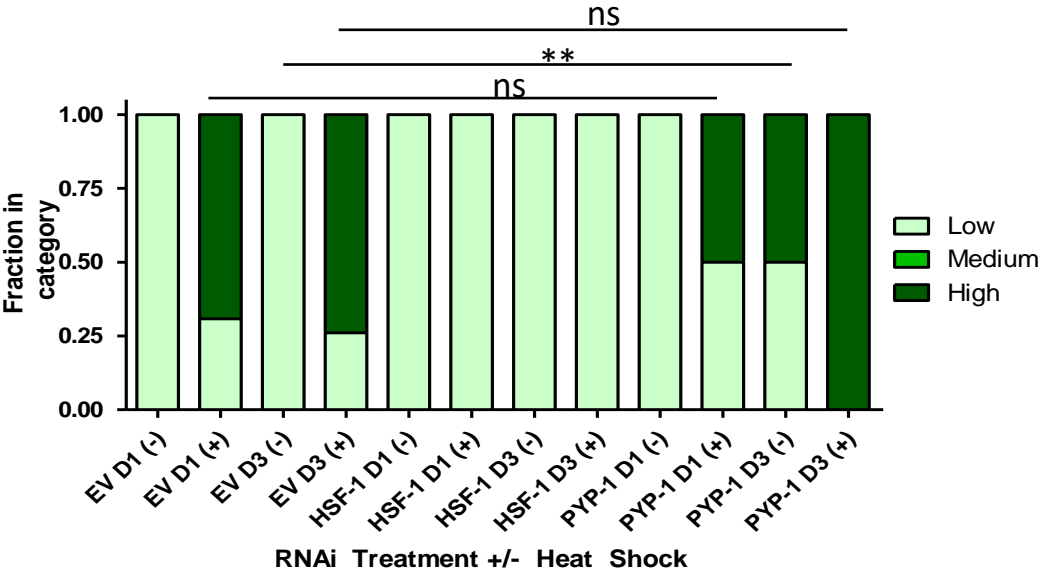
GFP

GFP + RFP + DIC

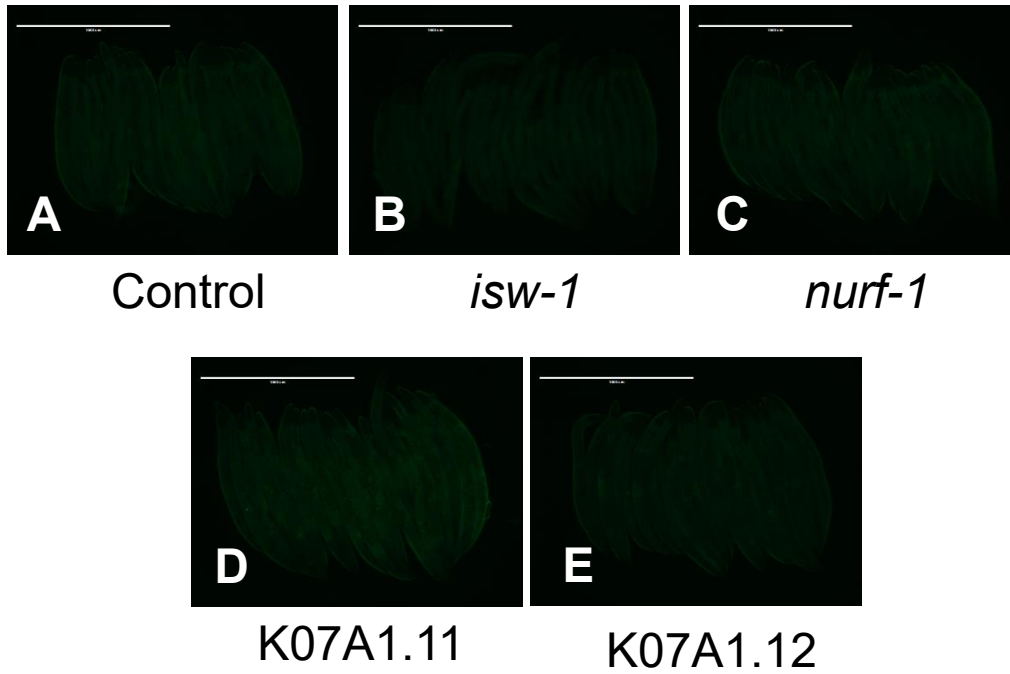
GFP

Appendix A6 Adult nerve ring neurons do not spontaneously form HSF-1 nuclear stress bodies. Confocal fluorescence images of gravid adult HSF-1::GFP CRISPR; *p_{mec-17}::RFP* worms (SDW077) are shown. Nerve ring neurons are identified by the pharyngeal bulbs in DIC and the ALM branch in the red TRN marker. Yellow dotted "nerve ring" box placement is around the location of the terminal pharyngeal bulb. Two examples are shown. Scale bar represents 10 microns.

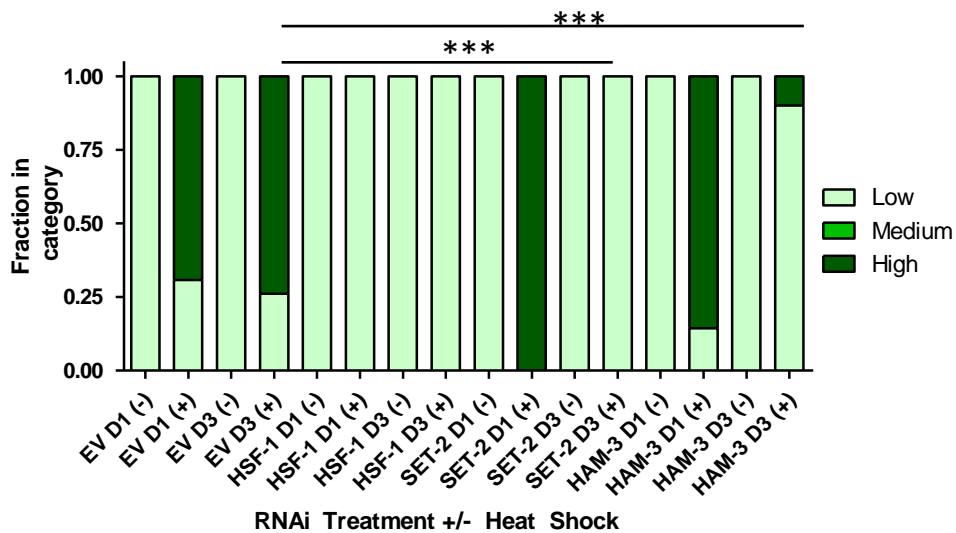
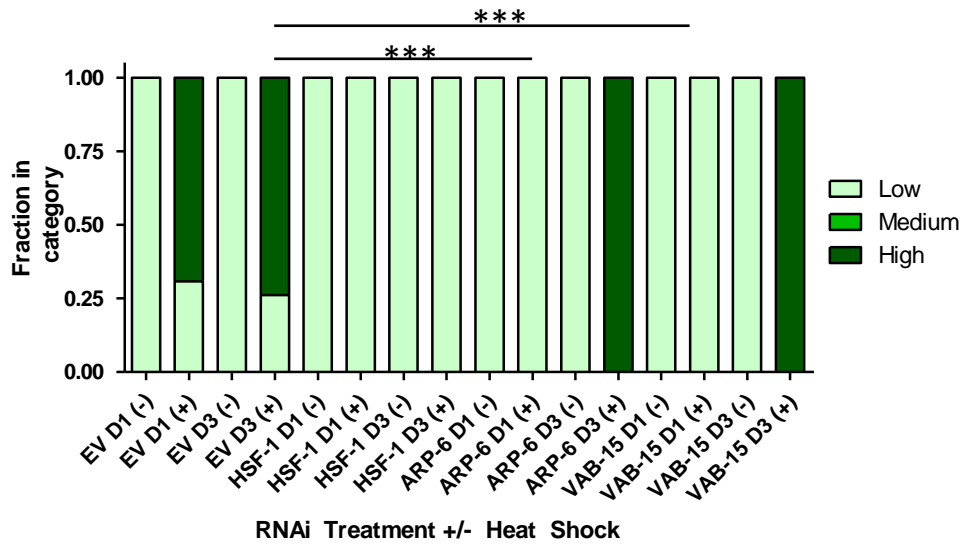
Appendix B: Supporting Figures for Chapter 3 Regulation of the Heat Shock Response by NuRF subunit *pyp-1*



Appendix B1 *pyp-1* negatively regulates the HSR. (A) TJ375 animals were fed the indicated RNAis and then assessed at L4/YA (Day 1) or two days later (Day 3). Worms were given no heat shock (-) or were exposed to 1 hour at 33°C and then recovered for 6 hours at 20°C (+). Worms were assessed qualitatively as low, medium, or high GFP expression.



Appendix B2 Other NuRF complex members do not regulate the HSR. TJ375 were fed the indicated RNAis from hatching. Two days post L4/YA worms were anesthetized using 10 mM Levamisole and mounted on agarose pads and imaged.



Appendix B3 *arp-6*, *vab-15*, *set-2*, *ham-3* modulate the HSR. (A) TJ375 animals were fed the indicated RNAis and then assessed at L4/YA (Day 1) or two days later (Day 3). Worms were given no heat shock (-) or were exposed to 1 hour at 33°C and then recovered for 6 hours at 20°C (+). Worms were assessed qualitatively as low, medium, or high GFP expression.

Appendix C: Extended Protocols

NGM Buffer (1L)

In a 2L bottle

1. Mix 3 g NaCl + 1000 ml H₂O. Autoclave
2. Cool to RT then aseptically add 1000 µl each of MgSO₄ (1M) and CaCl₂ (1M)
3. Add 25 ml KH₂PO₄ (1M pH:6.0)
4. Cap tightly and mix well.

NGM plates (1L)

In a 2L bottle

1. 3 g NaCl + 2.5 g Peptone + 17 g Agar + + 1L H₂O + stir bar, then autoclave.
2. Allow to cool to ~55-60C, if you can hold bottle for 10 sec without it being too hot this is around the right temperature, for 1L batch takes ~30-45 mins out of the autoclave.
3. Once cooled aseptically add 1000 µl each of MgSO₄ (1M) and CaCl₂ (1M), Cholesterol (5 mg/ml).
4. Aseptically add 25 ml KH₂PO₄ (1M pH:6.0)
5. Stir to combine all ingredients then pour plates.
6. For 10 cm plates ~25 ml, for 6 cm plates ~10 ml.

RNAi plates (1L)

In a 2L bottle

1. 3 g NaCl + 2.5 g Peptone + 17 g Agar + Stir bar, then autoclave.
2. Allow to cool to ~55-60C, if you can hold bottle for 10 sec without it being too hot this is around the right temperature, for 1L batch takes ~30-45 mins out of the autoclave.
3. Once cooled aseptically add 1000 μ l each of MgSO₄ (1M) and CaCl₂ (1M), Cholesterol (5 mg/ml).
4. Aseptically add 25 ml KH₂PO₄ (1M pH:6.0)
5. Aseptically add 10 ml of sterile 20% Lactose **OR** 1000 μ l of IPTG (1M), and 1000 μ l of Carbenicillin (50 mg/ml)
6. Stir to combine all ingredients then pour plates.
7. For 10 cm plates ~25 ml, for 6 cm plates ~10 ml.

Bleaching

1. Examine plate for high percentage of gravid adults.
2. Take out Clean NGM plate to warm to room temperature.
3. Wash plate NGM buffer, use a transfer pipet to place worms into a 15 ml tube, repeat plate wash one more time.
4. Cap tightly, invert 3-4 times, and allow to sit undisturbed in rack for ~5-7 mins to gravity settle out the adults.
5. Discard supernatant which contains excess bacteria + larval worms.
6. Wash adults with H₂O and allow them to gravity settle again for ~5-7 mins, you should have a clear supernatant now. If not rewash with H₂O until clean.
7. Remove supernatant to 3.5 ml. Discard transfer pipet.

The rest of the procedure must be **done to completion without stopping**.

Quickly add 1000 µl of bleach then 250 µl of NaOH to worms. Cap tube tightly, and shake for a maximum of 5 mins. Worms will typically be lysed around 3-4 mins.

8. Examine tube for unlyzed worm bodies, if you observe no bodies prior to 5 mins move on to the next step, but no matter what do not lyse for longer than 5 mins or eggs will begin to be destroyed.
9. Wash eggs with H₂O, centrifuge tube 1600 rpm for 30 sec, pour off supernatant carefully, and repeat egg washes 3 more times to give a total of 4 washes.
10. Use a fine tip transfer pipet to break up egg clumps (blow bubbles and gently pipet up and down a few times), then transfer eggs to clean NGM plate.
11. Observe plate for clean vs messy bleach (only eggs vs eggs + dead bodies).

12. Dry plate in sterile hood, wrap with parafilm, and place in incubator to hatch overnight.

CRISPR Transgenesis

Selection of guiding RNA. Enter 100-200 bp of target sequence on the CRISPR/Cas9 gRNA MIT website indicating the species and genome file were appropriate. The program will return hits ranked in order of computationally determined specificity and efficiency. Choose a gRNA with total score greater than 90. Take note of the entire gRNA sequence and PAM motif Mutate the plasmid pDD162 with site directed mutagenesis using forward primer 5'- N₂₀GTTTTAGAGCTAGAAATAGCAAGT-3' and reverse primer 5'-CAAGACATCTCGCAATAGG-3'. N₂₀ is your 20 bp targeting sequence from the CRISPR gRNA design tool. Sequence verify the insertional change.

Creation of HSF-1 Homologous Repair Template Plasmid

Each target region was amplified from the template source indicated in table appendix using Phusion Polymerase (NEB) After amplification, all fragments were ligated using Gibson Assembly (NEB) following the manufacturer's instructions for a 5 fragment assembly. After assembly, the resulting DNA was cloned into pDONR221 using Gateway technology BP cloning and transformed into ccdB sensitive Top10 cells according to manufacturer's instructions (Invitrogen). Candidate clones were screened using M13 F/R for insertions and subsequently sequence verified prior to injection into worms.

Gibson Assembly 4-6 fragments

1. On ice, mix 0.2-1 pmole of each fragment in a PCR tube
2. Add 10 ul Gibson assembly master mix
3. Bring final volume to 20 ul, do not exceed 20 ul.
4. Incubate samples in a thermocycler at 50°C for 60 minutes.
5. Store sample in -20°C or proceed to transformation.

Gateway Cloning

BP reaction

1. Add 20-50 fmoles of attB PCR product and 150 ng of pDONR vector in a PCR tube
2. Bring to 8 ul final volume with TE buffer.
3. Briefly vortex the BP Clonase enzyme mix and add 2 ul to the BP reaction.
4. Incubate reaction at RT overnight.
5. Add 1 ul proteinase K
6. Incubate at 37°C for 10 mins.
7. Proceed to transformation with Top10 cells.

Convert fmole to ng using

$$\text{ng} = (\text{X fmole}) * (\text{length in BP}) * (660/10^6)$$

Transformation

1. Thaw a vial of Top10 cells on ice for ~10 mins
2. Add 1 ul of the completed BP reaction to the tube of Top10 cells.
3. Flick gently to mix and incubate on ice for ~15 mins.
4. Heat shock cells at 42°C for 30 seconds.
5. Add 250 ul of SOC and shake horizontally for 1 hr at 37°C.
6. Spread 50-100 ul of the transformation reaction on pre-warmed LB-Kan plates.

Creation of isoform specific *pyp-1* RNAi plasmids

Each isoform specific section was amplified using Phusion Polymerase (NEB) with the indicated primers in table. After amplification, each product was cloned into L4440 Gtwy using BP cloning and transformed into *ccdB* sensitive Top10 cells according manufacturer's instructions (Invitrogen). Candidate clones were sequence verified and then utilized in RNAi experiments.

Single Worm PCR (for crossing)

Procedure:

1. Add proteinase K to lysis buffer (90 μ L lysis buffer + 10 μ L 10mg/mL proteinase K).
2. Place 3-10 μ L of lysis buffer in top of 1.5mL Eppendorf tube.
3. Pick single worm into lysis buffer.
4. Spin worm to the bottom of tube by spinning in centrifuge for 15 seconds at 14,000 rpm.
5. Flash freeze the tube in dry ice and ethanol or in liquid nitrogen (poke a hole in the tube's lid if freezing in liquid nitrogen so the tube does not explode).
6. Freeze tube at -80°C for at least 1 hour.
7. Lyse the worm and release the genomic DNA by heating tube to 65°C for 60-90 minutes.
8. Inactivate the proteinase K by heating to 95°C for 15 minutes.
9. Perform PCR - Run reaction for 30-35 cycles.

Recipes:

Worm PCR Lysis Buffer

50mM KCl

10mM Tris (pH 8.3)

2.5mM MgCl₂

0.45% NP-40 (IGEPAL)

0.45% Tween-20

0.01% Gelatin

Add 0.1mg/mL of proteinase K before use.

Gautam Kao Co-IP protocol

Co-immunoprecipitation protocol

(last change 12 Aug 2016)

Low salt wash buffer:

- 1M T-HCl (7.4) = 0.4mL
- 5M NaCl = 1.2mL
- 0.5M EDTA = 40uL
- H₂O = 38.4mL

High salt wash buffer

- 1M T-HCl (7.4) = 0.4mL
- 5M NaCl = 4mL
- 0.5M EDTA = 40uL
- H₂O = 35.4mL

Lysis buffer

- 1M T-HCl (7.4) = 0.4mL
- 5M NaCl = 1.2mL
- 0.5M EDTA = 40uL
- H₂O = 36.4mL
- 10% NP-40 = 2mL

Prior work: Add the 100X HALT protease/phosphatase cocktail (Thermo #78440)- to the lysis buffer. Keep on ice.

Start the experiment at 8:30am.

Switch on the refrigerated microfuge and set temp to 4C. We find that the Eppendorf 5424R centrifuge works better than the Beckman Coulter 22R machine.

Wash worms from 10-12 plates with M9 into a 15mL tube. Let them settle by gravity for 5-7 min till there is a pellet. Discard supernatant and add 5mL of M9, let it settle by gravity again.

Discard supernatant and add 5mL M9. Mix and centrifuge in the Hettich at 2.2K rpm for 2 min. Repeat 1 more time at least or until the supernatant looks free of bacteria.

After the last centrifugation, leave 0.5mL of the M9 in the tube with the worms

and transfer this to the screwcapped 2mL Axygen Eppendorf tubes with rubber gasket that is to be used with the bullet blender.

Centrifuge in the eppendorf at 2.2K rpm for 2 min and discard as much of the supernatant as possible.

Add 250uL lysis buffer supplemented with the protease inhibitor cocktail (LyP) to the worm pellet and mix well. Centrifuge as before. Remove the supernatant.

Add 400uL of LyP to the worm pellet. Then add 2 scoops of the 0.2mm stainless steel beads (SSB02/Next Advance) using a Corning 3013 microspatula. Use each microspatula only once. Can add the beads to the tubes before pipetting the worms into the tubes.

Lyse the worms with the Next Advance bead beater that is in the cold room. Setting of 8 for 3 min.

Centrifuge in refrigerated centrifuge for 20 min and 14K rpm at 4C.

Transfer the supernatant to a new labeled eppendorf. Do not pipette up the cloudy white layer just above the beads. Not always visible. There is also often white cloudy stuff that does not settle after the centrifugation. Cannot avoid taking this. The volume of the supernatant should be about 350-415uL. Keep on ice.

Thaw out the protein standards from the -20C after starting the centrifuge run.

Now need to make two 40uL dilutions of the lysate in MQ. These are 1:5 and 1:10 dilutions. These will be used for the protein concentration determinations.

Do protein estimation (separate protocol). We use the Pierce BCA protein assay kit. This takes about 40 minutes.

After protein estimation: From each lysate, pipette out the amount corresponding to between 800-1000ug protein (Can go up to 1200 ug of total protein). This is usually in approx. 100-350uL. Use the same total amount of protein for each lysate. Dilute this to 600-900uL (more if needed) with Chromotek low salt wash buffer (since it does not contain NP-40). It is important to dilute the NP-40 concentration to below 0.2% when doing pull-downs with GFP-trap beads from Chromotek.

NOTE: Supplement the dilution buffer with the sigma protease inhibitor cocktail! This dilution of the NP40 is important for when using Chromotek anti-GFP magnetic beads. Not necessary to do this when using anti-Flag (Sigma) beads.

The rest of the lysate is stored at -20C. 0.5ug will be needed for the “input” lanes in the western.

Preparation of beads and immunoprecipitation

Use 25uL of the GFP trap beads (or 40uL of anti-flag beads). Cut the pipette tip dispense the beads easily. Wash the antibody conjugated beads 3X with 600uL of cold Chromotek low salt

wash buffer using the magnetic separator. This is done in Axygen eppendorf tubes. It is important never to let the antibody conjugated beads dry up.

While washing the beads, dilute 1000 ug of protein lysates in a total of 900 uL. using protease inhibitor supplemented low salt wash buffer. (Can use less total protein if the protein concentration is lower)

After 3 washes, add the lysate mix to the washed beads.

If you are working alone you can wash the beads first and then make the lysate mix.

Incubate for 1 hour 15 min at 4C rotating in the end-over-end inverter. Make sure that the liquid is rolling properly in the tube.

TIME FOR A BREAK. The time should be around 12pm.

Separate the beads from the lysate using the magnet. Discard the supernatant. Wash with 600uL of low salt wash buffer (containing 150mM NaCl) for 10 min using the end-over end rotator at RT.

Separate, discard the wash buffer. Repeat with high salt wash buffer containing 500mM NaCl.

Repeat again with low salt wash buffer containing 150mM NaCl.

(Have done variations in which all 3 washes are in 150mM salt or all in 500mM salt.)

After the last wash, remove all possible wash buffer by doing a quick, low speed centrifugation to bring down all the liquids. Add twice 17.5uL of 2X SDS sample buffer + BME directly to the beads. (we elute in 35uL because our SDS_PAGE gels take a max of 50uL). Be careful not to tap the tubes too much, because the beads may not come down. Heat for 10 min at 95C. Quickly spin the tubes to bring down the droplets. Separate by the magnet and transfer the eluate to a new tube.

Preparing inputs samples.

Take 10ug of total protein in a total of 10uL. Add MQ water to get the final volume.

Add 5uL of 4X SDS sample buffer + BME to the inputs and boil them for 10 min at 95C.

Can freeze the samples at -20C now or run on a gel.

PROCEED FOR WESTERN BLOTTING.

SDS-PAGE GELS

MW standards used are Bio-Rad Precision Plus Protein Dual Extra (161-0377). Load 8uL in a Mini-Proean TGX Stain-free Gel (456-8124). [Robakowska thought that non-stain free gels give a high background).

The entire volume of the eluate is loaded (use the soft pipette P20). Because of the concerns of spill-over due to the large volume, an empty lane is kept between eluate lanes.

“Input” lanes (i.e. lysate before the IP): Use from 0.5 to 10ug (depending from strain) for each in a final volume of 10uL + 5uL of 4X SDS-sample buffer+BME. No need for empty lanes between input lanes since the volume is only 15uL.

Load 15uL of 1X SDS sample buffer to each empty lane.

Run the gel for 1 hour at 120V.

When the gel is done running, cut the gel to the minimum size possible.

Put the bottom part of the transfer pack (Trans-Blot Turbo Transfer Pack 170-4156) on the transfer box, roll out the bubbles.

Put the gel on the membrane, roll again to remove bubbles.

Put the top part of the transfer pack and rollout with the roller to remove bubbles.

Clamp on the top lid of the transfer block, then put the membrane with the gel into a Trans-blot machine. Start the machine, click on “turbo” then “minigel” and run the transfer. This should take 7 min.

When the transfer is done, turn off the machine and take out the membrane. Cut the membrane around the gel and put the membrane into 15mL of 5% Milk or 5% BSA in TBS-T (blocking solution). Make sure that the membrane does not dry. Then shake it at RT for 60-120 min (slow speed).

Discard the blocking solution and add 10mL primary antibody, anti-FLAG 1:1000 and shake overnight (at least 16h) at 4C. Or add 10mL primary antibody, anti-GFP 1:2000 and shake it for 60 min and RT.

Next day around 1pm (can be earlier also), put the primary Ab back into a Falcon tube and start washing the membrane with PBS-T 3 times 5 min each in RT with faster shaking.

Add 15mL secondary antibody, anti-Mouse 1:5000 or anti-Rat 1:5000, shake for 1h at RT with slow shaking.

Discard the secondary Ab and wash the membrane 3 times 5 min with PBS-T.

Discard the last wash and add 1mL Enhancer solution and 1mL Peroxide buffer to the membrane and pipette the solutions on the membrane to cover it equally.

Drain out excess liquid by touching the edge of the membrane to a paper towel.

Cut out a transparent plastic film and put the membrane in it. Streak out to avoid having bubbles.

Detect bands in the western blot detecting machine (LAS1000).

Take a picture of the gel in the LAS1000 using the light setting and 1/8 sec exposure.

Ptn estimation using 96 well plate and Pierce BCA reagent.

- 1) Mix 50 vols reagent A with 1 vol reagent B (3 mL or so should be enough). For making "3mL", add 3mL of reagent A and 60uL of reagent B.
- 2) In Column 1 of the plate add the **20uL** of standard BSA dilutions in this manner:
 - 1H: 25ug/ml
 - 1G 125ug/ml
 - 1F: 250
 - 1E:500
 - 1D:750
 - 1C: 1000
 - 1B 1500ug/ml
 - 1A: 2000ug/ml

These are made from a BSA solution supplied by Pierce. RG keeps premixed dilutions at -20C

- 3) In Column 2: **add 20ul of MQ to 2H. This is the blank. (see pic).**
- 4) Then add the samples to other wells as you wish. Can start from 2A onwards. The total volume here should also be 20uL QS with RIPA or MQ

- 5) To every well in use add 200uL of the A+B mix.
- 6) Incubate for 37C for 30 mins.

	1	2	3	4	5	6	7	8	9	10	11	12
A	1	1	8	16	24	32	40	48	56			
B	2	2	9	17	25	33	41	49	57			
C	3	3	10	18	26	34	42	50	58			
D	4	4	11	19	27	35	43	51	59			
E	5	5	12	20	28	36	44	52	60			
F	6	6	13	21	29	37	45	53	61			
G	7	7	14	22	30	38	46	54	62			
H	8	1	15	23	31	39	47	55	63			

Red: Standards; yellow: blank; Green: Samples.

Using the Viktor 300 machine

- 1) Switch on the machine. Switch is on the small box next to the reader.
- 2) Switch on computer.
- 3) Click on “wallac 1420 workstation” After it finishes initializing, minimize its window.
- 4) Click on “workout 2.0” on the desktop. Open “existing protocols”
- 5) Click on “Rahul BCA”
- 6) Click on start reading. When all is done you will get the results screen. Here click on “plate” or “results table” etc. Remember to multiply by the dilution factor
- 7) For N2 and COP264 lysates a dilution of 1:5 and 1:10 was used.